Russian Chemical Reviews **65** (5) 379–419 (1996)
© 1996 Russian Academy of Sciences and Turpion Ltd

UDC [41.12.017 + 548.3]: 666.5(047)

Phase equilibria in M–X–X′ and M–Al–X ternary systems (M = transition metal; X, X′ = B, C, N, Si) and the crystal chemistry of ternary compounds

A I Gusev

Contents

I.	Introduction	379
II.	Phase equilibria in M–B–C borocarbide systems	382
III.	M–B–N ternary boronitride systems	388
IV.	Phase relationships in the Si-containing M–B–Si, M–Si–C, and Me–Si–N systems	390
V.	Phase equilibria in M–Al–X ternary systems (X = C, N, Si)	402
VI.	Phase equilibria in X–X′–X″ ternary systems (X, X′, X″ = B, C, N, Si, Al)	414
VII.	Conclusion	415

Abstract. The published data on phase equilibria in the M–X–X′ and M–Al–X ternary systems (M is a Group III–VIII transition metal, X, X′ are B, C, N, Si) are surveyed. These systems provide a basis for the directed search for oxygen-free ceramic materials for various purposes. The phase diagrams for the ternary systems are presented; more than two hundred ternary phases formed in these systems are systematised and described for the first time. The typical crystal structures of the ternary compounds and of the phases are considered, the general and distinguishing features of these structures are analysed. It is shown that ternary compounds containing the XM_6 octahedral groups possess homogeneity regions. The bibliography includes 240 references.

I. Introduction

Ceramics are materials which have been in use for a very long time. Products of fired clay, faience, and porcelain have been traditionally referred to as ceramics. However, the range of ceramic materials has now considerably widened, and the term 'ceramics' is used in relation to polycrystalline materials based on compounds of Group III–VI nonmetals with one another and/or with metals, obtained by various methods such as sintering, pressing, precipitation from the gas phase or from the liquid colloidal state, etc. Borides, carbides, nitrides, oxides, and silicides are the initial compounds for the preparation of ceramics.

The interest in ceramic materials has substantially grown in the last few decades. In the developed countries, the amount of the manufactured ceramic products is rapidly increasing, new technologies appear, and the ceramic products have found wide application in industry, transport, energetics, electronics, and medicine. The new ceramics have revolutionised materials science. At present, ceramics are the third industrial material, regarding the tonnage of use, after metals and polymers, and it occupies a key position in the field of high technologies.

A I Gusev Laboratory of High-Melting Compounds, Institute of Solid State Chemistry, Ural Division of the Russian Academy of Sciences, ul. Pervomaiskaya 91, 620219 Ekaterinburg, Russian Federation.
Fax (7-343) 244 44 95. Tel. (7-343) 249 35 23.
E-mail: aig@gusev.e-burg.su.

Received July 6 1995
Uspekhi Khimii **65** (5) 407–451 (1996); translated by Z P Bobkova

An evaluation of the dynamics of the increase in the manufacture of ceramics over the period between 1990 and 1995 and up to 2000 indicates that the output volume is doubling every five years (Table 1). This is caused by the demand for the materials meant for performing new functions (for example, in force lasers, memory cells, superconducting devices, catalysts, electrodes, and heat- or radiation-resistant devices). Actually, the new ceramics often prove to be stronger than metals, though they are lighter; they may be elastic enough to be suitable for the manufacture of elastic units; ceramics withstand high temperatures and thermal shocks; they are highly resistant to corrosion and to wear.

The perfection of the existing ceramic materials and the development of new materials involves both the synthesis of complex compounds and heterogeneous compositions and the preparation of finely dispersed materials (with a particle size of ~1–10 nm) from these compounds and compositions, which ensures the stability and the high level of performance.

The new ceramic materials and the relevant technologies are extremely science-dependent. This accounts for the intense fundamental research in the field of physical chemistry, physics and chemistry of solids, and physical material technology. All the studies on physical chemistry and material technology dealing with the search for new solid-phase compounds and compositions for ceramics are based on phase equilibria and phase diagrams presented in many publications.

The aim of the present review is to generalise and systematise the data on the phase equilibria in the oxygen-free M–X–X′ and M–Al–X ternary systems (where M is a Group III–VIII

Table 1. Production of new ceramics and ceramic composite materials (in millions of US dollars) in developed countries over the period from 1990 to 1995 and a forecast for the production in 2000.

Field of application	1990	1995	2000
Electronics	3740	6565	11360
Aviation and astronautics	80	200	445
Motor-construction	81	310	820
Medicine and biology	15	34	60
Metal working, cutting tools	92	246	500
Industrial heat and power engineering	15	50	100
Other fields of application	150	320	720
Overall	4173	7725	14005

transition metal, X and X′ are B, C, N, Si) and on the crystal structure of the ternary compounds formed in these systems. These ternary systems serve as the constituents of more complex 4- and 5-component systems and cover largely the systems that are used or can be used for preparing new ceramic materials.

Before we discuss ternary systems, let us consider briefly some characteristic features of the structures of the binary compounds that are permanently involved in the phase equilibria in the M–X–X′ systems, namely, transition metal carbides, nitrides, borides, and silicides, and of binary high-melting compounds of nonmetals.

The cubic (with the *B*1 structure) and hexagonal (with the *L*′3 structure) carbides and nitrides of Group IV and V transition metals MC_y, M_2C_y, MN_y, and M_2N_y ($0.4 \leqslant y \leqslant 1.0$) belong to the group of nonstoichiometric interstitial compounds[1,2] and possess (in contrast to other compounds considered here) metallic electrical conductivity. The atomic radius of carbon is fairly small and is equal to ~0.077 nm, therefore, in compounds with transition metals carbon always acts as the interstitial element and is located in the interstices of the metal sublattice. The interstitial nonmetal atoms (carbon or nitrogen) in the cubic carbides and nitrides MC_y and MN_y occupy the octahedral interstices of the face-centred cubic (Fcc) metal sublattice and can populate either all of the interstices or only some of them. The octahedral interstices free from these atoms are referred to as structural vacancies. In hexagonal lower carbides and nitrides M_2C_y and M_2N_y, the interstitial atoms occupy half the octahedral interstices of the hexagonal close-packed metal sublattice. The interstitial atoms and the structural vacancies may be arranged in a crystal lattice either statistically (irregularly) or regularly.

The nonstoichiometric carbides and nitrides with the *B*1 and *L*′3 structures belong to the class of the so-called octahedral structures, that is to the structures in which each six transition metal atoms constitute the octahedral environment of an interstitial atom X or of a vacancy. These structures are built of the XM_6 octahedra joined with one another in various ways. For example, in the NaCl type structure (*B*1) the octahedra are joined through their edges (Fig. 1). Many of the ternary compounds considered below also incorporate regular or distorted XM_6 octahedra as the main structural motif.

Carbides and nitrides of Group VI–VIII transition metals have virtually no homogeneity regions and can have various crystal structures with a relatively high symmetry, namely, orthorhombic, tetragonal, hexagonal, or cubic.

A detailed description of the structures and properties of binary carbides and nitrides of transition metals with allowance for the short-range and long-range effects of nonstoichiometry has been published.[1–6]

Transition metal compounds with boron are built in a different manner. The boron atoms are larger than the carbon or nitrogen atoms; therefore, B–B bonds can arise in the crystal lattice of borides. In the borides M_2B, the boron atoms are separated from one another, and the M–B interactions are the most significant. With the increase in the boron content, changes occur from the structure with the separated boron atoms in M_2B to the ...–B–B–... zigzag-like chains in MB and to hexagonal chains in M_3B_4, and then to a two-dimensional hexagonal network of boron atoms bound to one another in the diborides MB_2 and to cage structures built of boron atoms in the borides MB_4, MB_6, and MB_{12}, which contain interpenetrating lattices of the metal and boron atoms.[7]

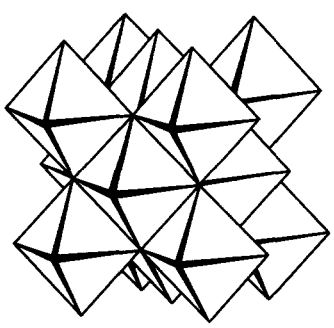


Figure 1. Crystal structure of the NaCl (*B*1) type of the cubic (space group *Fm*3*m*) monocarbides and mononitrides MX (X = C, N) represented by XM_6 octahedra.

The atom radius of silicon, an analogue of carbon, is much larger, being equal to ~0.117 nm. In compounds with Group IV and V transition metals, whose atoms are sufficiently large, silicon still acts as an interstitial element; the silicides of other transition metals occupy an intermediate position between interstitial compounds and intermetallides. Thus, silicon can be incorporated in a metallic lattice as an interstitial element or as a substituting element. In lower silicides (for example, in M_3Si), the silicon atoms are separated from one another, and only M–Si bonds exist. As the content of silicon atoms increases, isolated Si–Si pairs are formed initially; the further increase in the silicon content results in one-dimensional zigzag-shaped chains of the silicon atoms (in compounds of the M_5Si_3 type), two-dimensional close-packed networks (in MSi_2), and, finally, three-dimensional spatial frameworks of silicon atoms (for example, in lanthanide disilicides[8]). The crystal structures of borides and silicides are quite diverse.

Aluminium forms numerous intermetallic compounds with transition metals, many of which have homogeneity regions.

The great difference between the crystal structures of carbides and nitrides, on the one hand, and borides, silicides, and aluminides, on the other hand, result in their low mutual solubility.

Boron, carbon, nitrogen, silicon, and aluminium form solid solutions not only with metals, but also with one another, for example, in the X–X′ binary systems (B–C, B–N, Si–B, Al–B, C–N, Si–C, Al–C, Si–N, and Al–N). Let us discuss briefly the characteristic features of the crystal chemistry of these high-melting carbides, nitrides, and borides of nonmetals. The structural characteristics of the high-melting compounds are listed in Table 2.

The B–C system. The main phase in the B–C system is boron carbide B_4C ($B_{12}C_3$); the carbide $B_{13}C_2$ is also formed (see Table 2).

The twelve boron atoms in $B_{12}C_3$ are located at the vertices of an icosahedron. The B_{12} icosahedra constitute an Fcc-lattice, the three carbon atoms being located as the C–C–C chain in the large octahedral interstices. The terminal carbon atoms in this chain are linked to four boron atoms from the two nearest icosahedra (the B–C distance is 0.164 nm); and the central carbon atom of the carbon chain is bound only to the other carbon atoms of this chain, which are located at a distance of 0.139 nm from it.

The carbide $B_{13}C_2$ has a structure derived from that of B_4C ($B_{12}C_3$). This compound can be represented as $(B_{12})BC_2$, i.e., it may be regarded as $B_{12}C_3$ in which one of the C atoms has been substituted by boron. The boron atom and the two carbon atoms are located in the octahedral interstices of the B_{12} icosahedra as C–B–C chains.

The similarity of the crystal lattices of the carbides B_4C ($B_{12}C_3$) and $B_{13}C_2$ led some authors to suppose that there exists one phase with a broad homogeneity region. However, the dependence of the properties of boron carbide on the carbon content exhibits two extrema at the compositions $B_{12}C_3$ and $B_{13}C_2$, which attests to the existence of two different phases.

Table 2. Crystal-chemical characteristics of high-melting compounds of nonmetals.

Compound	Symmetry and type of structure	Space group	Z[a]	Unit cell parameters / nm			Ref.
				a	*b*	*c*	
B_4C ($B_{12}C_3$)	Hexagonal	$R\bar{3}m$	9	0.561	–	1.214	9
$B_{13}C_2$ ($B_{12}BC_2$)	"	$R\bar{3}m$	9	0.5633	–	1.2164	10
α-BN	"	$P6_3/mmc$	4	0.2504	–	0.6661	11
β-BN	Cubic, sphalerite ZnS (*B*3) type	$F\bar{4}3m$	8	0.3615	–	–	12
γ-BN	Hexagonal, wurtzite ZnS (*B*4) type	$P6_3mc$	4	0.255	–	0.423	13
SiB_4	Hexagonal	$R\bar{3}m$	9	0.635	–	1.269	7
SiB_6	Orthorhombic	*Pnnm*	40	1.4392	1.8267	0.9885	14
SiB_{14} (SiB_{12+x})	Hexagonal	$R\bar{3}m$	7	1.113	–	2.383	15
AlB_2	Hexagonal, *C*32 type	$P6/mmm$	1	0.3009	–	0.3262	16
α-AlB_{12}	Tetragonal	–	14	1.016	–	1.428	1
α-AlB_{12}	"	$P4_12_12$	4	1.0158	–	1.4270	18
γ-AlB_{12}	Orthorhombic	$P2_12_12_1$	4	1.6573	1.7510	1.0144	19
β-C_3N_4	Hexagonal, β-Si_3N_4 type	$P6_3/m$	2	0.63	–	0.246	20
α-SiC (2*H*)	Hexagonal	$P6_3mc$	2	0.3073	–	0.5028	21
α-SiC (4*H*)	"	$P6_3mc$	4	0.3073	–	1.0053	21
α-SiC (6*H*)	"	$P6_3mc$	6	0.3073	–	1.5079	21
α-SiC (15*R*)	Rhombohedral	$R3m$	5	0.3073	–	3.770	21
β-SiC (3*C*)	Cubic, sphalerite ZnS (*B*3) type	$F\bar{4}3m$	4	0.4349	–	–	21
Al_4C_3	Hexagonal, $D7_1$ type	$R\bar{3}m$	3	0.3330	–	2.489	22
α-Si_3N_4	Hexagonal, phenacite Be_2SiO_4 type	$P31c$	4	0.767	–	0.564	23
β-Si_3N_4	"	$P6_3/m$	2	0.759	–	0.292	23
AlN	Hexagonal, wurtzite ZnS (*B*4) type	$P6_3mc$	4	0.3113	–	0.4982	24
AlN	"	$P6_3mc$	4	0.3111	–	0.4978	22

[a] From here on, Z is the number of formula units in the unit cell.

The B–N system. In the B–N system only one compound is formed, namely, boron nitride BN, which exists in α, β, and γ modifications.

The nitride α-BN has a hexagonal graphite-like structure. The boron and nitrogen atoms in this ideal structure are regularly distributed in hexagonal networks; the networks are arranged one above the other in such a way that the boron and nitrogen atoms alternate along the *c* axis of the crystal. The distance between the layers in α-BN is larger than the interatomic distances in the networks by a factor of 2.5. This causes substantial anisotropy of the properties of α-BN. The α-BN modification can have various degrees of ordering ranging from an amorphous structure to a completely ordered structure. The resistance of α-BN to oxidation increases with an increase in the degree of ordering.

The cubic modification β-BN has a sphalerite-type structure (ZnS, *B*3), and γ-BN has a wurtzite-type structure (ZnS, *B*4). The structures of β- and γ-BN are very similar, and they may be regarded as polytypes. The cubic boron nitride β-BN is stable to attrition and possesses an extremely high hardness close to that of diamond. Only α- and β-BN are thermodynamically stable.[13]

The Si–B system. Three compounds, SiB_4, SiB_6, and SiB_{12+x} (SiB_{14}), are formed in this system (see Table 2).

The structure of the boride SiB_4 is similar to that of B_4C ($B_{12}C_3$): B_{12} icosahedra form an Fcc-lattice, the silicon atoms being located in its octahedral interstices; some of the silicon atoms can substitute the boron atoms in the B_{12} groups. The boride SiB_4 is stable at $T \leqslant 1640$ K; at higher temperatures it decomposes peritectically to give the orthorhombic boride SiB_6 and silicon.

The compound SiB_{12+x} (SiB_{14}), which also exists in the Si–B system, is sometimes regarded as being a solid solution of silicon in β-B (the groups of boron atoms in the β-B structure constitute a rhombohedrally distorted cubic close packing, the interstices of which may contain silicon and aluminium atoms, together with the boron atoms[25]).

The Al–B system. In the Al–B system, the existence of borides AlB_2 and α- and γ-AlB_{12} has been established reliably.

The boride AlB_2 has a hexagonal structure (space group $P6/mmm$) of the *C*32 type. In this structure, the aluminium atoms form trigonal prisms joined through all faces; the axes of the prisms are parallel to the *c* direction. The boron atoms are located at the centres of these prisms, therefore the structure of AlB_2 may be regarded as a filled structure of the WC type.

The borides α-AlB_{12} and γ-AlB_{12} have tetragonal and monoclinic structures of their own types (see Table 2). The orthorhombic boride β-AlB_{12}, which has been repeatedly described in the literature, is in fact the borocarbide $Al_3B_{48}C_2$.[25]

The C–N system. Gaseous cyanogen C_2N_2 exists in this system under equilibrium conditions. On heating to 870 K cyanogen polymerises to give a dark-brown solid (amorphous) and insoluble paracyanogen. When paracyanogen is heated to 1130 K in the absence of air, it is again converted to cyanogen.

In the system under consideration, the existence of a solid phase resembling a diamond-like solid solution of nitrogen in carbon C(N) cannot be ruled out. Furthermore, in recent years, information on crystalline carbon nitride has been reported. Liu and Cohen[26,27] who have used a model suggested previously[28] for the calculation of the crystal and electronic structures of solid phases, predicted the possible existence of crystalline β-C_3N_4. Later, this compound has been found as particles with a size of ~0.5 μm in a ~1 mm thick C,N-containing film obtained on a silicon support by atomisation of graphite ($T = 673-873$ K) under a nitrogen atmosphere ($P_{N_2} = 2.3$ Pa).[20] The carbon nitride β-C_3N_4 has a hexagonal structure of the β-Si_3N_4 type (see Table 2).

The Si–C system. In this system only one phase exists, namely, silicon carbide SiC having α- and β-modifications.

The structure of α-SiC consists of close-packed layers of silicon atoms and close-packed layers of carbon atoms, which are arranged between the silicon layers at a height equal to $\frac{3}{4}$ of the distance between them; the carbon atoms occupy the same crystallographic positions as the silicon atoms. Consequently, all the atoms of one kind in the carbide α-SiC are located in the tetrahedral environment of atoms of the other kind (SiC_4 and CSi_4). The number of the layers in the structure of α-SiC may differ, which accounts for the polytypism of silicon carbide. The carbide α-SiC forms more than 100 hexagonal and rhombohedral polytypes. More than 70 polytypes of α-SiC differing in the number of the layers have been described in a review.[21] The most commonly encountered structures are 4-, 6-, and 15-layered polytypes denoted as 4 H, 6 H, and 15 R (the letters H and R correspond to hexagonal and rhombohedral polytypes and the digits correspond to the numbers of the layers in the polytypes; the cubic close-packed structure is designated as 3*C*).

The cubic modification β-SiC crystallises with the sphalerite ZnS (*B*3) structural type; its formation is probably promoted by a slight excess of silicon.

The temperature of the peritectic decomposition of silicon carbide is 3030–3100 K.

The Al–C system. Al_4C_3 is formed as the only hexagonal carbide in the Al–C system (see Table 2). In this compound, the aluminium atoms constitute close-packed planes, with $\frac{2}{3}$ and $\frac{1}{3}$ of all the carbon atoms being located between these planes in the tetrahedral and octahedral interstices, respectively. Consequently, the Al_2C_2 and Al_2C layers alternate along the *c* axis (a rhombohedral unit cell contains 12 close-packed planes of aluminium atoms).

The Si–N system. The silicon nitride Si_3N_4 is the only stable silicon compound with nitrogen. It exists in two modifications: α-Si_3N_4 (trigonal) and β-Si_3N_4 (hexagonal) (see Table 2).

The nitride α-Si_3N_4 has a layered structure in which each silicon atom is in the tetrahedral environment of four nitrogen atoms, and three silicon atoms constitute the nearest environment of each nitrogen atom.

The structure of β-Si_3N_4 also consists of SiN_4 tetrahedra in which each nitrogen atom is shared by three tetrahedra. The nitride β-Si_3N_4 is stable up to 1700 K in the absence of nitrogen. The intercalation of admixtures into the lattice of β-Si_3N_4 can lead to the formation of the α-modification (for example, the structure of α-Si_3N_4 is stabilised by elemental silicon).

The Al–N system. In the Al–N system, too, only one compound is known, namely, the nitride AlN with a hexagonal structure of the wurtzite ZnS (*B*4) type. The nitrogen atoms in AlN occupy tetrahedral vacancies between the hexagonal close-packed layers of aluminium atoms. The sintering of an aluminium nitride powder prepared by the plasmochemical method yields a multilayer sphalerite polytype of AlN.[13] In all probability, this modification arises due to the presence of an admixture of oxygen.

Aluminium nitride possesses high hardness, heat conductivity, and thermal stability and low thermal expansion coefficient; it is resistant to oxidation up to 1000 K.

The Al–Si system. In this system no compounds have been detected.

II. Phase equilibria in M–B–C borocarbide systems

The transition metal borocarbide systems are among the ternary systems of transition metals with boron, carbon, nitrogen, and silicon studied most thoroughly. Nevertheless, virtually no survey papers devoted to them have been published. Some of the M–B–C systems have been described in monographs.[8,29–31]

1. Borocarbides of Group III transition metals

Borocarbides of scandium, yttrium, and lanthanides have not been studied adequately, though it is in these systems that most of the known ternary compounds $M_xB_yC_z$ (Table 3) have been found. In particular, scandium, yttrium, and all the lanthanides (except for Pm) form ternary borocarbides of the formula MB_2C_2.[33,34,36,37,41,44–46] For the lanthanide borocarbides LnB_2C_2, a small tetragonal unit cell containing one LnB_2C_2 formula unit and having similar a_0 and c_0 parameters was initially suggested.[36,41] The boron and carbon atoms in this structure are arranged randomly. Using YB_2C_2 as an example, Bauer and Nowotny have shown[34] that the crystal structure with disordered distribution of the B and C atoms is described by the *P*4/*mmm* space group, the small cell being regarded as only the first approximation to the structure of the borocarbides LnB_2C_2. Judging from the general views about bond lengths and directions, a tetragonal structure with a regular arrangement of B and C atoms (space group *P*4/*mbm* with $a = a_0\sqrt{2}$ and $c = c_0$) has been suggested for the compounds MB_2C_2. Bauer and Nowotny[34] have suggested a more plausible model for the ordering of the boron and carbon atoms in the compounds MB_2C_2 under consideration in relation to yttrium borocarbide YB_2C_2. According to this model, the small tetragonal unit cell with a statistical distribution of the atoms is doubled along the *c* axis, i.e. $a = a_0$ and $c = 2c_0$. In the unit cell thus obtained (space group $P\bar{4}2c$), the metal atoms occupy the 2(*e*) sites, the four boron atoms occupy the 4(*i*) sites with $y = 0.232$, and the four carbon atoms are at the 4(*h*) sites with $x = 0.168$ (Fig. 2).

A study of the crystal structure of LaB_2C_2 carried out by Bauer and Bars[37] has confirmed the validity of the ordering model described above.[34] The diffraction pattern of LaB_2C_2 was interpreted[37] in terms of several models: a small tetragonal unit cell with a disordered distribution of boron and carbon atoms [space group *P*422, $Z = 1$, the B and C atoms occupy the 4(*m*) sites with $x = 0.203$]; a small unit cell with an ordered distribution of nonmetal atoms [space group *Pmmm*, $Z = 1$, the B and C atoms occupy the 2(*p*) and 2(*l*) sites, respectively]; an ordered tetragonal structure with $a = a_0\sqrt{2}$ and $c = c_0$ (space group *P*4/*mbm*, $Z = 2$); and an ordered tetragonal structure (space group $P\bar{4}2c$, $Z = 2$). The latter model proved to be the most successful. This made it possible to conclude that all the borocarbides LnB_2C_2 crystallise with a tetragonal structure (space group $P\bar{4}2c$) with an ordered distribution of the carbon and boron atoms in the lattice. The unit cell parameters of the yttrium and lanthanide borocarbides MB_2C_2 with ordered and disordered distributions of the boron and carbon atoms are listed in Table 3.

Another common structure of scandium, yttrium, and heavy lanthanide borocarbides is MB_2C.[32,34,35] In the case of disordered distribution of the B and C atoms in the borocarbide YB_2C (space group *P*4/*mbm*), four Y atoms occupy the 4(*g*) sites, and twelve boron and carbon atoms are distributed statistically

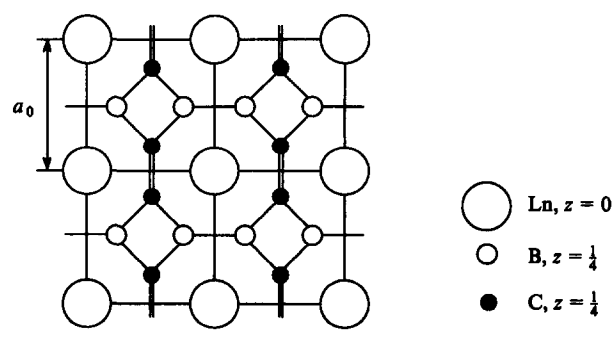


Figure 2. Projection along the [001] axis of the ordered crystal structure of the borocarbides MB_2C_2 of the YB_2C_2 type (space group $P\bar{4}2c$).[34] Only one half of the unit cell is shown; for $z = \frac{1}{4}$, the B–C network is rotated by 90°.

Table 3. Some ternary compounds in borocarbide systems of Group III transition metals and lanthanides.

Compound	Symmetry and type of structure	Space group	Z	Unit cell parameters / nm			Ref.
				a	b	c	
ScB_2C	Tetragonal, the YB_2C type	$P4_2/mbc$	8	0.6651	–	0.6763	32
ScB_2C_2	Orthorhombic	$Pbam$	4	0.5175	1.0075	0.3340	33
YBC	"	$Cmmm$	4	0.3388	1.3693	0.3627	34
Y_2BC_2	Isostructural to $Y_{15}C_{19}$ (?)	–	–	–	–	–	34
YB_2C	Tetragonal (disordered)	$P4/mbm$	4	0.6769	–	0.3715	34
YB_2C	Tetragonal (ordered)	$P4_2/mbc$	8	0.6769	–	0.7430	34
YB_2C	"	$P4_2/mbc$	8	0.6793	–	0.7438	34
YB_2C_2	Tetragonal (disordered)	$P4/mmm$	1	0.3796	–	0.3562	34
YB_2C_2	Tetragonal (ordered)	$P\bar{4}2c$	2	0.3796	–	0.7224	34
YB_2C_2	Tetragonal	–	–	0.3788	–	0.3551	36
CeB_2C_2	"	–	–	0.3817	–	0.3852	36
CeB_2C_2	"	$P\bar{4}2c$	2	0.3817	–	0.7704	37
CeB_2C_4	–	–	–	–	–	–	38
$Ce_5B_2C_6$	Tetragonal	$P4$	4	0.8418	–	1.2077	39
LaBC	–	–	–	–	–	–	40
LaB_2C_2	Tetragonal	$P\bar{4}2c$	2	0.3822	–	0.7924	37
LaB_2C_4	–	–	–	–	–	–	38
$La_5B_2C_6$	Tetragonal	$P4$	4	0.8585	–	1.2313	42
PrB_2C_2	"	–	–	0.382	–	0.381	41
PrB_2C_2	"	$P\bar{4}2c$	2	0.381	7	0.762	37
NdB_2C_2	"	–	–	0.3803	–	0.3794	41
NdB_2C_2	"	$P\bar{4}2c$	2	0.3803	–	0.7588	37
SmB_2C_2	"	–	–	0.3796	–	0.3696	36
SmB_2C_2	"	$P\bar{4}2c$	2	0.3796	–	0.7392	37
EuB_2C_2	"	$P\bar{4}2c$	2	0.3801	–	0.7602	37
GdB_2C_2	"	–	–	0.3792	–	0.3640	36, 41
GdB_2C_2	"	$P\bar{4}2c$	2	0.3792	–	0.7280	37
GdBc	Orthorhombic	$Cmmm$	4	0.4356	0.3796	0.3697	43
$Gd_{0.35}B_{0.45}C_{0.20}$ ($\sim Gd_7B_9C_4$)	–	–	–	–	–	–	41
$Gd_{0.3}B_{0.4}C_{0.3}$ ($\sim GdBC$)	–	–	–	–	–	–	41
$Gd_{0.4}B_{0.35}C_{0.25}$ ($\sim Gd_8B_7C_5$)	–	–	–	–	–	–	41
$Gd_{0.35}B_{0.19}C_{0.46}$ ($\sim Gd_2BC_2$)	Orthorhombic (?)	–	–	0.609	$\geqslant 0.8$	0.856	41
TbB_2C	Tetragonal, the YB_2C type	$P4_2/mbc$	8	0.6791	–	0.7522	35
TbB_2C_2	Tetragonal	–	–	0.3784	–	0.3591	41
TbB_2C_2	"	$P\bar{4}2c$	2	0.3784	–	0.7182	37
DyBC	Orthorhombic	$Cmmm$	4	0.3384	1.3727	0.3647	43
DyB_2C	Tetragonal, the YB_2C type	$P4_2/mbc$	8	0.6788	–	0.7452	35
DyB_2C_2	Tetragonal	–	–	0.3782	–	0.3560	41
DyB_2C_2	"	$P\bar{4}2c$	2	0.3781	–	0.7118	37
HoB_2C	Tetragonal, the YB_2C type	$P4_2/mbc$	8	0.6773	–	0.7399	35, 44
HoB_2C_2	Tetragonal	–	–	0.3780	–	0.3537	41
HoB_2C_2	"	$P\bar{4}2c$	2	0.3780	–	0.7074	37, 44
HoBC	Orthorhombic (high-temperature the YBC type	$Cmmm$	4	0.3384	1.3697	0.3594	44
HoBc	Tetragonal (long-period)	–	–	0.3546	–	4.640	44
Ho_2BC_3	Centred tetragonal (high-temperature)	–	–	0.3561	–	1.2455	44

Table 3 (continued).

Compound	Symmetry and type of structure	Space group	Z	Unit cell parameters / nm			Ref.
				a	b	c	
LaB_2C_2	Tetragonal	–	–	0.3816	–	0.3975	36, 41
Ho_2BC_3	Primitive tetragonal	–	–	0.3567	–	2.4515	44
$Ho_3B_2C_3$	–	–	–	–	–	–	44
$Ho_5B_2C_6$	Tetragonal, the $La_5B_2C_6$ type	$P4$	4	0.7981	–	1.1561	44
$Ho_5B_2C_5$	Tetragonal	–	–	0.8033	–	1.0812	44
$Ho_{15}B_2C_{17}$	Tetragonal (substitution of in $Ho_{15}C_{19}$ by B)	$P\bar{4}2_1c$	2	0.8004	–	1.5984	44
ErB_2C	Tetragonal	$P4_2/mbc$	8	0.6753	–	0.7321	35
ErB_2C_2	"	–	–	0.3778	–	0.3508	41
ErB_2C_2	"	$P\bar{4}2c$	2	0.3778	–	0.7016	37
TmB_2C	Tetragonal, the YB_2C type	$P4_2/mbc$	8	0.6735	–	0.7284	35
TmB_2C_2	Tetragonal	–	–	0.3776	–	0.3477	36
TmB_2C_2	"	$P\bar{4}2c$	2	0.3776	–	0.6954	37
YbB_2C	Tetragonal, the YB_2C type	$P4_2/mbc$	8	0.6724	–	0.7240	35
YbB_2C_2	Tetragonal	–	–	0.3775	–	0.3560	36, 41
YbB_2C_2	"	$P\bar{4}2c$	2	0.3775	–	0.7120	37
LuB_2C	Tetragonal, the YB_2C type	$P4_2/mbc$	8	0.6755	–	0.7178	32
LuB_2C_2	Tetragonal	–	–	0.3762	–	0.3453	36
LuB_2C_2	"	$P\bar{4}2c$	2	0.3762	–	0.7102	37

between the 8(j) and 4(h) sites. In the case of the borocarbides MB_2C with an ordered distribution of the B and C atoms (space group $P4_2/mbc$), the unit cell parameter c is twice as large as that for the disordered unit cell; the Y atoms occupy the 8(g) sites, sixteen boron atoms are arranged at the 8(h) sites of two types, and eight carbon atoms occupy the 8(h) sites.

Phase equilibria in the Y–B–C,[34] Eu–B–C,[31] Gd–B–C,[41] and Ho–B–C[44] systems have been studied; in these systems, four, two, five, and eight ternary compounds, respectively, have been found (Fig. 3). The state diagram for the Y–B–C system has been constructed using the data of an X-ray structural study of samples quenched from a melt. A phase

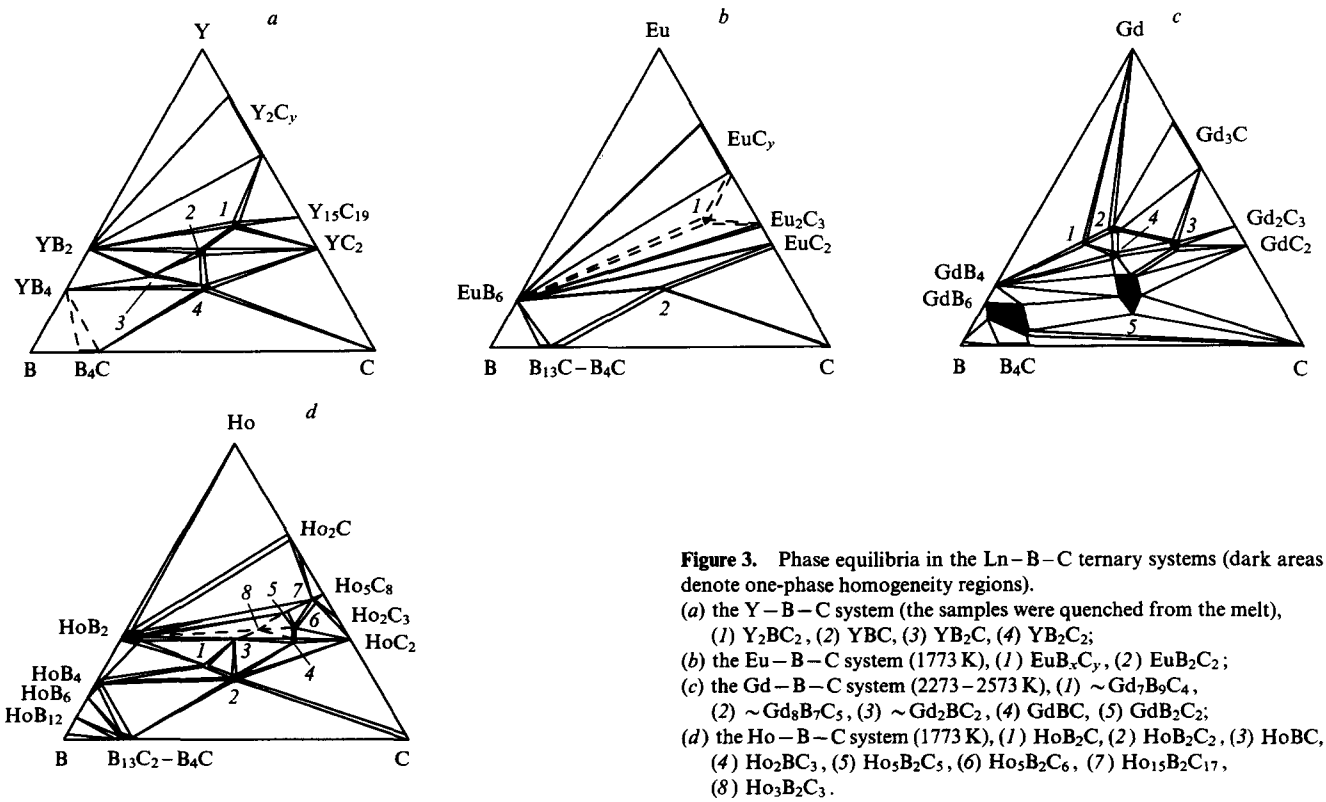


Figure 3. Phase equilibria in the Ln–B–C ternary systems (dark areas denote one-phase homogeneity regions).
(*a*) the Y–B–C system (the samples were quenched from the melt), (*1*) Y_2BC_2, (*2*) YBC, (*3*) YB_2C, (*4*) YB_2C_2;
(*b*) the Eu–B–C system (1773 K), (*1*) EuB_xC_y, (*2*) EuB_2C_2;
(*c*) the Gd–B–C system (2273–2573 K), (*1*) ~$Gd_7B_9C_4$, (*2*) ~$Gd_8B_7C_5$, (*3*) ~Gd_2BC_2, (*4*) GdBC, (*5*) GdB_2C_2;
(*d*) the Ho–B–C system (1773 K), (*1*) HoB_2C, (*2*) HoB_2C_2, (*3*) HoBC, (*4*) Ho_2BC_3, (*5*) $Ho_5B_2C_5$, (*6*) $Ho_5B_2C_6$, (*7*) $Ho_{15}B_2C_{17}$, (*8*) $Ho_3B_2C_3$.

diagram for the Ce – B – C system has been suggested [47] based on thermodynamic estimates; however, only one ternary compound, which was known at that time, was taken into account in this study.

2. Borocarbides of Group IV transition metals

Due to their high stability borides of Group IV transition metals exist in equilibrium with carbon, boron carbide B_4C, and non-stoichiometric monocarbides $M^{IV}C_y$. The mutual solubility of borides and carbides is very low.

The Ti – B – C system. The first version of the state diagram for this system was suggested by Brewer and Haraldsen.[47] According to the thermodynamic calculations made by them, four titanium borides, namely, Ti_2B, TiB, TiB_2, and Ti_2B_5, are formed in this system. The existence of the Ti_2B and Ti_2B_5 phases has not been confirmed reliably in experimental studies. The phase diagram for the Ti – B – C system, commonly accepted at present, has been constructed using the results of a detailed study[48] and has been refined later in another study;[49] this variant has also been presented in a paper by Schouler et al.[50] (Fig. 4). The isothermal cross-section through the Ti – B – C system at 2273 K [51] coincides almost exactly with that presented in Fig. 4*a*.

There is almost no mutual solubility of titanium carbide $TiC_{1.0}$ and titanium diboride TiB_2 at temperatures below 2273 K. When the stoichiometric composition of titanium carbide is disturbed, the solubility of TiB_2 in it increases. In fact, at 1873 K, ~3 mol % of TiB_2 is dissolved in the carbide $TiC_{0.95}$, whereas $TiC_{0.68}$ dissolves ~7 mol % of TiB_2. The increase in the solubility of TiB_2 is in good agreement with the conclusion made by Gusev [2] that an increase in the concentration of structural vacancies creates new interstitial positions and is favourable for the increase in the solubility. Note that the hardness of titanium carbide increases on the addition of TiB_2.

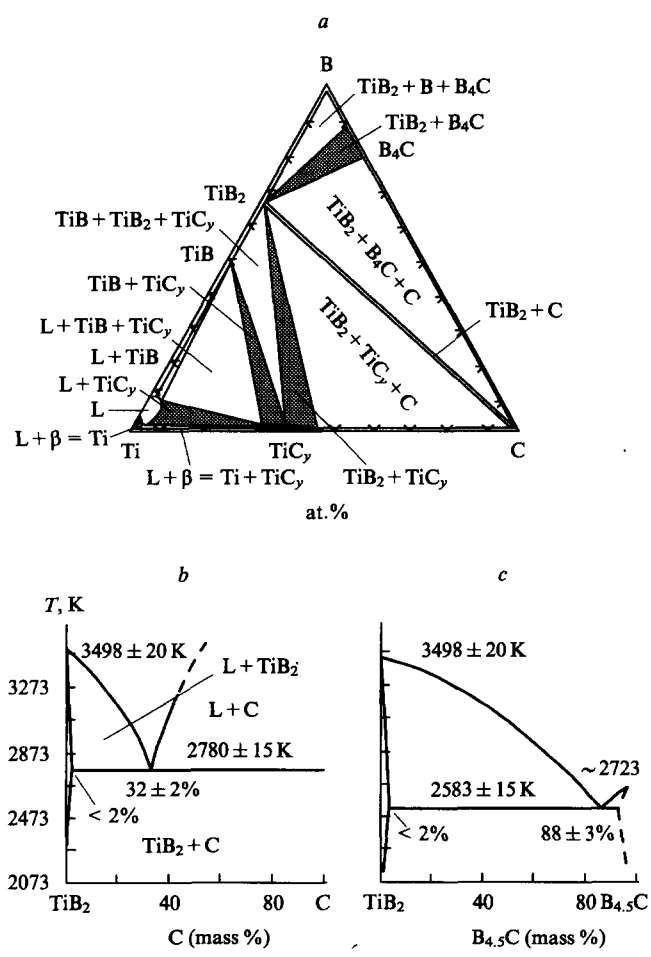


Figure 4. State diagram for the Ti – B – C ternary system and its pseudobinary cross-sections.[49, 50]
(*a*) the isothermal cross-section through the Ti – B – C system at 1873 K (dark areas denote one-phase homogeneity regions); (*b*) polythermal pseudobinary TiB_2 – C cross-section; (*c*) polythermal pseudobinary TiB_2 – $B_{4.5}C$ cross-section.

In the TiC_y – TiB_2, TiB_2 – C, and TiB_2 – B_4C pseudobinary cross-sections, ordinary eutectics at 2900, 2780, and 2600 K, respectively, are formed. The mutual solubility of titanium boride and titanium carbide along the TiC_y – TiB pseudobinary cross-section should most likely be unlimited, if these compounds have identical structures of the *B*1 type, and their unit cells have similar sizes. In the TiC_y – TiB system, there is a possibility of the formation of solid solutions, but it is prevented by the decomposition of TiB at temperatures above 2200 K. [52]

The Zr – B – C system. The state diagram of this system has been studied in a number of papers.[47, 53, 54] The ZrC_y – ZrB_2, ZrB_2 – C, and ZrB_2 – B_4C pseudobinary equilibria were found in the Zr – B – C ternary system; later, their existence has been confirmed experimentally. In addition, the ZrC_y – ZrB equilibrium exists at $T \leqslant 1523$ K and the ZrB_{12} – B_4C equilibrium exists at $T > 1923$ K.[47] ZrB has not been detected.[53] The solubility of ZrB_2 in the carbide ZrC_y increases with an increase in the concentration of structural vacancies in the carbon sublattice of the carbide.

The Hf – B – C system. The phase diagram for the Hf – B – C ternary system was constructed for the first time by Nowotny et al.[53] It proved to be fairly similar to the state diagram of the Ti – B – C system. The HfB – HfC_y, HfB_2 – HfC_y, HfB_2 – C, and ZrB_2 – B_4C pseudobinary equilibria exist in the Hf – B – C system. In the HfB_2 – HfC_y, HfB_2 – C, and ZrB_2 – B_4C pseudobinary cross-sections, ordinary eutectics at temperatures of 3410, 2790, and 2600 K, respectively, are formed. The solubility of HfB_2 in HfC_y increases with an increase in the defectiveness of the carbon sublattice of the carbide.

A general feature of the interaction of boron with titanium, zirconium, and hafnium carbides is the formation of limited MB_xC_{1-x} borocarbide solid solutions. The solubility of boron in carbides increases in the sequence $TiC_y \rightarrow ZrC_y \rightarrow HfC_y$ and with a decrease in the carbon content. Hafnium carbide dissolves up to 6 at.% of boron.

No ternary compounds are formed in the titanium, zirconium, and hafnium borocarbide systems.[47–50, 53–55]

The Th – B – C system. Only binary carbides ThC, ThC_2, and B_4C and borides ThB_4 and ThB_6 exist in this system. There are four pseudobinary phase equilibria in the Th – B – C ternary system, namely, ThC – ThB_4, ThC_2 – ThB_6, ThB_6 – C, and ThB_6 – B_4C.[47] It has been shown by experimental studies that in this system (in contrast to the titanium, zirconium, and hafnium borocarbide systems), four ternary compounds $Th_3B_2C_3$, ThBC, ThB_2C, and $ThBC_2$, are formed (Table 4). They all have homogeneity regions, the homogeneity region of ThBC being fairly large. A state diagram for the Th – B – C system has been reported.[56] Five ternary compounds, namely, ThBC, ThB_2C, $ThBC_2$, Th_2BC, and Th_2BC_2, were found in this diagram (the ternary monoclinic thorium borocarbide $Th_3B_2C_2$ reported in another paper [58] was not taken into account in this diagram). The compounds ThBC and ThB_2C melt congruently at 2370 and 2310 K, respectively.

A characteristic feature of the Th – B – C system is that carbon is almost insoluble in borides, and boron is almost insoluble in carbides.

3. Borocarbides of Group V – VIII transition metals

The ternary systems of Group V transition metals with boron and carbon differ from the analogous systems containing Group IV transition metals in that new binary borides, M_3B_4 and M_3B_2, arise in these systems. No ternary borocarbides of Group V transition metals were detected in the M^V – B – C systems.

Chromium, molybdenum, and uranium form borocarbides with boron and carbon, whereas in the W–B–C system no ternary compounds were detected.

The V–B–C system. The state diagram for the V–B–C system has been constructed by Markovsky et al.[69] In this system, all the carbides and borides are in equilibria with one another: $V_2C_y-V_3B_2$, V_2C_y-VB, VC_y-VB, $VC_y-V_3B_4$, VC_y-VB_2, and VB_2-B_4C. The VB_2-C pseudobinary equilibrium also exists. The solubility of boron in vanadium carbides is low, but it is somewhat higher than the solubility of carbon in vanadium borides.

The Nb–B–C system. This system involves the same phase equilibria as the V–B–C system.[69] The NbC_y-NbB_2 pseudobinary cross-section is eutectic with an eutectic temperature of ~2900 K. The solubility of boron in the carbide NbC_y increases with a decrease in y and can reach 5 at.%. The hardness of the niobium carbide NbC_y increases noticeably on the dissolution of boron.

The Ta–B–C system. In this system, the existence of borides Ta_2B and Ta_3B, in addition to the borides TaB_2, Ta_3B_4, and TaB, which are also characteristic of the V–B–C and Nb–B–C systems, has been reported.[47] Later, the existence of Ta_2B has been confirmed, and the boride Ta_3B_2 has also been found. The existence of Ta_3B has not been confirmed. The Ta–B–C system, unlike the V–B–C and Nb–B–C systems, involves one more pseudobinary equilibrium, namely, $Ta_2C_y-Ta_2B$. The TaC_y-TaB_2 pseudobinary cross-section has a eutectic at a temperature of ~3000 K. The solubility of boron in TaC_y increases with an increase in the concentration of carbon vacancies and can reach 6 at.%. The solubility of carbon in TaB_2 is no more than 2 at.%. The dissolution of boron in TaC_y leads to a substantial increase in the microhardness.

The Cr–B–C system. Chromium carbides, in contrast to carbides of other transition metals, can dissolve substantial quantities of boron. This is caused by the significant differences between the crystal structures of chromium carbides and carbides of other transition metals. For example, at 1723 K, about 30% of the carbon can be substituted by boron in the carbide $Cr_{23}C_6$, about 36% in Cr_7C_3, and about 5% in Cr_3C_2.[29] The state diagram for the Cr–B–C ternary system has been constructed;[70] however, the phase relationships in the region rich in carbon and boron have been studied inadequately. Chromium forms four ternary phases with boron and carbon, namely, the $Cr_3(B,C)_2$, $Cr_7(B,C)_3$, and $Cr_{23}(B,C)_6$ solid solutions and the compound Cr_7BC_4 (see Table 4).

The boron atoms and some of the carbon atoms in Cr_7BC_4 fill the trigonal prismatic interstices and the rest are arranged in the octahedral vacancies of the metal sublattice.[60] This compound is stable in the temperature range 1820 K–1980 K. A neutron-diffraction study has shown that the borocarbide Cr_7BC_4 has a filled structure of the Re_3B type (space group *Cmcm*) (Fig. 5), which is also peculiar to other ternary compounds (for example, zirconium and hafnium aluminidonitrides).[61] In the borocarbide

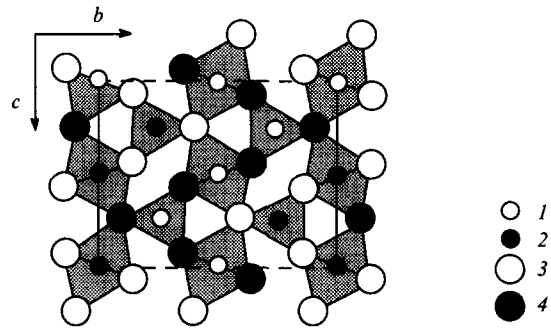


Figure 5. Projection along the [001] axis of the crystal structure of the Re_3B type (space group *Cmcm*).
(*1*, *2*) nonmetal atoms located at heights $x = 0$ and $x = \frac{1}{2}$, respectively; (*3*, *4*) metal atoms located at heights $x = 0$ and $x = \frac{1}{2}$, respectively.

Table 4. Some ternary compounds in borocarbide systems of Group IV and Group VI–VIII transition metals.

Compound	Symmetry and type of structure	Space group	Z	Unit cell parameters/ nm			Ref.
				a	b	c	
ThBC	Tetragonal	$P4_122$	8	0.3762	–	2.5246	56, 57
$Th_3B_2C_3$	Monoclinic	$P2/m$	1	0.3703	0.9146	0.3773[a]	58
ThB_2C	Hexagonal	$P6/mmm$	3	0.3868	–	0.3810	56
ThB_2C	Trigonal (rhombohedral)	$R\bar{3}m$	9	0.6676	–	1.1376	59
$ThBC_2$	–	–	–	–	–	–	56
Cr_7BC_4	Orthorhombic filled structure of the Re_3B type	$Cmcm$	4	0.2870	0.9260	0.6982	60
$Cr_3(B_{0.44}C_{0.56})C_{0.85}$	"	$Cmcm$	4	0.2857	0.9233	0.6967	61
Mo_2BC	Orthorhombic	$Cmcm$	4	0.3086	1.735	0.3047	62
UBC	Monoclinic	$C2/m$	4	0.3591	1.195	0.3372	57
UBC	Orthorhombic	$Cmcm$	4	0.3591	1.195	0.3372	63
UBC	"	$Cmcm$	4	0.3591	1.1985	0.3348	64
UB_2C	Trigonal, the ThB_2C type (high-temperature modification)	$R\bar{3}m$	9	0.6535	–	1.0781	64
$U_5B_2C_7$	Tetragonal, the $La_5B_2C_6$ type (?)	–	–	–	–	–	64
$Mn_{23}C_3B_3$	Cubic, the $Cr_{23}C_6$ ($D8_4$) type, a solid solution of boron in $Mn_{23}C_6$	$Fm3m$	4	1.071	–	–	65
Mn_7BC_2	Orthorhombic, a solid solution of boron in Mn_7C_3	$Pnma$	4	0.4521	0.6986	1.2099	31
$Fe_{23}C_3B_3$	Cubic, the $Cr_{23}C_6$ ($D8_4$) type	$Fm3m$	4	1.0594	–	–	67
$Fe_3(B,C)$ $(Fe_3C_{0.2}B_{0.8})$	Orthorhombic, the cementite Fe_3C ($D0_{11}$) type	$Pnma$	4	–	–	–	68
$Co_{11}B_2C$	Cubic, the $Cr_{23}C_6$ ($D8_4$) type	$Fm3m$	8	1.047	–	–	69

[a] In the unit cell $\beta = 100.06°$.

Cr_7BC_4 with the Re_3B type of structure, the carbon atoms at the 4(*b*) sites populate 85% of the octahedral interstices, and the rest of the carbon atoms together with the boron atoms share the 4(*c*) sites at the centres of trigonal prisms. Thus, the more exact structural formula of this compound should be written as $Cr_3(B_{0.44}C_{0.56})C_{0.85}$.

The Mo–B–C system. The possible phase equilibria in the Mo–B–C system were first estimated by a thermodynamic calculation.[47] According to this estimate, six pseudobinary phase interactions exist in this system, and ternary compounds are absent. More recently,[69] the Mo–B–C phase diagram has been made substantially more precise.

One ternary compound Mo_2BC with a small homogeneity region and an orthorhombic structure (space group *Cmcm*) of its own type (see Table 4), typical also of a number of other ternary compounds discussed in this review, is formed in this system. The structure of Mo_2BC is a combination of the boride and carbide sublattices (Fig. 6). The carbon atoms are located at the centres of the octahedra formed by the molybdenum atoms. The CMo_6 octahedra are connected to one another by eight edges and form double-stranded octahedral layers. The boron atoms in Mo_2BC linked in zigzag-shaped chains are arranged between the octahedral layers. Each boron atom is located at the centre of a trigonal prism, molybdenum atoms serving as the vertices of the prism. This distribution of boron atoms is specific and typical of transition metal monoborides. This gives grounds for regarding the borocarbide Mo_2BC as a derivative of β-MoB in which the octahedral interstices of the molybdenum sublattice are occupied by carbon atoms.

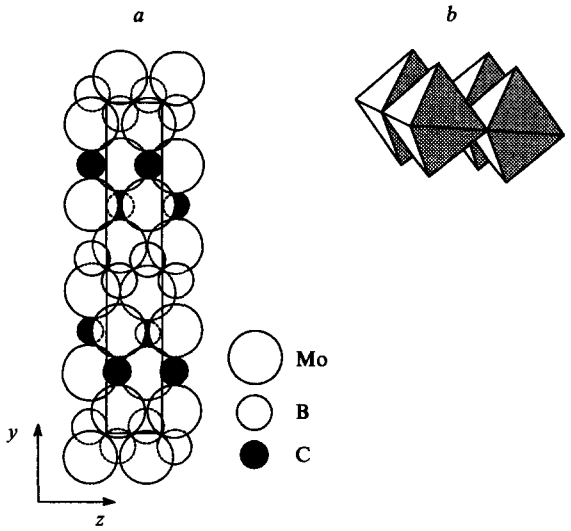


Figure 6. Crystal structure of Mo_2BC (space group *Cmcm*).
(*a*) projection along the [100] axis (the wholly visible atoms are located at height $x = 0$; the atoms that are partly seen are located at height $x = \frac{1}{2}$); (*b*) the layer of the CMo_6 octahedra joined through their edges, parallel to the (010) plane; in Mo_2BC, these layers are joined in pairs in such a way that each octahedron is linked to the neighbouring octahedra via its eight edges.

At 1573 K, three borides Mo_2B, MoB, and Mo_2B_5, molybdenum carbide Mo_2C, boron carbide B_4C, and ternary compound Mo_2BC exist in the Mo–B–C system. The following equilibria are established between these compounds: $Mo_2B–Mo_2C$, $MoB–Mo_2C$, $MoB–Mo_2BC$, $MoB–C$, $Mo_2BC–Mo_2C$, $Mo_2BC–C$, $Mo_2B_5–B_4C$, and $Mo_2B_5–C$. At 2073 K, the $Mo_2B_5–C$ equilibrium disappears, since the boride MoB_2 arises, and the $MoB_2–C$ equilibrium is established; in addition, carbide Mo_3C_2 arises distinct from Mo_2C; 1–2 at.% of boron dissolves in both carbides. Boron stabilizes the high-temperature carbide phases of molybdenum. The $MoB_2–C$ and $MoB–C$ pseudobinary cross-sections are eutectic systems.

The W–B–C system. This system contains only binary tungsten carbides W_2C and WC, tungsten borides W_2B, WB, and W_2B_5, and boron carbide B_4C.[47] Tungsten borides WB_{12}[69] and WB_4[49,50] have also been detected. The existence of the boride WB_4 is more probable. Six pseudobinary cross-sections, namely, $W_2B–W_2C$, $W_2B–WC$, $WB–WC$, $WB–C$, $W_2B_5–C$, and $W_2B_5–B_4C$ contain ordinary eutectics with temperatures 2640, 2560, 2600, 2630, 2550, and 2500 K, respectively.[49] In all probability the $WB_4–B_4C$ pseudobinary cross-section is also an eutectic system.

The U–B–C system. The phase equilibria in this system have been studied.[63,64] It was originally believed that the U–B–C system contains one ternary compound UBC (see Table 4) with an extended homogeneity region, which exists at 1573 K in equilibrium with UC, UC_2, C, UB_2, and UB_4. In addition, there are $UC–UB_2$, $UB_4–C$, $UB_4–B_4C$, and $UB_{12}–B_4C$ pseudobinary equilibria. The ternary borocarbide UBC lies at the $UC_2–UB_2$ pseudobinary cross-section. The distribution of the carbon and boron atoms in this orthorhombic phase is intermediate between those in the tetragonal carbide UC_2 and the hexagonal boride UB_2.

In a more recent study of the U–B–C system, two other ternary compounds UB_2C and $U_5B_2C_7$ have been detected, apart from UBC (see Table 4). The isothermal cross-section through the U–B–C system at 1873 K at an argon pressure of 1×10^5 Pa has been constructed by Rogl et al.[64] The phase equilibria at 1273, 1673, 1873, and 2073 K are virtually identical. The high-temperature modification of UB_2C has a structure of the ThB_2C type and has a narrow homogeneity region; with an increase in carbon content the unit cell volume of U_2BC somewhat decreases. At temperatures below 1900 K, the low-temperature modification of UB_2C is formed; its structure is unknown. The compound $U_5B_2C_7$ probably has a tetragonal structure similar to that of $La_5B_2C_6$.[42] The temperatures of the congruent melting of UBC and UB_2C are 2420 ± 25 K and 2550 ± 30 K, respectively. The borocarbide UB_2C exists in equilibrium with UBC, UB_4, and C, and $U_5B_2C_7$ is in equilibrium with UBC, UC, and UC_2.

The Mn–B–C system. Among the ternary systems formed by boron and carbon with manganese, technetium, and rhenium, only the Mn–B–C system has been studied fairly extensively. An isothermal cross-section through the manganese-rich part of the phase diagram of this system at 1073 K has been reported.[65] At 1073 K the borocarbide formed on the dissolution of boron in the cubic carbide $Mn_{23}C_6$ has the composition $Mn_{23}C_{4.6}B_{1.4}$ (a = 1.064 nm), and at 1273 K, its composition is $Mn_{23}C_3B_3$. The dissolution of boron in the carbide Mn_7C_3 at 1273 K yields the Mn_7BC_2 ternary phase (see Table 4).[65,66] At 1273 K the boride Mn_4B exists in equilibrium with $Mn_{23}C_3B_3$ and Mn_7BC_2, MnB is in equilibrium with Mn_7BC_2 and C; two other equilibria, namely, $Mn_3B_4–C$ and $Mn_3B_4–B_4C$, also exist in the system.[71]

The borocarbide $Mn_{23}C_3B_3$ has a structure of the $Cr_{23}C_6$ type, which is also typical of the iron borocarbide $Fe_{23}B_3C_3$, the cobalt borocarbide $Co_{11}B_2C$, and some other ternary compounds.

The unit cell of the carbide $Cr_{23}C_6$ and the borocarbides $Mn_{23}C_3B_3$ and $Fe_{23}B_3C_3$ (space group *Fm3m*) is a cube including 4 formula units, i.e. 92 metal atoms and 24 atoms of the nonmetals. Each metal atom occupies a cube vertex and is surrounded by 12 metal atoms constituting a cubooctahedron. Similar cuboctahedra formed by 12 metal atoms surround the centre of each face of the cube. Eight metal atoms occupy the 8(*c*) and equivalent sites and the remaining metal atoms are at the 32(*f*) sites and form simple cubes surrounding the middle of each unit cell edge. Each nonmetal atom in compounds with the $Cr_{23}C_6$ type of structure is surrounded by eight metal atoms located at the vertices of a tetragonal antiprism.

Among ternary systems of boron and carbon with Group VIII transition metal, only the Fe–B–C system has been studied in detail. In the Co–B–C system, a ternary compound $Co_{11}B_2C$ has been found (see Table 4).[69]

The Fe–B–C system. Iron forms a carbide Fe_3C (cementite) and borides Fe_2B and FeB. Up to 80 at.% of the carbon in Fe_3C can be substituted by boron; carbon is markedly soluble in both borides. Two ternary compounds $Fe_{23}C_3B_3$ and $Fe_3(B,C)$ have been found in this system (see Table 4). Boron introduced to the cementite Fe_3C can replace not only the carbon atoms, but also the iron atoms, the boron atoms being predominantly distributed over the crystallographic planes of cementite.[68] The borocarbide $Fe_{23}C_3B_3$ (the τ-phase) having fairly extended homogeneity regions both for boron and carbon has been studied most thoroughly. The borocarbide $Fe_{23}C_3B_3$ melts congruently. As the temperature increases, the homogeneity region of the τ-phase decreases, and at 1240 K, the τ-phase decomposes to give the γ-phase (austenite) and $Fe_3(B,C)$.[73]

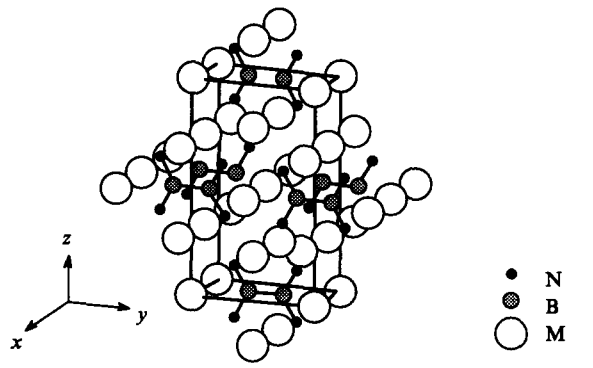


Figure 7. Orthorhombic structure of the lanthanide boronitrides $M_3B_2N_4$ (M = La, Ce, Pr, Nd) of the $(W_2Co)B_2\square_4$ type (space group *Immm*).[74]

III. M–B–N ternary boronitride systems

The properties of the boronitride systems of transition metals are largely similar to those of the borocarbide systems. For a long time, no ternary compounds were found in the M–B–N systems; however, since 1983, several boronitrides of lanthanides and also a ternary compound in the Nb–B–N system were detected (Table 5). The phase equilibria in the M–B–N ternary systems have been analysed in a number of studies.[80–83]

Rogl et al.,[74] who have studied ternary systems containing lanthanides, boron, and nitrogen, have found a family of new ternary lanthanum, cerium, praseodymium, and neodymium boronitrides $M_3B_2N_4$ with the orthorhombic structure of the W_2CoB_2 type. In the M–B–N-systems (M = Sc, Y, Gd → Lu), the $M_3B_2N_4$ ternary phases are not formed. The boronitride $Nd_3B_2N_4$ is unstable at temperatures above 1673 K. The structure of boronitrides $M_3B_2N_4$ can be regarded as a variant of the $(W_2Co)B_2\square_4$ filled structure. The boron atoms in this structure are located in trigonal prisms consisting of six metal atoms and form B–B pairs; in addition, each boron atom is bound to two nitrogen atoms (Fig. 7). In turn, the nitrogen atoms of $M_3B_2N_4$ occupy the 8(*l*) sites, which are vacant in $(W_2Co)B_2\square_4$. In other words, the nitrogen atoms are located in the distorted octahedral interstices and are surrounded by five metal atoms (the M atoms are in the vertices of a rectangular pyramid) and by one boron atom, i.e. NM_5B groups are formed. There are no direct N–N interactions in the structure of the boronitrides $M_3B_2N_4$.

Ternary compounds MBN_2 of the same type have been found in the M–B–N systems (M = Pr, Nd, Sm, Gd) (see Table 5). The boronitride $GdBN_2$ is stable only at $T > 1763$ K.[76] The boronitride $Ce_{15}B_8N_{25}$ has been detected in the Ce–B–N system.[75] Scandium, yttrium, and lanthanides from Tb to Lu do not form compounds MBN_2.[81] In the M–B–N systems (M = Tb → Lu, Y), the boron nitride BN exists in equilibrium with a metal nitride MN and with all the existing borides beginning with MB_4 and ending with MB_{66}, and MN coexists with borides MB_2 and MB_4; in the Sc–B–N system, there are only two borides, ScB_2 and ScB_{12}, existing in equilibrium with BN; and ScN is in equilibrium with ScB and BN.[63] The mutual solubilities of boron nitride and lanthanide borides and nitrides are extemely limited.[81]

Table 5. Some ternary compounds in boronitride systems of transition metals.

Compound	Symmetry and type of structure	Space group	*Z*	Unit cell parameters / nm			Ref.
				a	*b*	*c*	
$La_3B_2N_4$	Orthorhombic, filled structure of the W_2CoB_2 type	*Immm*	2	0.3634	0.6414	1.0974	74
$Ce_3B_2N_4$	"	*Immm*	2	0.3565	0.6316	1.0713	74
$Ce_{15}B_8N_{25}$	Trigonal (rhombohedral)	$R\bar{3}c$	2	1.0946[a]	–	–	75
$Pr_3B_2N_4$	Orthorhombic, filled structure of the W_2CoB_2 type	*Immm*	2	0.3540	0.6310	1.0795	74
$PrBN_2$	Trigonal (rhombohedral)	*R3c*	18	1.2114	–	0.7013	76
$Nd_3B_2N_4$	Orthorhombic, filled structure of the W_2CoB_2 type	*Immm*	2	0.3520	0.6278	1.0756	74
$NdBN_2$	Trigonal (rhombohedral)	*R3c*	18	–	–	–	76
$NdBN_2$	Monoclinic	$P2_1/m$ or $P2_1/c$	10	0.6950	1.2077	0.5856[b]	77
$SmBN_2$	"	$P2_1/m$ or $P2_1/c$	10	0.6897	1.1928	0.5783[c]	77
$SmBN_2$	Trigonal (rhombohedral)	*R3c*	18	–	–	–	76
$GdBN_2$	"	*R3c*	18	–	–	–	76
Nb_2BN	Orthorhombic	*Cmcm*	4	0.3172	1.7841	0.3114	78, 79
$Nb_{2-x}V_xBN$	"	*Cmcm*	4	0.3172	1.7841	0.3113	78
$Nb_{2-x}Ta_xBN$	"	*Cmcm*	4	0.3171	1.7846	0.3114	78

[a] In the unit cell $\alpha = 82.96°$. [b] In the unit cell $\beta = 99.32°$. [c] In the unit cell $\beta \approx 99.84°$.

The Ti–B–N system. Studies of the phase equilibria in ternary systems containing Group IV transition metals, boron, and nitrogen have shown that no ternary compounds are formed in these systems. According to thermodynamic data,[47] six pseudobinary equilibria are possible in the Ti–B–N system, namely, TiN_y–Ti_2B, TiN_y–TiB, TiN_y–TiB_2, TiB_2–N, TiB_2–BN, and Ti_2B_5–BN. There are no reliable experimental data supporting the existence of the borides Ti_2B and Ti_2B_5. The phase diagram for the Ti–B–N system has been constructed by Nowotny et al.[48] Four binary compounds, namely, TiB, TiB_2, TiN_y, and BN, exist in this system; ternary compounds are absent. The titanium nitride TiN_y exists in equilibrium with the borides TiB and TiB_2 and with BN. The lower boride TiB is in equilibrium with the solid solution of nitrogen in α-Ti and the higher boride TiB_2 is in equilibrium with BN. The solubility of boron in the titanium nitride is low, but it is higher than that in the carbide TiC_y. When the composition of nitride TiN_y deviates from the stoichiometric composition, the solubility of boron in it increases. The solubility of nitrogen in titanium borides is negligibly small. The TiN_y–BN equilibrium at a nitrogen pressure of 0.05 MPa exists only below 1900 K, and at $T > 1900$ K, the boride TiB_2 exists in equilibrium with nitrogen.[47]

The Zr–B–N system. The phase equilibria in this system have been investigated in a number of studies.[47,54,84] Brewer and Haraldsen[47] suggested the existence of three zirconium borides, ZrB, ZrB_2, and ZrB_{12}, therefore, five possible pseudobinary equilibria, ZrN_y–ZrB, ZrN_y–ZrB_2, ZrB_2–N, ZrB_2–BN, and ZrB_{12}–BN, were considered in the Zr–B–N system. ZrB_2 is the main boride phase of zirconium. In this system, four binary equilibria exist: zirconium diboride exists in equilibrium with the solid solution of nitrogen and boron in α-Zr and with the nitrides ZrN_y and BN; and the nitride ZrN_y is in equilibrium with BN. The latter equilibrium can exist at a pressure of nitrogen of 0.05 MPa (0.5 atm) up to a temperature of 1820 K; at $T > 1820$ K, the zirconium diboride ZrB_2 exists in equilibrium with nitrogen.[47] The solubility of boron in zirconium nitride ZrN_y is much higher than that in TiN_y, and it increases from 8 at.% to 25 at.% as the composition of the zirconium nitride varies from $ZrN_{1.00}$ to $ZrN_{0.55}$.

The Hf–B–N system. In the state diagram of the Hf–B–N ternary system, the borides HfB and HfB_2 exist in an equilibrium with the solid solution of nitrogen and boron in α-Hf. The HfB_2–HfN_y, HfB_2–BN, and HfB_2–N equilibria exist in this system [the latter exists at a nitrogen pressure of more than 0.1 MPa (1 atm)].[84] The solubility of boron in the nitride HfN_y at the lower boundary of the homogeneity region reaches 40–50 at.%. The solubility of nitrogen in HfB and HfB_2 is low, but it is higher than that in the titanium and zirconium borides.

The V–B–N system. The phase equilibria in the V–B–N ternary system have been studied by Spear et al.[85] (Fig. 8*a*). No ternary compounds exist in this system, but there are eight binary compounds including five borides (V_3B_2, VB, V_3B_4, V_2B_3, and VB_2), two vanadium nitrides (V_2N_y and VN_y), and one boron nitride (BN). At a pressure of nitrogen of 0.1 MPa (1 atm), eight pseudobinary equilibria are possible in the V–B–N system depending on the temperature, namely, VB–BN, V_3B_2–V_2N_y, VB–V_2N_y, VB–VN_y, V_3B_4–BN, V_2B_3–BN, VB_2–BN, and VN_y–BN. The central three-phase VB + BN + VN_y field exists at $T < 2010$ K, the VB + BN + V_3B_4 field exists at $T < 2180$ K, and the V_3B_4 + BN + V_2B_3 and V_2B_3 + BN + VB_2 fields exist at $T < 2290$ K.[84] Boron is hardly soluble in vanadium nitrides, and nitrogen is almost insoluble in vanadium borides.

The Nb–B–N system. The phase equilibria in this system have been studied in a number of works.[78,79,86] The Nb–B–N system is the only one among the boronitride systems of Group V–VIII transition metals in which ternary compounds have been found. Rogl et al.[79] have constructed an isothermal cross-section through the Nb–B–N system at 1473 K and a pressure of argon of 1×10^5 Pa (Fig. 8*b*). The phase equilibria in this system involve three ternary compounds, among which Nb_2BN is formed most easily (at 1473 K). The other two ternary compounds were observed in the NbB–Nb_2BN–BN region. The boronitride Nb_2BN exists in equilibrium with ε-NbN, δ-NbN, γ-Nb_4N_3, BN, and NbB; besides, the niobium nitride β-Nb_2N coexists with Nb_3B_2 and NbB; γ-Nb_4N_3 coexists with the boride NbB, and boron nitride is in equilibrium with ε-NbN, Nb_3B_4, and NbB_2.

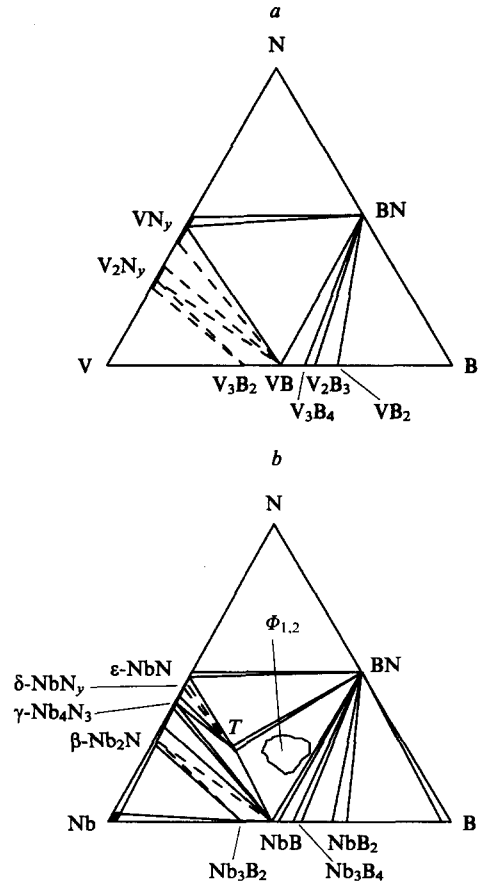


Figure 8. Isothermal cross-sections through the M–B–N (M = V, Nb) ternary systems at 1473 K.
(*a*) the V–B–N system at a nitrogen pressure of 1×10^5 Pa (dark areas denote one-phase homogeneity regions);[85] (*b*) the Nb–B–N system at an argon pressure of 1×10^5 Pa [T = Nb_2BN, $\Phi_{1,2}$ is the designation for two (or more) unknown ternary phases, observed in the BN + Nb_2BN + NbB region].[79]

The crystal structure of only one of the ternary compounds, Nb_2BN_{1-x}, has been determined.[78,79] This compound has a very narrow homogeneity region and the orthorhombic structure of the Mo_2BC type (space group *Cmcm*).[78] The structure of the boronitride Nb_2BN is shown in Fig. 9. The boron atoms are located at the centres of trigonal prisms formed by six niobium atoms, and

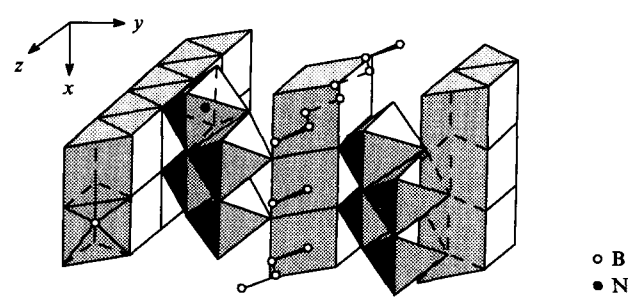


Figure 9. Crystal structure of Nb_2BN (the Mo_2BC type, space group *Cmcm*).[78]

the seventh niobium atom is located at the centre of one of the square faces of the prism. The nitrogen atoms in Nb_2BN occupy the octahedral interstices of the niobium sublattice. The boron atoms are joined in zigzag-shaped chains parallel to the c axis; the N–N and N–B bonds are missing. Similar compounds V_2BN and Ta_2BN could not be obtained even by the thermobaric treatment (pressure 65×10^8 Pa, temperature 1273 K). The boronitride Nb_2BN forms limited solid solutions with V and Ta, $Nb_{2-x}V_xBN$ ($x \approx 0.1$) and $Nb_{2-x}Ta_xBN$ ($x \approx 0.2$). The substitution of niobium by vanadium or tantalum is accompanied by a slight decrease in the unit cell volume.

The Ta–B–N system. In this system, boron is insoluble in nitrides and nitrogen is insoluble in borides.[86]

The Cr–B–N system. The phase equilibria in ternary systems of Group VI–VIII transition metals with boron and nitrogen have not been adequately studied. The Cr–B–N system involves eight pseudobinary equilibria:[47] Cr_4B–N, Cr_2B–N, Cr_5B_3–N, CrB–N, Cr_3B_4–N, CrB_2–N, CrB_2–BN, and Cr_2B_5–BN. Three additional pseudobinary equilibria are possible at a nitrogen pressure of 0.05 MPa. The CrN–BN equilibrium can exist at temperatures below 1300 K, Cr_2N–BN exists from 1300 K to 1500 K, and the Cr–BN equilibrium exists from 1500 K to 2000 K. An experimental study has confirmed the absence of ternary compounds in the Cr–B–N system and has shown the existence of one more chromium nitride, Cr_3N.[87] Later it was shown that at 1873 K and a nitrogen pressure of 0.1 MPa, the Cr_2B–Cr_2N, Cr_2B–N, Cr_5B_3–N, and Cr_5B_3–BN pseudobinary equilibria are observed in the Cr–B–N system.[29]

The W–B–N system. In this system, at a nitrogen pressure of 0.05 MPa, the tungsten borides W_2B (at $T > 1600$ K), WB, and W_2B_5 exist in equilibrium with nitrogen; a W_2B_5–BN pseudobinary equilibrium also exists.[47] At the same nitrogen pressure, the W_2B–BN and WB–BN equilibria as well as the W–BN equilibrium (at $T < 1600$ K) are also possible. Only binary compounds are formed in the W–B–N system.[87] Boron is virtually insoluble in tungsten nitrides, and nitrogen is virtually insoluble in tungsten borides.

The Fe–B–N system. Studies of the phase equilibria in the Fe–B–N–system[87,88] have shown the presence of binary compounds Fe_2B, FeB, Fe_2N (ζ), Fe_3N (ε), Fe_4N (γ'), and BN. Nitrogen is insoluble in iron borides, and boron is insoluble in iron nitrides.

IV. Phase relationships in the Si-containing M–B–Si, M–Si–C, and Me–Si–N systems

1. The common type of structures of ternary Si-containing compounds

The ternary systems of transition metals with boron and silicon are of interest as refractory materials resistant to the oxidation at high temperatures. The similarity of the structures of silicides and borides facilitates their mutual solubility and the formation of ternary compounds. The phase equilibria in the M–B–Si systems have been studied.[89–100]

An investigation of doping of high-melting silicides with boron, carbon, nitrogen, and oxygen[89] and some more recent studies[90–92] have shown that in all the M–Si–X systems (M is a transition metal, X = B, C, N, O) a number of ternary phases are formed on the basis of the silicides M_5Si_3, namely, M_5Si_3X or $M_5Si_3X_2$ with hexagonal structure of the Mn_5Si_3 type ($D8_8$) and/or M_5SiX_2 [the Cr_5B_3 type (α-Nb_5Si_3) (T_2 — $D8_l$)], and M_5Si_2X [the W_5Si_3 type (β-Nb_5Si_3) (T_1 — $D8_m$)].

The hexagonal filled structure of the Mn_5Si_3 type (the $D8_8$ structural type, space group $P6_3/mcm$) (Fig. 10) is characteristic of many transition metal silicoborides, carbosilicides, and silicononitrides M_5Si_3X as well as for aluminocarbides and aluminonitrides. It is likely to be the commonest structure of ternary compounds in the M–X–X′ systems being considered. Its unit cell incorporates two M_5Si_3X formula units. The transition atom metals M occupy the 4(d) and 6(g) sites in this structure.

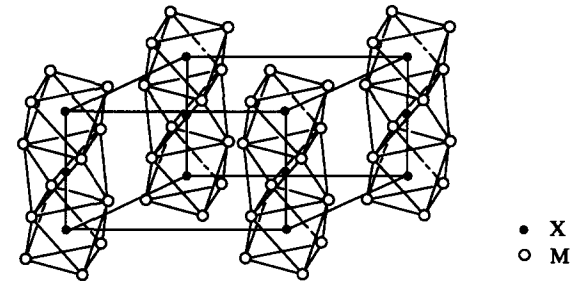


Figure 10. Filled crystal structure of the Mn_5Si_3 ($D8_8$) type of the ternary compounds M_5Si_3X (space group $P6_3/mcm$). Only the transition metal atoms M at the 6(g) sites and the interstitial nonmetal atoms X at the 2(b) sites forming the XM_6 octahedra are shown. The XM_6 octahedra are linked to one another through two faces and form columns directed along the [001] axis.

The silicon atoms also occupy the 6(g) sites, but with other coordinates, and are located within distorted trigonal prisms constituted by two metal atoms at the (d) sites and four metal atoms at the (g) sites. The M atoms located at the 6(g) sites form octahedra; the nonmetal atoms X (C, N, O) can be arranged inside these octahedra at the 2(b) sites (see Fig. 10). Each XM_6 octahedron is joined with two neighbouring octahedra through its opposite faces; thus, parallel chains of octahedra are formed along the c axis. An important characteristic feature of the phases with the $D8_8$ structure is the presence of a broad homogeneity region, since the interstitial atoms can occupy not all the octahedra, but only some of them.

The M_5Si_2X tetragonal phases of the W_5Si_3 type [β-Nb_5Si_3, the $D8_m$ (T_1) structural type] and M_5SiX_2 of the Cr_5B_3 type [α-Nb_5Si_3, the $D8_l$ (T_2) structural type] belong to the same space group $I4/mcm$ (D_{4h}^{18}) and have very similar structures. Their unit cells incorporate 4 formula units each, i.e. 20 metal atoms and 12 nonmetal atoms. A characteristic feature of the structure of these phases is that the silicon atoms at the 8(h) sites are isolated and form the localised Si–Si pairs. These phases may be regarded as resulting from the substitution of silicon in the silicides M_5Si_3 by the X atoms.

It is of interest that the tetragonal silicides M_5Si_3 are very sensitive to admixtures of the C, B, N, and O nonmetal atoms; their introduction leads to the transition to ternary phases with the Mn_5Si_3 ($D8_8$) type of structure. When this transformation takes place, the X nonmetal atoms occupy the octahedral interstices of the metal sublattice, whereas the displaced silicon atoms occupy the points in the metal sublattice. In the tetragonal silicoborides M_5Si_2B (T_1), the boron atoms occupy the vacant positions in the silicon sublattice, whereas the silicon atoms replace some of the metal atoms in the metal sublattice.

Phases with the $D8_8$ structure are stabilised most effectively by carbon and somewhat less effectively by boron, they are very slightly stabilised by nitrogen and not at all by oxygen.

2. The ternary M–B–Si silicoboride systems

The ternary phases formed in the M–B–Si systems are presented in Table 6. Typically, boron possesses substantial initial solubility in all the M_5Si_3 phases with the $D8_8$, $D8_m$, and $D8_l$ structures. The addition of boron to pure silicides leads to an expansion of the $D8_8$ lattice caused by the intercalation of boron to the vacant points of the silicon sublattice and to the compression of the T_1 and T_2 lattices due to the direct substitution of the silicon atoms by boron.

The Ti–B–Si system. This system involves four titanium borides Ti_2B, TiB, TiB_2, and Ti_2B_5 and three titanium silicides Ti_5Si_3, TiSi, and $TiSi_2$.[8] No reliable experimental data on the temperature-dependent concentration ranges for the existence of the borides Ti_2B and Ti_2B_5 have been reported. In all probability, the TiB–TiSi, TiB_2–$TiSi_2$, and TiB_2–Si (or Ti_2B_5–Si)

Table 6. Some ternary compounds in silicoboride systems of Group IV–VIII transition metals.[89–100]

Compound	Symmetry	Type of structure[a]	Unit cell parameters / nm		
			a	*b*	*c*
$Ti_5Si_3(B)$	Hexagonal	$D8_8$	–	–	–
$Zr_5Si_3(B)$	"	$D8_8$	0.7788	–	0.5558
$Hf_5Si_3(B)$	"	$D8_8$	0.789	–	0.556
$V_5Si_3B_{0.45}$	"	$D8_8$	0.718	–	0.489
V_5SiB_2	Tetragonal	$D8_l(T_2)$	0.581	–	1.079
$Nb_5Si_3B_2$	Hexagonal	$D8_8$	0.754	–	0.525
$Ta_5Si_3B_2$	"	$D8_8$	0.747	–	0.523
Cr_5Si_3B	"	$D8_8$	0.706	–	0.473
Mo_5SiB_2	Tetragonal	$D8_l(T_2)$	0.601	–	1.103
$W_5(Si,B)_3$	"	$D8_l(T_2)$	0.6047	–	1.009
Mn_5SiB_2	"	$D8_l(T_2)$	0.561	–	1.044
Fe_5SiB_2	"	$D8_l(T_2)$	0.554	–	1.032
$Fe_3Si_{0.2}B_{0.8}$	Orthorhombic	$D0_{11}$	0.446	0.536	0.666
$Fe_{4.8}Si_2B$	Tetragonal	$D8_m(T_1)$	0.882	–	0.434
$Co_{4.7}Si_2B$	"	$D8_m(T_1)$	0.862	–	0.425
Ni_6Si_2B	Hexagonal	$C22$	0.6105	–	0.2895

[a] $D8_8$ is a filled structure of the Mn_5Si_3 type (space group $P6_3/mcm$), $Z = 2$; $D8_l(T_2)$ is a structure of the Cr_5B_3–α-Nb_5Si_3 type (space group $I4/mcm$), $Z = 4$; $D0_{11}$ is a structure of the Fe_3C type (space group $Pnma$), $Z = 4$; $D8_m(T_1)$ is a structure of the W_5Si_3 – β-Nb_5Si_3 type (space group $I4/mcm$), $Z = 4$; $C22$ is a structure of the Fe_2P type (space group $P\bar{6}2m$), $Z = 3$.

pseudobinary equilibria exist in the Ti–B–Si system. The existence of the ternary hexagonal silicoboride Ti_5Si_3B formed from Ti_5Si_3 via the substitution of a minor portion (~1–2 at.%) of the silicon atoms by the boron atoms is also quite probable.

The Zr–B–Si system. The state diagram of the Zr–B–Si ternary system (Fig. 11) shows eight binary zirconium compounds.[93] They include three borides ZrB, ZrB_2, and ZrB_{12} and five silicides Zr_2Si, Zr_5Si_3 (Zr_3S_2), Zr_4Si_3, ZrSi, and $ZrSi_2$. The existence of the boride ZrB at 1623 K is doubtful, because it is stable only within a narrow temperature range and decomposes already at 1500 K. In addition, the silicon borides SiB_3, SiB_4, and SiB_6 are not shown in the diagram. In the zirconium diboride ZrB_2 up to 20 at.% of boron can be substituted by silicon, i.e. a limited solid solution of $ZrSi_2$ in ZrB_2, namely $Zr(B,Si)_2$, is formed. An important characteristic feature of the Zr–B–Si system is the presence of the ternary hexagonal compound $Zr_5Si_3(B)$ containing from 5 to 8 at.% of boron. The phase diagram of this system (see Fig. 11) exhibits ten pseudobinary equilibria, namely, $Zr(B,Si)_2$–Zr, $Zr(B,Si)_2$–ZrSi, $Zr(B,Si)_2$–$Zr_5Si_3(B)$, $Zr(B,Si)_2$–$ZrSi_2$, $Zr(B,Si)_2$–Si, $Zr_5Si_3(B)$–Zr, $Zr_5Si_3(B)$–Zr_2Si, $Zr_5Si_3(B)$–Zr_3Si_2, $Zr_5Si_3(B)$–Zr_4Si_3, and $Zr_5Si_3(B)$–ZrSi. In all probability, three more pseudobinary equilibria of $Z(B,Si)_2$ with the silicon borides SiB_3, SiB_4, and SiB_6 also exist.

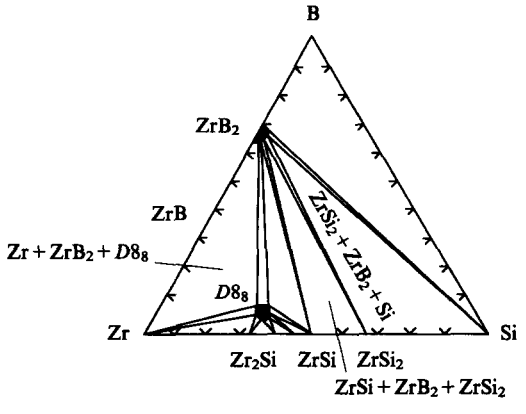


Figure 11. Isothermal cross-section through the Zr–B–Si system at 1623 K (dark areas denote one-phase homogeneity regions).[93]

The Hf–B–Si system. This system includes the borides HfB and HfB_2, the silicides Hf_5Si_3, HfSi, and $HfSi_2$, and compound $Hf_5Si_3(B)$ with a minor (2–3 at.%) content of boron, which substitutes silicon.[8]

The V–B–Si system. The V–B–Si ternary system has been studied.[90,91] Kudielka et al.[90] suggested a scheme for the triangulation of the V angle (V–VB–VSi) of the state diagram of the V–B–Si system, which incorporates two ternary compounds, namely, $V_5Si_3B_{0.45}$ with a hexagonal lattice and V_5SiB_2 (the T_2 type) with a tetragonal lattice (see Table 6). The former of these compounds crystallises with the $D8_8$ structural type and is formed via partial substitution of the silicon atoms in the silicide V_5Si_3 by boron atoms. Six pseudobinary equilibria exist in the system, namely, V_2B–V_5SiB_2, VB–V_5SiB_2, V_3Si–V_5SiB_2, $V_5Si_3B_{0.45}$–V_5SiB_2, V_3Si–$V_5Si_3B_{0.45}$, and V_5Si–$V_5Si_3B_{0.45}$. One may expect that six more pseudobinary equilibria, VB–$V_5Si_3B_{0.45}$, VSi_2–$V_5Si_3B_{0.45}$, VB–VSi_2, V_3B_4–VSi_2, VB_2–VSi_2, and VB_2–Si, will be found.

The Nb–B–Si system. The state diagram of the Nb–B–Si system has been studied rather comprehensively.[92] This system incorporates ten binary compounds (the niobium borides Nb_3B_2, NbB, Nb_3B_4, and NbB_2, the niobium silicides Nb_4Si, Nb_5Si_3, and $NbSi_2$, and the silicon borides SiB_3, SiB_4, and SiB_6) and two ternary compounds based on Nb_5Si_3, namely, Nb_5Si_3B with the $D8_8$ structure and Nb_5SiB_2 with the $D8_l$ structure. Both ternary compounds have fairly extended homogeneity regions, and the nonmetal sublattice of these silicoborides can contain a substantial number of vacancies, apart from the boron and silicon atoms. The boride NbB_2 which has a homogeneity region can dissolve up to 2 at.% of silicon.

The Ta–B–Si system. The phase diagram of state of the Ta–B–Si ternary system has been studied.[90,94] It is very similar to the state diagram of the Nb–B–Si system, but differs from it by the greater numbers of binary compounds (twelve) and ternary compounds (three). Two ternary phases (of the $D8_8$ and T_2 types) are based on the silicide Ta_5Si_3 and the third one is based on Ta_2Si.

The Cr–B–Si system. This system contains six chromium borides, four chromium silicides, and two ternary phases with the $D8_8$ and T_1 structures; the phase with the T_2 structure is a limited solid solution of silicon in the boride Cr_5B_3.[95] The Cr_5Si_3B ternary phase (the $D8_8$ type) (see Table 6) has virtually no homogeneity region.

The Mo–B–Si system. The phase equilibria in this system (Fig. 12*a*) have been studied in a number of works.[91,96,97] The state diagram of the Mo–B–Si system is simpler than the analogous diagram for the system containing chromium, since it incorporates a smaller number of binary compounds. There are two ternary phases with structures of the T_1 and T_2 types, but the ternary phase with the $D8_8$ type of structure is missing. It has been shown that silicon is insoluble in the molybdenum borides Mo_2B, MoB, Mo_2B_5, and boron does not dissolve in $MoSi_2$.[97]

The W–B–Si system. Two ternary phases exist in this system: $W_{10}Si_3B_3$ [$W_5(Si,B)_3$] with the T_2 type of structure and W_5Si_2B with the T_1 type of structure (Fig. 12*b*).[91]

The Mn–B–Si system. In the Mn–B–Si system, the ternary compound Mn_5SiB_2 with the tetragonal structure of the T_2 type (see Table 6) existing in an equilibrium with the hexagonal silicide Mn_5Si_3 has been found.[99]

The Fe–B–Si system. The phase equilibria in this system have been studied in detail in the Fe-angle of the state diagram.[98,99] Four ternary phases were discovered, namely, Fe_5SiB_2 with the structure of the T_2 type and with a small homogeneity region formed on the B ↔ Si mutual substitution; $Fe_{4.8}Si_2B$ with the T_1 type of structure; $Fe_3(Si,B)$ (with the composition $Fe_3Si_{0.2}B_{0.8}$) with the cementite Fe_3C structure and with a small homogeneity

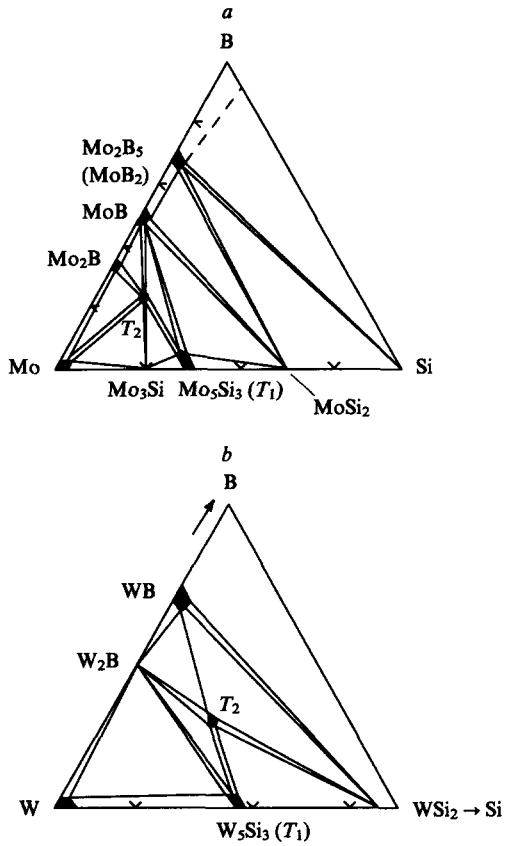


Figure 12. Isothermal cross-sections through the Mo–B–Si system at 1873 K (*a*) and through the W–B–Si system at 2073 K (*b*); dark areas denote one-phase homogeneity regions.[91]

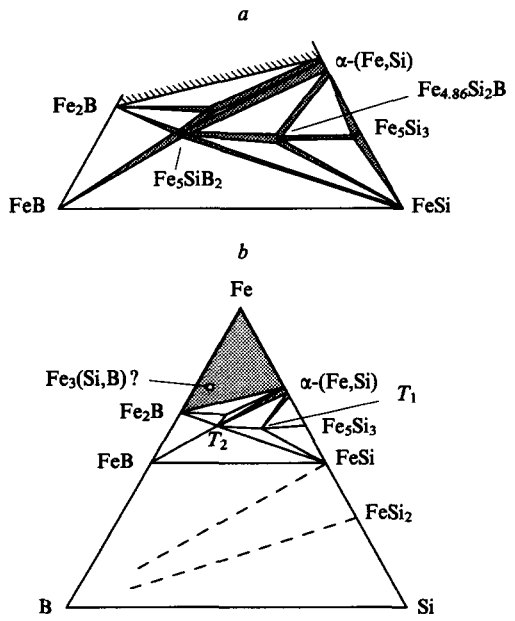


Figure 13. State diagram and isothermal cross-section for the Fe–B–Si system at 1273 K; dark spots denote one-phase regions, two-phase regions are cross-hatched).[99]
(*a*) a cross-section in the silicoboride region with iron contents ranging from 50 to 70 at.%; (*b*) the contours of the state diagram for the whole Fe–B–Si ternary system.

region; and $Fe_2(Si,B)$ (with the composition $Fe_2Si_{0.4}B_{0.6}$), the structure of which is unknown (Fig. 13). It was found that a minor amount of boron can be dissolved in Fe_5Si_3. The other binary iron borides and silicides are absolutely insoluble in one another.

The Co–B–Si system. Only one ternary phase $Co_{4.7}Si_2B$ with the T_1 type of structure and a small homogeneity region is formed in this system. It exists in an equilibrium with the cobalt borides CoB and Co_2B and with the cobalt silicides CoSi and Co_2Si; in addition, there are the CoB–CoSi and Co_2B–Co_2Si pseudobinary equilibria.[98]

The Ni–B–Si system. The ternary compound Ni_6Si_2B with a hexagonal structure of the *C*22 type, isomorphous to the phosphides Mn_2P, Fe_2P, and Ni_2P, has been found in this system (see Table 6).

3. The M–Si–C ternary carbosilicide systems

The atomic radius of carbon is small (~0.077 nm); therefore, carbon always acts as the interstitial element in compounds with transition metals and is located in the interstices of the metal sublattice. Silicon, which is an analogue of carbon in the Periodic System, has a substantially larger atomic radius, equal to ~0.117 nm. In compounds with Group IV and V transition metals, the atoms of which are fairly large, silicon can act as an interstitial element; silicides of other transition metals occupy an intermediate position between interstitial compounds and intermetallic compounds. Thus, silicon can enter into the metal lattice either as an interstitial element or as a substituting element. The same dual behaviour of silicon is exhibited in transition metal carbosilicides.

The ternary hexagonal phases of the $M_5Si_3(C)$ type, similar to the $M_5Si_3(B)$ silicoboride ternary phases with the filled structure of the Mn_5Si_3 type ($D8_8$) are characteristic of the majority of the M–Si–C systems. The main ternary carbosilicide phases are

Table 7. Some ternary compounds in carbosilicide systems of Group IV–VIII transition metals.

Compound	Unit cell parameters / nm			Ref.
	a	*b*	*c*	
$Ti_5Si_3C_x$	–	–	–	89, 101–103
Ti_3SiC_2 [a]	0.3064–0.3068	–	1.7646–1.7669	104–106
$Zr_5Si_3C_x$	0.7914–0.7909	–	0.5559–0.5579	89, 107
$V_5Si_3C_x$	0.7135	–	0.4842	107
$Nb_5Si_3C_x$	0.7536	–	0.5249	107
$Ta_{4.8}Si_3C_{0.5}$	0.7494	–	0.5242	108
$Cr_{5-x}Si_{3-y}C_{x+y}$	0.6993	–	0.4726	109
$Cr_{5\pm0.2}Si_{3\pm0.1}C_x$ (0.25 < *x* < 1.05)	0.6980–0.6983	–	0.4726–0.4737	110
$Mo_{5-x}Si_{3-y}C_{x+y}$	0.7285	–	0.5030	109
$Mo_{4.8}Si_3C_{0.6}$	0.7286	–	0.5046	111
Mo_5Si_3C	0.7303	–	0.5057	112
$W_{5-x}Si_{3-y}R$ [b]	0.7205	–	0.4850	109
$U_3Si_2C_3$ [c]	0.3598	0.3535	1.896	113, 114
$U_{20}Si_{16}C_3$ [c]	1.0385	–	0.8013	113, 115
$U_3Si_2C_x$ [c]	0.7306	–	0.3901–0.3942	116
$Mn_5Si_3C_x$	0.6915	–	0.4823	117
Mn_8Si_2C	–	–	–	117
Mn_5SiC	–	–	–	117

Note. All the ternary compounds listed in the Table, except for Mn_8Si_2C and Mn_5SiC (the structures of which are unknown), Ti_3SiC_2, and uranium ternary phases, have hexagonal filled structure of the Mn_5Si_3 ($D8_8$) type with space group $P6_3/mcm$, $Z = 2$. [a] This compound crystallises with a hexagonal structure and with space group $P6_3/mmc$, $Z = 2$. [b] $R = (C,N,O)_{x+y}$. [c] $U_3Si_2C_3$ has the orthorhombic symmetry, $Z = 2$; $U_{20}Si_{16}Si_3$ crystallises with the hexagonal symmetry, $Z = 1$; $U_3Si_2C_x$ is a tetragonal (space group $P4/mbm$) solid solution of carbon in U_3Si_2, $Z = 2$.

listed in Table 7. The phase diagrams for a number of M–Si–C ternary systems have been surveyed.[101–103]

a. Carbosilicides of Group IV–VI transition metals

The Ti–Si–C system. The kinetics and thermodynamics of the reactions of titanium silicides with carbon were studied for the first time by Kudielka et al.[90] They found that the titanium carbide TiC_y exists in equilibrium with the silicon carbide SiC and the titanium silicides Ti_5Si_3, TiSi, and $TiSi_2$, whereas SiC is in equilibrium with $TiSi_2$. It has been shown[89] that the addition of carbon stabilizes the Ti_5Si_3 hexagonal phase and leads to the formation of a ternary phase $Ti_5Si_3C_x$, which contains[101] up to 11 at.% of carbon. The Ti_5Si_3C phase belongs to the group of ternary silicoborides and carbosilicides M_5Si_3X with the hexagonal structure of the $D8_8$ type. The Ti–Si–C system includes one more ternary compound, Ti_3SiC_2, with a hexagonal structure (space group $P6_3/mmc$) (Fig. 14).[101–103] In this compound, the carbon atoms occupy the octahedral vacancies in the octahedra formed by the titanium atoms. Each CTi_6 octahedron is joined to the neighbouring octahedra through its nine edges in such a way that one octahedral layer is superimposed onto another (see Fig. 14*b*). A half of all the titanium atoms are located in the middle of the double octahedral layer and each of these atoms is shared by six octahedra. The remaining titanium atoms are located on the upper and lower surfaces of the double octahedral layer, and each of them is shared by three neighbouring octahedra. The chemical formula of the double octahedral layer is Ti_3C_2. The octahedral layers contain open and closed tetragonal interstices, the open tetragonal vacancies of one double octahedral layer being located over the same vacancies of another double octahedral layer. The silicon atoms are arranged halfway between the centres of the tetrahedral vacancies of the neighbouring double octahedral layers and also constitute a layer.

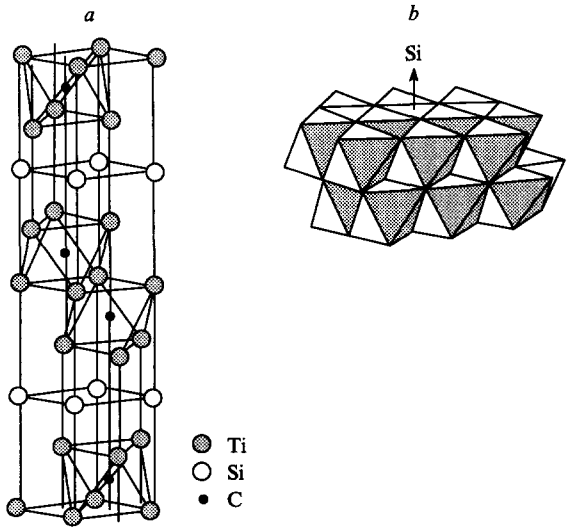


Figure 14. Crystal structure of the titanium carbosilicide Ti_3SiC_2.
(*a*) unit cell (space group $P6_3/mmc$) with distinct CTi_6 octahedra; (*b*) the double layer of the CTi_6 octahedra joined via nine edges; the silicon atoms are arranged over the centres of the open tetrahedral vacancies.

The carbosilicide Ti_3SiC_2 exists in equilibrium with the carbides TiC_y and SiC, with the disilicide $TiSi_2$, and with the Ti_5Si_3C ternary phase. The phase equilibria in the Ti–Si–C system at 1373 K and 1523 K have been studied.[118,119] The ternary compounds and multiphase materials present in the Ti–Si–C system have been investigated by Auger spectroscopy.[120] The isothermal cross-sections through the Ti–Si–C system at 1473 K[121] and 1523 K[118,119] are very similar. At a lower temperature of 1373 K, titanium silicide Ti_3Si appears. It exists in equilibrium with Ti_5Si_3C and with the solid solution of Si and C in β-Ti.

A schematic phase diagram for the Ti–Si–C system, which does not take into account the actual existing ternary phases has been reported.[122]

The compatibility of phases in the Ti–Si–C system at 1473–1773 K has been studied under the conditions of confining compression at a pressure of $(1-2) \times 10^8$ Pa.[123] At high pressures, the titanium silicide Ti_3Si becomes stable and dissolves up to 9 at.% of carbon (without external pressure, Ti_3Si decomposes at the same temperatures to give TiC_y, Ti_5Si_3, and a solid solution of silicon and carbon in titanium). It is of interest that at high pressures carbon is insoluble in the silicide Ti_5Si_3, although under ambient conditions the solubility of carbon in this compound reaches 11 at.%.

The Zr–Si–C system. The first scheme for the triangulation of the phase diagram for the Zr–Si–C ternary system has been suggested by Brewer and Krikorian.[108] According to the data obtained by Nowotny et al.,[89] the silicide Zr_5Si_3 dissolves a substantial amount of carbon to give the $Zr_5Si_3C_x$ ternary phase. The Zr–Si–C system incorporates seven binary compounds (the carbides ZrC_y and SiC and the silicides Zr_2Si, $Zr_5Si_3(Zr_3Si_2)$, Zr_5Si_4, ZrSi, and $ZrSi_2$) and one ternary phase $Zr_5Si_3C_x$. The silicon carbide exists in equilibrium with ZrC_y, $ZrSi_2$, and ZrSi, whereas the zirconium carbide ZrC_y is in equilibrium with SiC, ZrSi, Zr_2Si, and $Zr_5Si_3C_x$.[101] Pseudobinary equilibria connect the ternary phase also to the silicides Zr_2Si, $Zr_5Si_3(Zr_3Si_2)$, Zr_5Si_4, and ZrSi. The isothermal cross-section at 1573 K through the Zr–Si–C ternary system has been studied.[124]

The Hf–Si–C system. According to a number of studies,[101–103] the phase diagrams for this system and for the system discussed above are similar. The existing differences are due to the fact that the hafnium carbide HfC_y is in equilibrium with $HfSi_2$; therefore, the SiC–HfSi pseudobinary equilibrium is missing. Taking into account the data on the stabilisation by carbon of hexagonal phases with the Mn_5Si_3 type of structure ($D8_8$) and also the similarity of the phase diagrams for Hf–Si–C and Zr–Si–C, one may assume that the Hf–Si–C system contains a $Hf_5Si_3C_x$ ternary phase.

The V–Si–C system. In the V–C, Nb–C, and Ta–C binary systems, rhombohedral ζ-phases of the composition M_4C_3 are formed in narrow concentration and temperature intervals ($1200\ K < T < 1800\ K$).[125,126] The carbides ζ-M_4C_3 cannot be isolated as individual phases, therefore equilibria involving these compounds are not discussed in the ternary carbosilicide systems of vanadium, niobium, and tantalum. Vanadium forms three silicides, namely, V_3Si, V_5Si_3, and VSi_2. The dissolution of up to 10 at.% of carbon in V_5Si_3 leads to the formation of the $V_5Si_3C_x$ ternary phase.[101,107] It exists in an equilibrium with the carbides SiC and VC_y and with the silicides V_5Si_3 and VSi_2. In addition, five pseudobinary equilibria, $SiV-VS_2$, $SiV-VC_y$, $VC_y-V_5Si_3$, $V_2C_y-V_5Si_3$, and $V_2C_y-V_3Si$, exist in the V–Si–C system. The phase diagrams for the V–Si–C ternary system have been reported.[122,127]

The Nb–Si–C system. In this system, the carbide NbC_y is in equilibrium with two silicides $NbSi_2$ and Nb_5Si_3, with the silicon carbide SiC,[101,108] and with the $Nb_5Si_3C_x$ ternary phase.[107] The quantity of carbon dissolved in the $Nb_5Si_3C_x$ phase is likely to be less than that dissolved in the analogous $V_5Si_3C_x$ phase. The $Nb_5Si_3C_x$ ternary phase is in equilibrium with NbC_y and with the niobium silicides $NbSi_2$ and Nb_5Si_3, whereas the carbides SiC and Nb_2C_y are in equilibrium with $NbSi_2$ and Nb_5Si_3, respectively. The phase diagram for the Nb–Si–C ternary system has been reported by Brukl.[121]

The Ta–Si–C system. The phase equilibria in this system have been studied repeatedly.[89,101,108,127] The isothermal cross-sections through the phase diagram of the Ta–Si–C system at 1273 K,[127] 1823 K,[89] and 1873 K[89] are virtually identical. All the workers noted that the $Ta_5Si_3C_x$ ($Ta_{4.8}Si_3C_{0.5}$) ternary phase with the hexagonal structure of the Mn_5Si_3 type ($D8_8$) exists in this

system.[108] This phase is isomorphous to the hexagonal silicide Ta_5Si_3 stabilised by carbon (the pure silicide Ta_5Si_3 has a tetragonal structure) and forms a continuous series of solid solutions with it. The $Ta_5Si_3C_x$ phase is in an equilibrium with the carbides TaC_y and Ta_2C_y and with the silicides Ta_2Si, Ta_5Si_3, and $TaSi_2$. The system also includes five pseudobinary equilibria: $SiC-TaSi_2$, $SiC-TaC_y$, TaC_y-TaSi_2, $Ta_2C_y-Ta_2Si$, and $Ta_2C_y-Ta_3Si$.

The Cr–Si–C system. At 1673 K, eight binary compounds (SiC, Cr_3C_2, Cr_7C_3, $Cr_{23}C_6$, $CrSi_2$, CrSi, Cr_5Si_3, and Cr_3Si),[110] the $Cr_5Si_3C_x$ ternary phase having a homogeneity region,[109,110] a solid solution of silicon in chromium Cr(Si), and a substitution solid solution based on the silicide Cr_3Si exist in this system. The $Cr_5Si_3C_x$ ternary phase has the hexagonal structure of the $D8_8$ type and exists in an equilibrium with silicon carbide SiC, chromium carbides Cr_3C_2 and Cr_7C_3, chromium silicides CrSi and Cr_5Si_3, and the substitution solid solution based on Cr_3Si. The solid solution based on Cr_3Si exists in equilibrium with the carbides Cr_7C_3 and $Cr_{23}C_6$ and with the solid solution of silicon in chromium Cr(Si). In addition, there are four equilibria, namely, $SiC-CrSi_2$, $SiC-CrSi$, $SiC-Cr_3C_2$, and $Cr_{23}C_6-Cr(Si)$. The diagram of the phase equilibria in the Cr–Si–C system has been reported.[122]

Parthe et al.[109] believed that the $Cr_5Si_3C_x$ ternary phase results from the substitution of chromium and silicon atoms by carbon. However, later it was shown[110] that the unit cell parameters and the unit cell volume of the $Cr_{5\pm0.2}Si_{3\pm0.1}C_x$ ternary phase ($0.25 < x < 1.05$) increase with an increase in x. This means that the carbon atoms do not replace Cr or Si atoms, as was believed previously,[109] but are located in the vacant octahedral interstices of the structure of the $D8_8$ type of this compound. Evidence that the carbon atoms fill the octahedral interstices of the metallic sublattice of the $M_5Si_3C_x$ phases with the $D8_8$ type of structure has also been obtained in another study.[111]

The Mo–Si–C system. The first variant of the phase diagram for the Mo–Si–C ternary system has been suggested by Brewer and Krikorian.[108] This diagram reflects fairly adequately all the characteristic features of this system including the existence of a stable ternary hexagonal compound with an extended homogeneity region and a temperature of congruent melting of ~2340 K. The composition Mo_4Si_3C has been suggested for this compound. This ternary compound exists in equilibrium with carbon, with the carbides SiC, MoC_y (Mo_3C_2), and Mo_2C, and with the silicides $MoSi_2$ and Mo_5Si_3 (Mo_3Si_2); SiC is in equilibrium with $MoSi_2$, and Mo_2C is in equilibrium with Mo_5Si_3 (Mo_3C_2) and Mo_3Si.[128]

It has been shown[112] that the ternary molybdenum carbosilicide has the stoichiometric composition Mo_5Si_3C and belongs to the M_5Si_3X type of ternary hexagonal phases common for the M–Si–X systems (X = B, C, N); the homogeneity region of Mo_5Si_3C is much narrower than has been found by Nowotny et al.[128] The isothermal cross-section through the Mo–Si–C system at 1473 K has been reported.[112] According to this study, at 1473 K, the silicon carbide SiC exists in equilibrium with Mo_5Si_3, and the $MoSi_2-Mo_5Si_3C_x$ pseudobinary equilibrium is absent.

The reason for the discrepancies between the results obtained by Van Loo et al.[112] and Nowotny et al.[128] concerning these pseudobinary equilibria can be elucidated by additional investigations of the phase relationships in the Mo–Si–C system. The isothermal cross-section through the Mo–Si–C system at 1873 K[128] virtually coincides with the cross-section at 1673 K reported by Spear et al.[85]

It has been suggested[109] that the carbon atoms in the ternary molybdenum carbosilicide $Mo_{5-x}Si_{3-y}C_{x+y}$ substitute the molybdenum and silicon atoms; however, it has been shown in another study[111] that such a substitution does not occur, and the carbon atoms are located in the octahedral interstices formed by the molybdenum atoms.

The W–Si–C system. In this system, no ternary compounds exist;[108] however, when a minor amount of nitrogen or oxygen is present, a quasi-ternary hexagonal phase $W_{5-x}Si_{3-y}(C,N,O)_{x+y}$ arises.[109] In the absence of nitrogen or oxygen admixtures, the pseudobinary equilibria existing in the W–Si–C system at 2073 K involve only binary compounds: $SiC-WSi_2$, $SiC-W_5Si_3$, SiC–WC, $WC-W_5Si_3$, and $W_2C-W_5Si_3$.[49] The conclusion reached by Parthe et al.[109] that the tungsten and silicon atoms in the ternary phase have been substituted by interstitial atoms (C, N, O) was erroneous, since the carbon and nitrogen atoms in the compounds M_5Si_3X with the $D8_8$ structure behave as interstitial elements and are arranged in octahedral interstices formed by the metal atoms.[110,111]

The U–Si–C system. The phase equilibria in this system at 1000–1773 K under an argon atmosphere have been investigated.[113] Two ternary compounds $U_3Si_2C_3$ and $U_{20}Si_{16}C_3$ with orthorhombic and hexagonal crystal lattices, respectively, have been found in the U–Si–C system (see Table 7).[114,115] It has also been shown[113,116] that the silicide U_3Si_2 dissolves up to 4 at.% of carbon thus forming the $U_3Si_2C_x$ interstitial solid solution. At 1100 K (Fig. 15) the ternary compound $U_3Si_2C_3$ exists in the U–Si–C system in equilibrium with UC, SiC, and U_3Si_5; SiC is in equilibrium with U_2C_3, UC, U_3Si_5, USi_2, and USi_3; UC coexists with U_3Si, $U_3Si_2C_x$, $U_{20}Si_{16}C_3$, and U_3Si_5; the carbosilicide $U_{20}Si_{16}C_3$ coexists with $U_3Si_2C_x$, USi, and U_3Si_5; and U_3Si exists in equilibrium with $U_3Si_2C_x$.

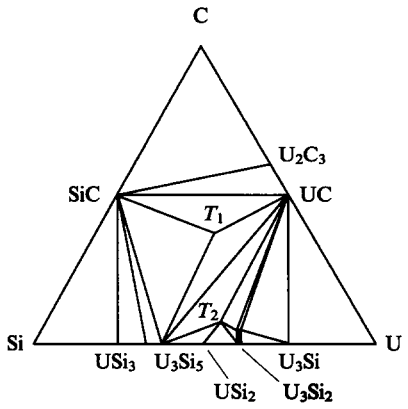


Figure 15. Isothermal cross-section through the U–Si–C system at 1100 K (*the dark area denotes the homogeneity region of the* $U_3Si_2C_x$ solid solution).[113]
$T_1 = U_3Si_2C_3$, $T_2 = U_{20}Si_{16}C_3$.

Later the phase equilibria in the alloys with large proportions of uranium have been studied at 1023–1223 K.[116] At temperatures below 1090 K, the phase equilibria in the U–UC–USi region were the same as those in the diagram shown in Fig. 15. At 1100–1150 K, the UC–U_3Si pseudobinary equilibrium disappears and the U–$U_3Si_2C_x$ equilibrium appears instead and, at temperatures above 1200 K, the silicide U_3Si and the $U_3Si-U_3Si_2C_x$ equilibrium do not exist.[116,129] According to the data obtained by Guinet et al.,[116] the solubility of carbon in U_3Si_2 reaches 4 at.%. On the dissolution of carbon, the c parameter of the unit cell of U_3Si_2 increases by 0.0042 nm thus becoming equal to 0.3942 nm. The maximum solubility of carbon in the U_3Si silicide at 1083 K is 0.15 at.%.[130]

b. Carbosilicides of Group VII and VIII transition metals

The Mn–Si–C system. The phase diagram for this system (Fig. 16*a*), in addition to eight binary compounds, contains the $Mn_5Si_3C_x$ ternary phase (a solid solution of carbon in Mn_5Si_3), Mn_8Si_2C, and Mn_5SiC.[101–103] Silicon carbide exists in equilibrium with the silicides $Mn_{15}Si_{26}$ and MnSi, with the $Mn_5Si_3C_x$ and Mn_8Si_2C ternary phases, and perhaps with Mn_5SiC. The unit cell parameters of the $Mn_5Si_3C_x$ ternary phase are larger than the corresponding unit cell parameters of Mn_5Si_3;[107] this implies that

the carbon atoms are located in the octahedral interstices formed by the manganese atoms. The $Mn_5Si_3C_x$ hexagonal phase with a structure of the $D8_8$ type is in equilibrium with MnSi, Mn_5Si_3, Mn_3Si, Mn_9Si_2, and Mn_8Si_2C; and the Mn_8Si_2C phase coexists with Mn_9Si_2. The pseudobinary equilibria involving the Mn_5SiC ternary phase are given hypothetically. The scheme of phase equilibria in the Mn–Si–C system have been reported by Lyakishev et al.[122]

The Re–Si–C system. This system contains no ternary phases.[101–103,131] The scheme of triangulation of the phase diagram of the Re–Si–C system at 1873 K suggested by Searcy and Finnie [131] involves four pseudobinary equilibria of the silicon carbide SiC with rhenium and three rhenium silicides. Figure 16*b* presents the isothermal cross-section through this system at 1273 K constructed using published data;[101–103] rhenium silicides are in equilibrium with carbon, and SiC coexists with $ReSi_2$.

Jeitschko et al.,[117] who have studied the phase equilibria in the M–Ga–C and M–Ge–C systems, also have paid attention to the M–Si–C systems (M = Mn, Re, Fe). In the Re–Si–C system they discovered a ternary phase containing 45 at.% Re, 40 at.% Si, and 15 at.% C; the structure of this phase was not determined. There is no other evidence in support of the existence of a ternary phase in this system.

The Fe–Si–C system. The phase relationships in the Fe–Si–C system have been considered in many studies, because they are related to the problems of the production of cast iron, steel, various iron-based alloys, and refractory materials. The equilibrium and nonequilibrium phase transformations in the Fe–C system become substantially more complicated on the addition of silicon, since the silicon atom is much larger than the carbon atom.

When silicon substitutes iron, the ferrite solid solution is stabilised and the γ-region (solid solution of C and Si in Fe) narrows. At the same time this substitution promotes decomposition and graphitisation of the cementite Fe_3C. In all probability, the Fe–Si–C system contains no stable ternary phase. The information concerning ternary iron carbosilicides (for example, a ternary phase of an unknown composition of the type of the Nowotny phase with the $D8_8$ structure has been observed in this system;[117] and the carbosilicide $Fe_{10}Si_2C_3$ containing about 9 mass % of silicon has been mentioned in a monograph [8]) refers most probably to a metastable phase. It is even possible that there are several metastable phases in which silicon substitutes either iron [$(Fe,Si)_3C$] or carbon [$Fe_3(C,Si)$]. The formation of a ternary metastable phase based on austenite also cannot be ruled out.

No stable ternary phases have also been found in the recent studies of the phase diagram of the Fe–Si–C ternary system at 1123 K[132] and 1243 K.[101–103] At temperatures below 1100 K (the temperature of the decomposition of the Fe_5Si_3 high-temperature phase) silicon carbide exists in equilibrium with the silicides $FeSi_2$, FeSi, and Fe_3Si. Above this temperature the equilibrium silicide Fe_5Si_3 with a hexagonal structure of the $D8_8$ type appears in this system, and silicon carbide is in equilibrium with the disilicide $FeSi_{2+x}$ having a homogeneity region and with the silicides FeSi and Fe_5Si_3 [according to a study by Schuster,[101] instead of the $SiC-FeSi_{2+x}$ equilibrium, two equilibria exist, $SiC-Fe_2Si_5$ and $SiC-FeSi_2(h)$]. The silicides Fe_5Si_3 and Fe_3Si as well as α-Fe and γ-Fe are in equilibrium with carbon. The isothermal cross-section through the Fe–Si–C system at 1243 K is presented in Fig. 16*c*. The scheme of the main phase equilibria in this system have been reported by Lyakishev et al.[122]

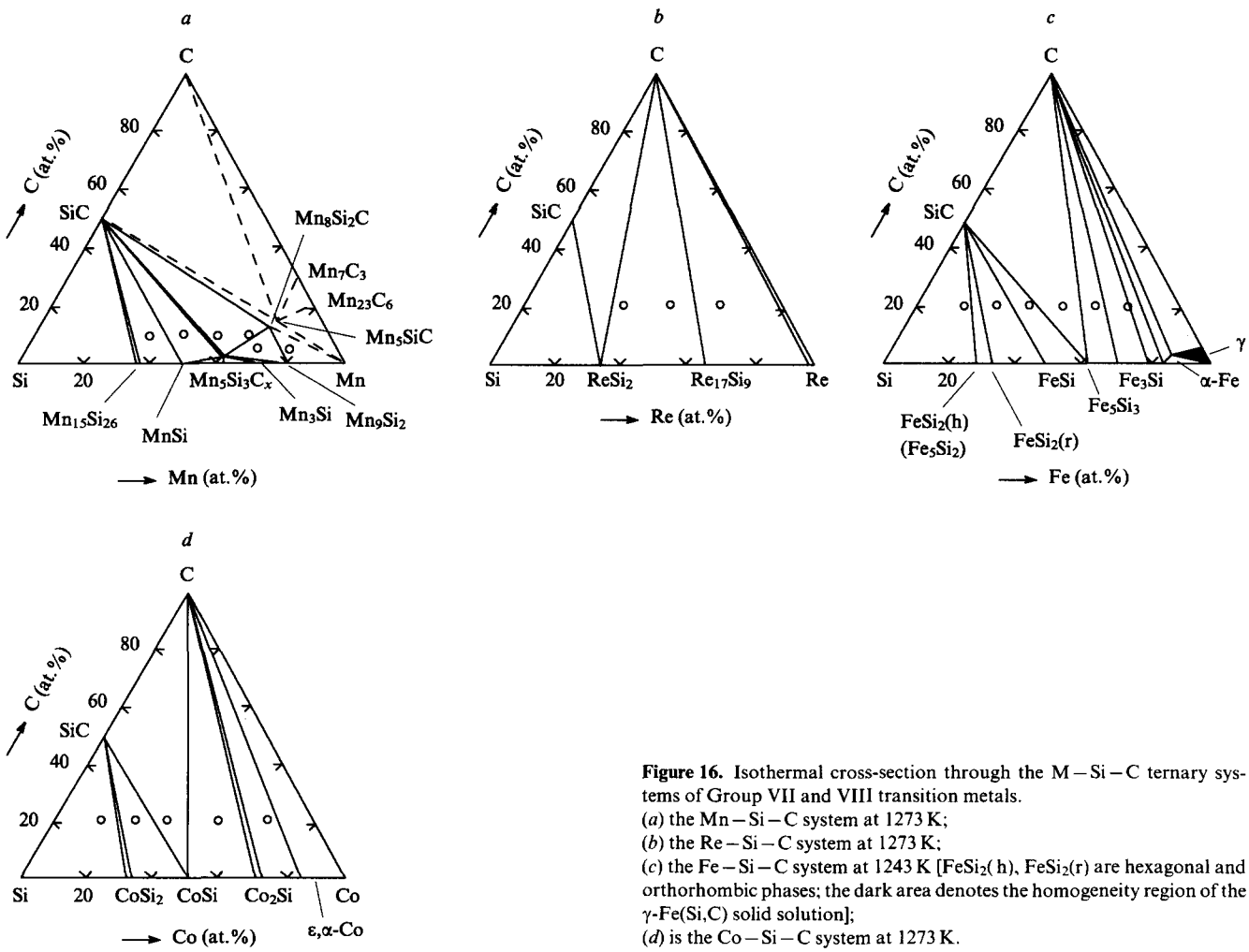


Figure 16. Isothermal cross-section through the M–Si–C ternary systems of Group VII and VIII transition metals.
(*a*) the Mn–Si–C system at 1273 K;
(*b*) the Re–Si–C system at 1273 K;
(*c*) the Fe–Si–C system at 1243 K [$FeSi_2$(h), $FeSi_2$(r) are hexagonal and orthorhombic phases; the dark area denotes the homogeneity region of the γ-Fe(Si,C) solid solution];
(*d*) is the Co–Si–C system at 1273 K.

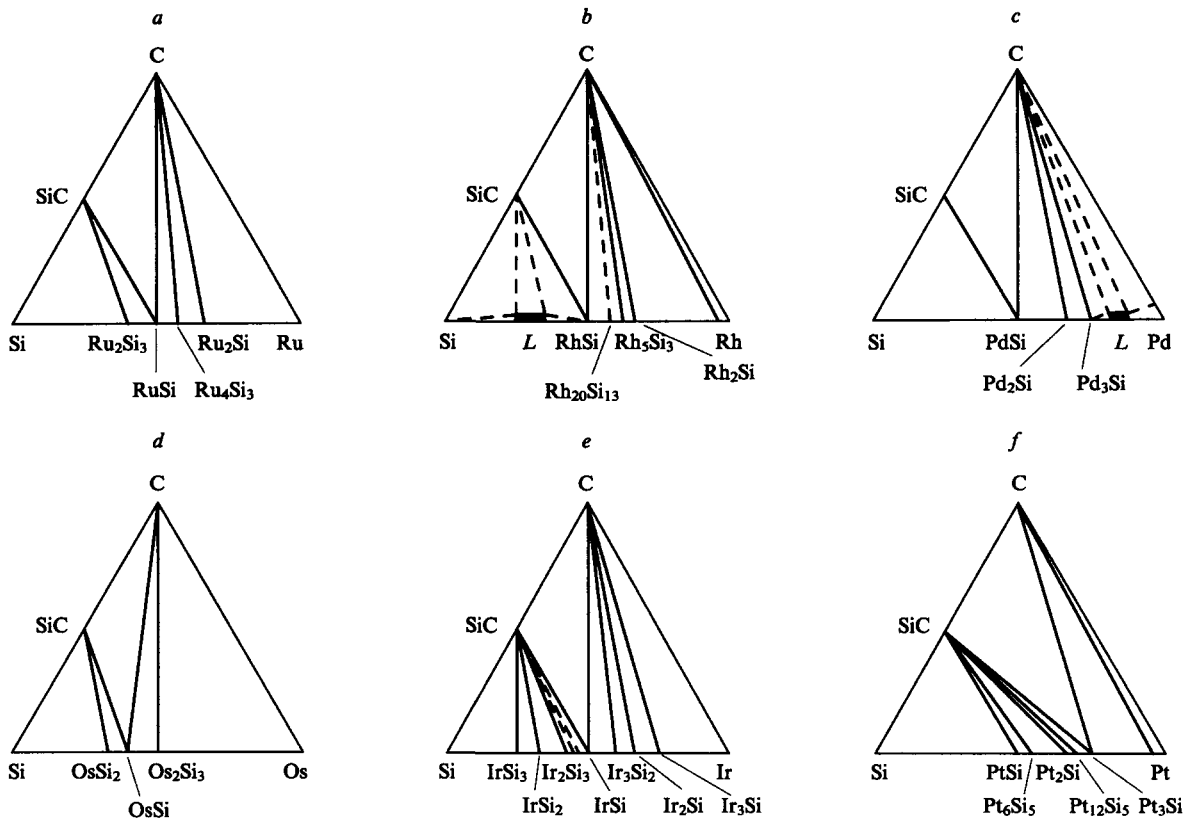


Figure 17. State diagrams for platinum group metal–silicon–carbon ternary systems, dark areas denote the regions of the existence of a liquid phase.[103,131]

Two metastable cubic phases of an unknown composition have been discovered in the Fe–Si–C system under the conditions of rapid cooling; the unit cell of one of these phases belongs to the $P4_132$ or $P4_332$ space group and has the period $a = 0.63$ nm, and the second metastable phase has a body-centred cubic (Bcc) lattice with the period $a = 0.89$ nm.[133]

The Co–Si–C system. There are hardly any stable ternary phases in the Co–Si–C system. The silicon carbide SiC is in an equilibrium with the silicides $CoSi_2$ and CoSi, whereas carbon coexists with CoSi, Co_2Si, and with the extended solid solution of silicon in cobalt (Fig. 16*d*).[101–103]

The Ni–Si–C system. The phase diagram for the Ni–Si–C system has been studied and constructed at 1123 K[132] and 1423 K.[134] No ternary compounds were found. At 1123 K, the silicon carbide SiC is in equilibrium with four silicides: $NiSi_2$, NiSi, Ni_3Si_2, and Ni_2Si, whereas Ni_2Si, Ni_5Si_2 ($Ni_{31}Si_{12}$), Ni_3Si, and the solid solution of silicon and carbon in nickel Ni(Si,C) are in equilibrium with carbon. At 1423 K the SiC–Ni_2Si–C three-phase region is still retained. At higher temperatures the silicides Ni_5Si_2 and Ni_3Si no longer exist, and Ni_2Si coexists directly with the Ni(Si,C) solid solution and also with carbon and SiC.

On rapid cooling, the $Ni_{67.5}Si_{17.5}C_{15}$ nonequilibrium ordered Bcc phase with the period $a = 0.2744$ nm containing 4 at.% of carbon and 15–21 at.% of silicon is formed in the Ni–Si–C system.[135]

(Ru,Rh,Pd,Os,Ir,Pt)–Si–C systems. The phase equilibria in the M–Si–C systems (M = Ru, Rh, Pd, Os, Ir, Pt) have been studied by Searcy and Finnie[131] and have been refined later by Schuster[103] (Fig. 17). The platinum-group metals do not form carbides, and no stable ternary compounds of these meals with silicon and carbon exist; thus, only equilibria between carbon and silicon carbide on the one hand, and platinum metal silicides on the other hand, are possible in the (Ru, Rh, Pd, Os, Ir, Pt)–Si–C systems.

The SiC–MSi–C three-phase regions exist at 1613 K in the Ru–Si–C system, at 1443 K in the Rh–Si–C system, at 1100 K in the Pd–Si–C system, and at 1613 K in the Ir–Si–C system. The silicides with the highest proportions of silicon are in equilibrium with SiC, and the silicides with high proportions of metal coexist with carbon. In the Rh–Si–C system, the Rh_2SiC unstable ternary phase can be formed in the temperature range 1770–1870 K, whereas in the Pt–Si–C system, the formation of the $Pt_3(Si_{2-x}C_x)$ phase is possible. In more recent papers these phases have not been mentioned. According to the data reported by Chou,[136] in the Pt–Si–C system at 1073 K silicon carbide SiC exists in an equiibrium with all the platinum silicides, and carbon coexists with Pt_3Si, i.e. the phase equilibria differ from those reported by Searcy and Finnie[131] (see Fig. 17).

4. The M–Si–N ternary siliconitride systems

The ceramics based on silicon nitride Si_3N_4 preserve their high hardness, wear resistance, and strength up to high temperatures, which accounts for its wide industrial application. The composite ceramic materials based on silicon nitride usually also contain a metallic component. This has necessitated the investigation of the phase equilibria in the M–Si–N ternary systems formed by the transition metal M, silicon, and nitrogen. The studies on the M–Si–N ternary systems have been surveyed in a monograph.[80]

The ternary phases formed in the M–Si–N systems are few in number, as in the M–Si–C carbosilicide systems. As a rule, these are $M_5Si_3N_x$ phases with a filled structure of the Mn_5Si_3 type ($D8_8$). Ternary phases with a different crystal structure are present in the siliconitride systems of some lanthanides and manganese. The structural characteristics of the ternary phases formed in the M–Si–N systems are presented in Table 8.

a. Siliconitrides of Group III transition metals

Based on the classification of the M–Si binary systems (M = Sc, Y, La → Lu) in terms of their composition and the crystal

Table 8. Some ternary phases in siliconitride systems of Group III–VII transition metals.

Compound	Symmetry and type of structure	Space group	Z	Unit cell parameters/ nm			Ref.
				a	b	c	
$LaSi_3N_5$	Orthorhombic	$P2_12_12_1$	4	0.7838	1.1236	0.4807	137, 138
$Sm_3Si_6N_{11}$	Tetragonal	–	4	0.9993	–	0.4836	139
$Ho_5Si_3N_x$ ($0 \leqslant x \leqslant 0.4$)	Hexagonal [a] (a solid solution of nitrogen in Ho_5Si_3)	$P6_3/mcm$	2	0.8356–0.8324	–	0.6273–0.6477	140
$Ti_5Si_3N_x$ ($0 \leqslant x \leqslant 1.0$)	Hexagonal [a] (a solid solution of nitrogen in Ti_5Si_3)	$P6_3/mcm$	2	–	–	–	119
$Zr_5Si_3N_x$ ($0.1 \leqslant x \leqslant 0.3$)	Hexagonal [a]	$P6_3/mcm$	2	0.7949	–	0.5573	89, 141
$Hf_5Si_3N_x$ ($x \leqslant 0.1$)	Hexagonal phase [a], stabilised by nitrogen	$P6_3/mcm$	2	0.7801	–	0.5523	141, 142
$V_5Si_3N_x$ ($0.2 \leqslant x \leqslant 1.0$)	Hexagonal [a]	$P6_3/mcm$	2	0.7121	–	0.4847	89, 141
$Nb_5Si_3N_x$ ($x < 0.3$)	"	$P6_3/mcm$	2	0.7517	–	0.5249–0.5310	89, 108, 141
$Ta_5Si_3N_x$ ($0.3 \leqslant x \leqslant 1.2$)	"	$P6_3/mcm$	2	0.7501	–	0.5229–0.5246	89, 108, 141
$MnSiN_2$	Orthorhombic	$Pna2_1$	4	0.5248	0.6511	0.5070	143,144
$MnSiN_2$	"	$Pna2_1$	4	0.5266–0.5268	0.6522–0.6521	0.5074–0.5069	145

[a] Hexagonal (space group $P6_3/mcm$) $M_5Si_3N_x$ phases, among which there are ternary compounds (M = Zr, Hf, V, Nb, Ta) and solid solutions (M = Ho, Ti), have the filled structure of the Mn_5Si_3 ($D8_8$) type, $Z = 2$.

structure of the silicides formed, Weitzer et al.[140] have divided the M–Si–N ternary siliconitride systems into three groups: (1) (La,Ce,Pr,Nd)–Si–N; (2) (Sm,Gd,Tb,Dy,Ho,Er,Y)–Si–N; and (3) (Tm,Yb,Lu,Sc)–Si–N. They chose one M–Si–N ternary system from each group and studied the phase equilibria in it assuming that the phase equilibria in all the siliconitride systems of the same group are similar. This assumption is true only within certain limits: for example, no ternary compounds were found in the Ce–Si–N system (the first group) or in the Ho–Si–N system (the second group), but ternary compounds $LaSi_3N_5$ and $Sm_3Si_6N_{11}$ were discovered in the La–Si–N and Sm–Si–N systems, which belong to the same groups (see Table 8).[139] Thus, the phase equilibria in the M–Si–N ternary systems of the same group are not entirely similar.

The Sc–Si–N system. The isothermal cross-sections through this system at 1073 K and 1273 K have been reported[140] (Fig. 18*a*,*b*). No ternary compounds were found in this system. At 1073 K only two scandium silicides ScSi and Sc_5Si_3 are stable. The scandium silicides, silicon, and the silicon nitride Si_3N_4 exist in equilibrium with the scandium nitride ScN. At 1273 K one more stable silicide appears, namely, $ScSi_{2-x}$ (Sc_3Si_5), which coexists with silicon nitride and scandium nitride; ScN is also in equilibrium with Si_3N_4, ScSi, and Sc_5Si_3.

The Ce–Si–N system. In the absence of external nitrogen pressure the Ce–Si–N system contains no ternary compounds at 1273 K.[140] The cerium nitride CeN exists in equilibrium with Si_3N_4 and six cerium silicides — $CeSi_2$, $CeSi_{2-x}$, CeSi, Ce_5Si_4, Ce_3Si_2, and Ce_5Si_3; the silicon nitride Si_3N_4 exists in equilibrium with $CeSi_2$ (Fig. 18*c*). The solubility of a third component in the binary phases is negligibly small.

The Ho–Si–N system. Based on an X-ray diffraction study and a metallographic study and on the determination of the melting points, Weitzer et al.[140] have constructed the phase diagram of the Ho–Si binary system. In this system, they detected all of the six known holmium silicides. The holmium disilicide $HoSi_2$ melts incongruently at 2153 K, whereas $HoSi_{2-x}$ and HoSi melt congruently at temperatures above 2260 K. In the Ho–Si alloys containing less than 50 at.% Ho, HoSi has a structure of the FeB ($B27$) type; in the alloys containing more than 50 at.% Ho, the HoSi modification with a structure of the CrB (B_f, $B33$) type predominates. The Ho_5Si_4 phase melts incongruently at $T > 2120$ K, and in the 1870 K > T > 1270 K range it decom-

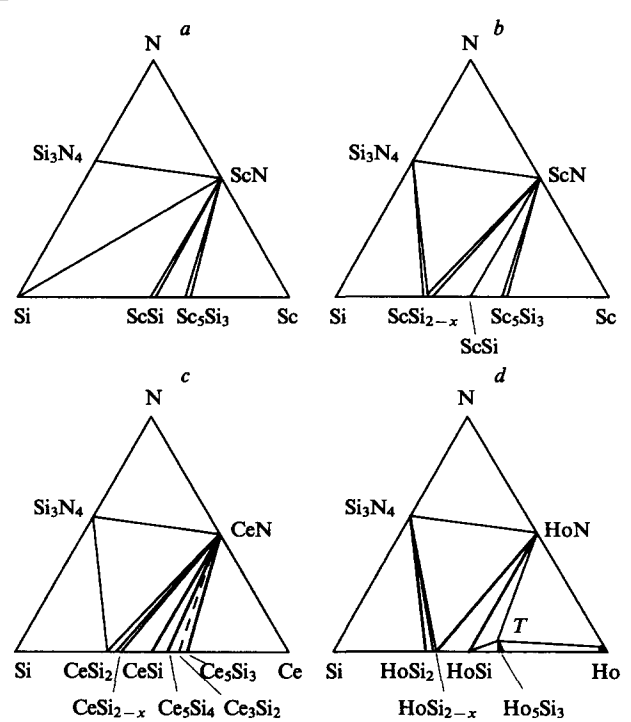


Figure 18. Isothermal cross-section through the M–Si–N ternary systems of Group III transition metals.[140]
(*a*) the Sc–Si–N system at 1073 K; (*b*) the Sc–Si–N system at 1273 K; (*c*) the Ce–Si–N system at 1273 K; (*d*) the Ho–Si–N system at 1273 K (dark areas denote the homogeneity regions of the $Ho_5Si_3N_x$ solid solution and of the solid solution of silicon and nitrogen in holmium), $T = Ho_5Si_3N_x$.

poses to HoSi (the CrB structural type) and Ho_5Si_3. The temperature of the congruent melting of Ho_5Si_3 is 1983 K.

The Ho–Si–N system incorporates no ternary compounds at 1273 K (Fig. 18*d*); however, up to 4 at.% of nitrogen is dissolved in Ho_5Si_3 to form the $Ho_5Si_3N_x$ limited solid solution having a filled structure of the Mn_5Si_3 ($D8_8$) type (see Table 8). The holmium nitride HoN is in equilibrium with Si_3N_4, $HoSi_{2-x}$, HoSi, and $Ho_5Si_3N_x$; in addition, there exist Si_3N_4–$HoSi_2$, HoSi–$Ho_5Si_3N_x$, and Ho–$Ho_5Si_3N_x$ equilibria. Metallic holmium dissolves up to 2 at.% of nitrogen. The holmium silicide HoSi coexisting with HoN and $Ho_5Si_3N_x$ has a structure of the CrB type.

b. Siliconitrides of Group IV and V transition metals

The Ti–Si–N system. According to thermodynamic estimates,[146,147] the interaction of metallic titanium with silicon nitride Si_3N_4 in the 300 K < $T \leqslant$ 1800 K temperature range most probably yields the silicide Ti_5Si_3 and the nitride TiN_y. This type of interaction is retained up to 2300 K. Taking into account these data and also the results of a study[148,149] of the interaction between silicon nitride and titanium nitride under an atmosphere of NH_3 and H_2 [at a total pressure in the gas phase of $(1.33-10.7)\times10^3$ Pa] at 1323–1723 K, Schuster and Nowotny[141] concluded that under these conditions, Si_3N_4 exists in equilibrium with TiN_y and with the silicide $TiSi_2$, whereas TiN_y coexists with all the titanium silicides. The study of the phase equilibria in the Ti–Si–N ternary system at 1273 K (in vacuo) and at 1573 K (under an argon atmosphere) has shown that the above phase equilibria are retained under these conditions (Fig. 19*a*). From the authors' viewpoint,[141] the phase equilibria in the Ti–Si–N system are insensitive to the variations of the temperature or nitrogen pressure. No ternary compounds were found in the Ti–Si–N system; no solubility of nitrogen in the silicide Ti_5Si_3 with the structure of the Mn_5Si_3 type or in other binary phases was observed.

The isothermal cross-section through the Ti–Si–N system at 973–1273 K has been constructed by Beyers et al.,[150] who have studied phase equilibria in thin films. These researchers[150] (in contrast to Schuster and Nowotny[141]) did not note the equilibrium between Si_3N_4 and $TiSi_2$, because there exists an equilibrium between TiN_y and silicon. The other equilibria reported in these two papers[141,150] are the same. Thermodynamic calculations[119,151] have shown that the TiN_y–Si equilibrium exists most likely up to 1573 K; in particular, the variation in the Gibbs energy for the reaction $4TiSi_2 + Si_3N_4 \rightarrow 4TiN + 11Si$ at 1373 K is −11.1 kJ (g-at)$^{-1}$.

The most recent studies[119,151] of the phase equilibria in the Ti–Si–N system at 1373 K have been carried out in relation to the diffusion pairs of the Ti–Si_3N_4, $Ti_{1-x}Si_x$–Si_3N_4, and $Ti_{1-x}Si_x$–TiN types. A study involving the nitriding of Ti,Si alloys proved to be impossible due to the formation of a thin film of titanium nitride on the surface of the samples, which prevents further diffusion of nitrogen. The isothermal cross-section through the Ti–Si–N system at 1373 K (Fig. 19*b*) largely coincides with the cross-section obtained by Beyers et al.[150] The titanium nitride TiN_y coexists with Si, Si_3N_4, $TiSi_2$, and the $Ti_5Si_3N_x$ ternary phase, which is a solid solution of nitrogen in Ti_5Si_3. The solubility of nitrogen in Ti_5Si_3 reaches 11 at.%.[119,151] The silicide Ti_3Si decomposes to β-Ti and $Ti_5Si_3N_x$ at 1373 K on the addition of even small amounts of nitrogen. Similar effects (substantial solubility of carbon or oxygen in Ti_5Si_3 and decomposition of Ti_3Si on the addition of a third element) have also been observed in the Ti–Si–C and Ti–Si–O systems.[118,119,151]

In all probability, the disagreement between the results of Schuster and Nowotny[141] and those obtained by other workers[119,150,151] is caused by the experimental procedure: Schuster and Nowotny[141] studied the phase equilibria in the Ti–Si–N system using massive samples, Beyers et al.[150] used thin films, whereas in the other two studies[119,151] diffusion pairs were employed. The phases formed in thin films due to diffusion are not always reproduced in massive samples and are probably nonequilibrium phases. Also in massive samples the real equilibrium is not always reached due to the short durations of the annealing (sometimes, annealing requires hundreds or even thousands of hours).

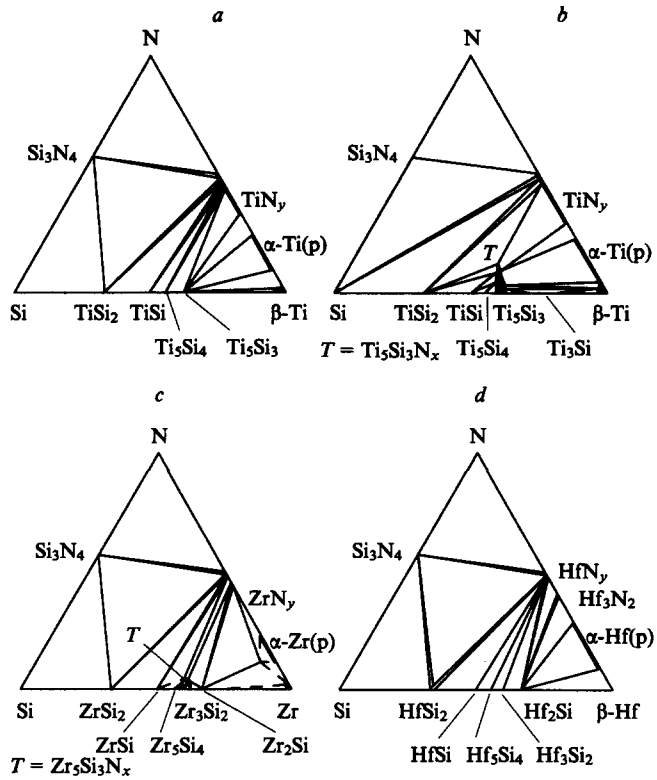


Figure 19. Isothermal cross-sections through M–Si–N ternary systems of Group IV transition metals (dark areas denote one-phase homogeneity regions).
(*a*) the Ti–Si–N system at 1573 K; (*b*) the Ti–Si–N system at 1373 K, $T = Ti_5Si_3N_x$; (*c*) the Zr–Si–N system at 1573 K, $T = Zr_5Si_3N_x$; (*d*) the Hf–Si–N system at 1573 K.
The cross-sections *a*, *c*, and *d* were constructed using the results of a study of samples sintered under an argon atmosphere at 1573 K; the cross-section *b* was constructed by a layer-by-layer study of the samples obtained by sintering diffusion pairs at 1373 K.

The Zr–Si–N system. In the first investigation of this system,[89] a ternary zirconium siliconitride with a structure of the Mn_5Si_3 ($D8_8$) type has been detected. This compound contains up to 10 at.% of nitrogen and its chemical formula and crystal structure are similar to those of the zirconium carbosilicide $Zr_5Si_3C_x$. The distribution of phase fields in the Zr–Si–N system was reported[89] to be identical to that in the Zr–Si–C system at 1873 K. The experimental results obtained with the samples sintered at 1573 K under argon[141] have confirmed the views[89] of the phase equilibria in the Zr–Si–N system.

The isothermal cross-section through the Zr–Si–N system at 1573 K is shown in Fig. 19*c*.[141] The nitride ZrN_y is in equilibrium with Si_3N_4, with the ternary compound $Zr_5Si_3N_x$, with the silicides $ZrSi_2$, ZrSi, and Zr_2Si, and with the α-Zr(N) solid solution; Si_3N_4 is in equilibrium with $ZrSi_2$, and $Zr_5Si_3N_x$ also coexists with ZrSi, Zr_5Si_4, Zr_3Si_2, Zr_2Si, and with the solid solution of nitrogen in α-Zr.

At a lower temperature, namely at 1273 K, all the phases existing in the Zr–Si–N system at 1573 K are retained, but the content of nitrogen in $Zr_5Si_3N_x$ noticeably decreases ($x \leqslant 0.2$), and the Si_3N_4–ZrSi, ZrN_y–Zr_5Si_4, and ZrN_y–Zr_3Si_2 equilibria arise instead of $Zr_5Si_3N_x$–Zr_5Si_4 and ZrN_y–$ZrSi_2$.

The Hf–Si–N system. The phase equilibria in this system at 1273 and 1573 K are virtually identical and are similar to those in the

Zr–Si–N system at these temperatures.[141] The main distinction between the isothermal cross-section through the Hf–Si–N system at 1273 K and the corresponding cross-section through the Zr–Si–N system is the existence of the Si_3N_4 + $HfSi_2$ + HfN three-phase field. The ternary compound $Hf_5Si_3N_x$ with a very low content of nitrogen ($x \leqslant 0.1$) is formed in the Hf–Si–N system. It has a structure of the Mn_5Si_3 ($D8_8$) type and exists in an equilibrium with HfN_y and Hf_2Si. The isothermal cross-section through the Hf–Si–N system at 1573 K is presented in Fig. 19*d* (the position of the ternary compound $Hf_5Si_3N_x$ is not shown).[124]

The V–Si–N system. The heating of V_5Si_3 to 1673 K under an NH_3 atmosphere leads to the formation of the ternary compound $V_5Si_3N_x$ with a filled structure of the Mn_5Si_3 ($D8_8$) type and the nitride VN_y.[89] The phase equilibria in the V–Si–N system at 1273 K (in vacuo) and at 1773 K (under an argon atmosphere) (Fig. 20*a*,*b*) have been studied.[141] At 1273 K the ternary compound is in equilibrium with Si_3N_4, VSi_2, V_6Si_5, V_5Si_3, V_3Si, and V_9N_4; the silicon nitride Si_3N_4 coexists with VSi_2, VN_y, and V_9N_4; and the silicide V_3Si coexists with V_9N_4 and with the solid solution of nitrogen in vanadium.

As the temperature increases, the nitrogen content in $V_5Si_3N_x$ increases substantially, as indicated by the increase in the unit cell parameters from $a = 0.7121$ nm and $c = 0.4847$ nm at 1273 K to $a = 0.7155$ nm and $c = 0.4852$ nm at 1773 K. The nitrides Si_3N_4 and VN_y are unstable under an argon atmosphere at 1773 K. Thus, the ternary compound $V_5Si_3N_x$ and the silicide VSi_2 in the V–Si–N system coexist directly with nitrogen, whereas the other equilibria are retained (Fig. 20*b*). The solubility of a third component in the binary phases is negligibly small.[141]

The compound V_9N_4 crystallises with a hexagonal ordered structure with the periods $a = a_V\sqrt{3}$ and $c = c_V$ (a_V and c_V are the parameters of the hexagonal close-packed vanadium sublattice). According to the data obtained by Onozuka,[152] the nitrides stable in the V–N binary system at temperatures above 900 K are VN_y and V_9N_4 (rather than V_2N_y as has been believed previously), whereas at $T < 900$ K, the $V_{32}N_{26}$ (space group $P4_2/nmc$) and V_9N_4 (space group $P6_322$) ordered phases are stable. The VN_y ($y = 0.78$) → $V_{32}N_{26}$ ordering occurs at 793 K as a first-order phase transition.

The Nb–Si–N system. A thermodynamic calculation[146] implies that the reaction between the silicon nitride Si_3N_4 and metallic niobium at 1300 K most probably yields the silicide Nb_5Si_3 and the nitride Nb_2N. This is in agreement with the experimental data.[141] The isothermal cross-section through the Nb–Si–N system at 1273 K (in vacuo) is shown in Fig. 20*c*.[141] There are no ternary phases in the Nb–Si–N system at this temperature, the nitride Si_3N_4 coexists with all the binary niobium silicides and nitrides, whereas the silicide Nb_5Si_3 exists in equilibrium with Nb_2N.

The annealing of the alloys existing in the Nb–Si–N system at 1773 K led to the appearance of the ternary compound $Nb_5Si_3N_x$ with a filled structure of the Mn_5Si_3 ($D8_8$) type.[141] This compound exists in equilibrium with $NbSi_2$, Nb_5Si_3, Nb_2N, δ-NbN, and probably with nitrogen. The equilibria of $Nb_5Si_3N_x$ ($Nb_{5-x}Si_{3-y}N_z$) with N_2 and $NbSi_2$ have been reported.[108] The assumption that in the ternary compound, nitrogen substitutes niobium and silicon[108] have not been confirmed: the interstitial atoms X in the compounds $M_5M'_3X$ with the Mn_5Si_3 ($D8_8$) type of structure fill the octahedral vacancies formed by the M atoms. The $Nb_5Si_3N_x$ ternary phase has been obtained by heating Nb_5Si_3 under an atmosphere of NH_3 at 1673 K.[89] The parameter c of the crystal lattice of $Nb_5Si_3N_x$ has been reported[89,141] to increase from 0.5249 nm to 0.5310 nm with an increase in the nitrogen content, with the invariable parameter $a = 0.7517$ nm. The invariability of the parameters of the crystal lattices of the binary phases in the Nb–Si–N system indicates that the solubility of the third component in these phases is negligibly small.

The Ta–Si–N system. This system has been the most comprehensively studied among the siliconitride systems of group IV and V transition metals (except for titanium). The first investigation of the phase equilibria in this system was carried out by Kudielka et

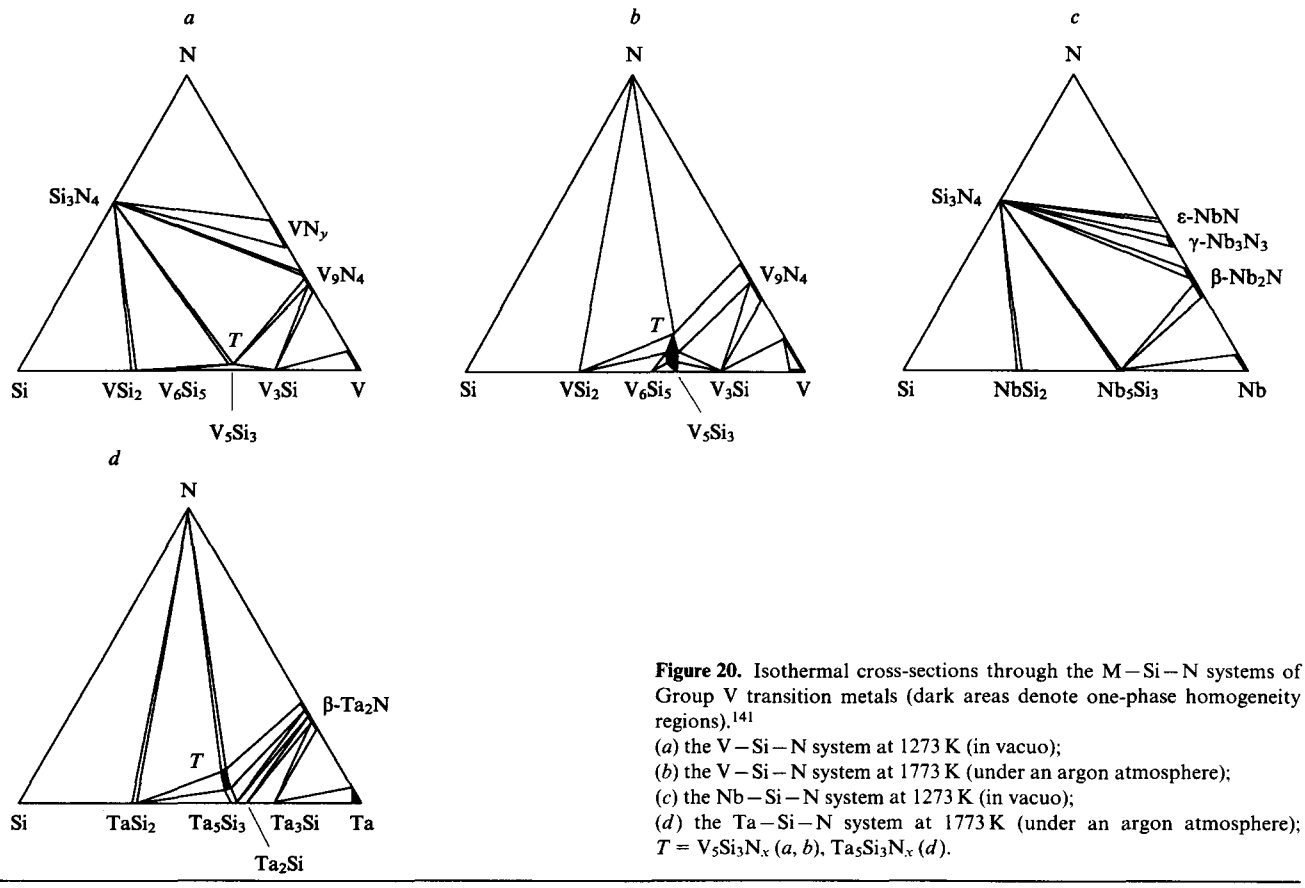


Figure 20. Isothermal cross-sections through the M–Si–N systems of Group V transition metals (dark areas denote one-phase homogeneity regions).[141]
(*a*) the V–Si–N system at 1273 K (in vacuo);
(*b*) the V–Si–N system at 1773 K (under an argon atmosphere);
(*c*) the Nb–Si–N system at 1273 K (in vacuo);
(*d*) the Ta–Si–N system at 1773 K (under an argon atmosphere);
$T = V_5Si_3N_x$ (*a*, *b*), $Ta_5Si_3N_x$ (*d*).

al.[90] They constructed the isothermal cross-section through the Ta–Si–N system at 1600 K and a nitrogen pressure of 0.75×10^5 Pa. The ternary compound $Ta_{5-x}Si_{3-y}N_z$ with a broad homogeneity region exists in this system; it exists in equilibrium with nitrogen, the silicon nitride Si_3N_4 and with the tantalum nitrides and silicides TaN_y, Ta_2N, Ta_5Si_3, and $TaSi_2$.[108] The formation of the $Ta_5Si_3N_x$ ternary phase on nitriding the silicide Ta_5Si_3 at 1673 K by various methods and on the interaction of Si_3N_4 with tantalum at 1873 K has also been observed in another study.[89] The ternary compound $Ta_5Si_3N_x$ has a filled structure of the Mn_5Si_3 ($D8_8$) type common to the $M_5Si_3N_x$ phases. The phase equilibria in the Ta–Si–N system have been studied at 1273 K (in vacuo) and at 1773 K (under an argon atmosphere).[141] It was found that at 1273 K, no ternary phase exist, and the silicon nitride is in equilibrium with $TaSi_2$, Ta_5Si_3, TaN_y, and Ta_2N, whereas the nitride Ta_2N coexists also with Ta_5Si_3, Ta_2Si, and Ta_3Si. At 1773 K, the ternary compound $Ta_5Si_3N_x$ exists in the Ta–Si–N system. It is in equilibrium with nitrogen, Ta_2N, Ta_2Si, and Ta_5Si_3 (Fig. 20*d*). When the content of nitrogen in $Ta_5Si_3N_x$ increases, the parameter c of the crystal lattice increases from 0.5229 nm to 0.5246 nm with the parameter $a = 0.7501$ nm being constant. The solubility of the third component in the binary phases of the Ta–Si–N system is negligibly small.[141]

c. Siliconitrides of Group VI–VIII transition metals

The Cr–Si–N system. The interaction of the silicon nitride Si_3N_4 with chromium can yield Cr_3Si, Cr_5Si_3, CrSi, $CrSi_2$, Cr_2N, Si, and gaseous nitrogen, depending on the amount of chromium.[146] Heating a mixture of Cr, Si, and Si_3N_4 to 1673 K in a moist atmosphere leads to the formation of Cr_5Si_3 (structure of the W_5Si_3 type), containing up to 10 at.% of nitrogen, and Cr_3Si, containing up to 20 at.% of nitrogen; chromium nitrides are not formed in the absence of an external nitrogen pressure.[89]

A detailed study of the phase equilibria in the Cr–Si–N system[153] has shown that at 1273 K and under an argon atmosphere, the nitride Si_3N_4 coexists in this system with all the chromium silicides, namely, $CrSi_2$, CrSi, Cr_5Si_3, and Cr_3Si, whereas Cr_3Si and the solid solution of silicon in chromium are in equilibrium directly with nitrogen. However, at 1273 K, even a low nitrogen pressure is sufficient to stabilise Cr_2N existing in equilibrium with Cr_3Si and with the solid solution of silicon in chromium; the other equilibria in the Cr–Si–N system under a low nitrogen pressure are the same as the equilibria under argon. At a higher temperature of 1673 K under an argon atmosphere, the silicides Cr_5Si_3 and Cr_3Si are in equilibrium with nitrogen, whereas Si_3N_4 coexists with Cr_5Si_3. Nitrogen is insoluble in chromium silicides.[153]

The isothermal cross-section through the Cr–Si–N system at 1873 K and at a nitrogen pressure of 1×10^5 Pa has been constructed[153] with the aid of the results obtained in another study.[154] The equilibria existing at 1673 K under argon are retained under these conditions; in addition, new equilibria arise, due to the stabilisation of the chromium nitride Cr_2N and the appearance of the liquid phase of chromium.

The Mo–Si–N system. The nitriding of Mo_5Si_3 at 1673 K gives Mo and Mo_3Si, whereas the nitriding of $MoSi_2$ under the same conditions is accompanied by the appearance of Mo_5Si_3.[89] The annealing of a mixture of Mo, Si, and Si_3N_4 powders at 1973 K affords Mo_5Si_3 and nitrogen.[89] The reaction between Mo and Si_3N_4 at 1273 K proceeds very slowly; in the absence of an external pressure of nitrogen, Si_3N_4 coexists with $MoSi_2$ and Mo_5Si_3, whereas the silicides Mo_5Si_3 and Mo_3Si exist in equilibrium with nitrogen.[153] The same phase equilibria are retained in the Mo–Si–N system at 1673 K under argon. At 1850 K, the silicon nitride Si_3N_4 is unstable, and all the molybdenum silicides are in equilibrium with nitrogen. No ternary compounds have been found in the Mo–Si–N system.

The phase equilibria in the Mo–Si–N system have been studied at 1573 K and at various nitrogen pressures (Fig. 21).[137] At $p_{N_2} < 18$ Pa, the Mo–Si–N system incorporates only the silicides $MoSi_2$, Mo_5Si_3, and Mo_3Si existing in equilibrium with nitrogen. At 18 Pa $< p_{N_2} <$ 3000 Pa all the molybdenum silicides are still in equilibrium with nitrogen, and $MoSi_2$ coexists with Si_3N_4. The phase equilibria in the Mo–Si–N system at higher nitrogen pressures (3×10^3 Pa $\leqslant p_{N_2} < 7 \times 10^5$ Pa) are the same as shown in Fig. 21*c*. At a nitrogen pressure of 7×10^5 Pa $\leqslant p_{N_2} < 88 \times 10^5$ Pa, the silicon nitride Si_3N_4 exists in equilibrium with all the molybdenum silicides, and Mo_3Si coexists with nitrogen. When the nitrogen pressure is $(88-98) \times 10^5$ Pa, the nitride Mo_2N becomes stable, and one more equilibrium appears, namely, Mo_2N-Mo_3Si. At $p_{N_2} > 98 \times 10^5$ Pa, the Mo_3Si-N equilibrium disappears, and the $Si_3N_4-Mo_2N$ equilibrium arises instead; silicon nitride coexists also with all the molybdenum silicides, and Mo_2N is in equilibrium with Mo_3Si (Fig. 21*f*).

The W–Si–N system. The nitriding of W_5Si_3 at 1673–2073 K under an NH_3 atmosphere does not lead to the formation of a phase with the structure of the Mn_5Si_3 ($D8_8$) type observed in the M–Si–N systems of Group V transition metals.[89] It has been shown[153] that silicon nitride does not react with tungsten or with the silicides WSi_2 and W_5Si_3 at 1273 K, but exists in equilibrium with them. The Si_3N_4-W equilibrium is retained up to 1400 K. At higher temperatures, Si_3N_4 and tungsten interact to give W_5Si_3 and nitrogen that exist in equilibrium with each other. At 1773 K, the silicides WSi_2 and W_5Si_3 are in equilibrium with nitrogen.

The Re–Si–N system. The phase equilibria in this system have been studied at 1273 K and 1673 K under argon.[153] At 1273 K, the silicon nitride Si_3N_4 coexists with rhenium and with its silicides $ReSi_2$ and $Re_{17}Si_9$. At a higher temperature Si_3N_4 reacts with rhenium, and thus the $Re_{17}Si_9-N$ equilibrium arises instead of Si_3N_4-Re. No ternary phases in the Re–Si–N system have been found.

The Mn–Si–N system. The interaction of liquid manganese with the silicon nitride Si_3N_4 in vacuo, under an inert gas, or under nitrogen is accompanied, in particular, by the formation of the ternary compound $MnSiN_2$.[156] The nitrogen atoms in the siliconitride $MnSiN_2$ are located at the centres of the distorted tetrahedra comprising two manganese atoms and two silicon atoms.[143,144] The decomposition of $MnSiN_2$ to the silicide MnSi and gaseous nitrogen begins at 1570 K (at a nitrogen pressure of 1×10^5 Pa) or at 1070 K (under argon).

The study of the phase equilibria in the Mn–Si–N system carried out by Weitzer and Schuster[145] has confirmed the presence of only one ternary compound $MnSiN_2$ with an orthorhombic lattice (see Table 8). It has a narrow homogeneity region. In the absence of an external nitrogen pressure at 1273 K the siliconitride $MnSiN_2$ is in equilibrium with nitrogen, with the silicon nitride Si_3N_4, with β-Mn (the solid solution of silicon in manganese), and with the silicide Mn_3Si; Si_3N_4 also coexists with $MnSi_2$, MnSi, Mn_5Si_3, and Mn_3Si. Nitrogen is insoluble in manganese silicides.

In the presence of an external nitrogen pressure, γ-Mn (the solid solution of nitrogen in manganese) arises in the system. This leads to the appearance of β-Mn–γ-Mn and $MnSiN_2$–γ-Mn phase equilibria. With an increase in the external pressure of nitrogen, manganese nitrides (in particular, ε-Mn_4N) appear in the system and equilibria between them and $MnSiN_2$ are established.

The Fe–Si–N system. The combined influence of the nitrogen and silicon admixtures in iron and its alloys on the properties of the latter have been studied in connection with the development of siliceous sheet transformer steel. In steels with high silicon contents (up to 4 at.%), the nitride Si_3N_4 can segregate from the solid solution of silicon in iron. The silicon nitride is also formed in the nitriding of steels with low contents of silicon.

The phase equilibria in the Fe–Si–N system have been studied at 1173 K and 1423 K.[145] In the absence of an external nitrogen pressure at 1173 K, Si_3N_4 coexists with all the iron silicides stable at this temperature and with α-Fe (the solid

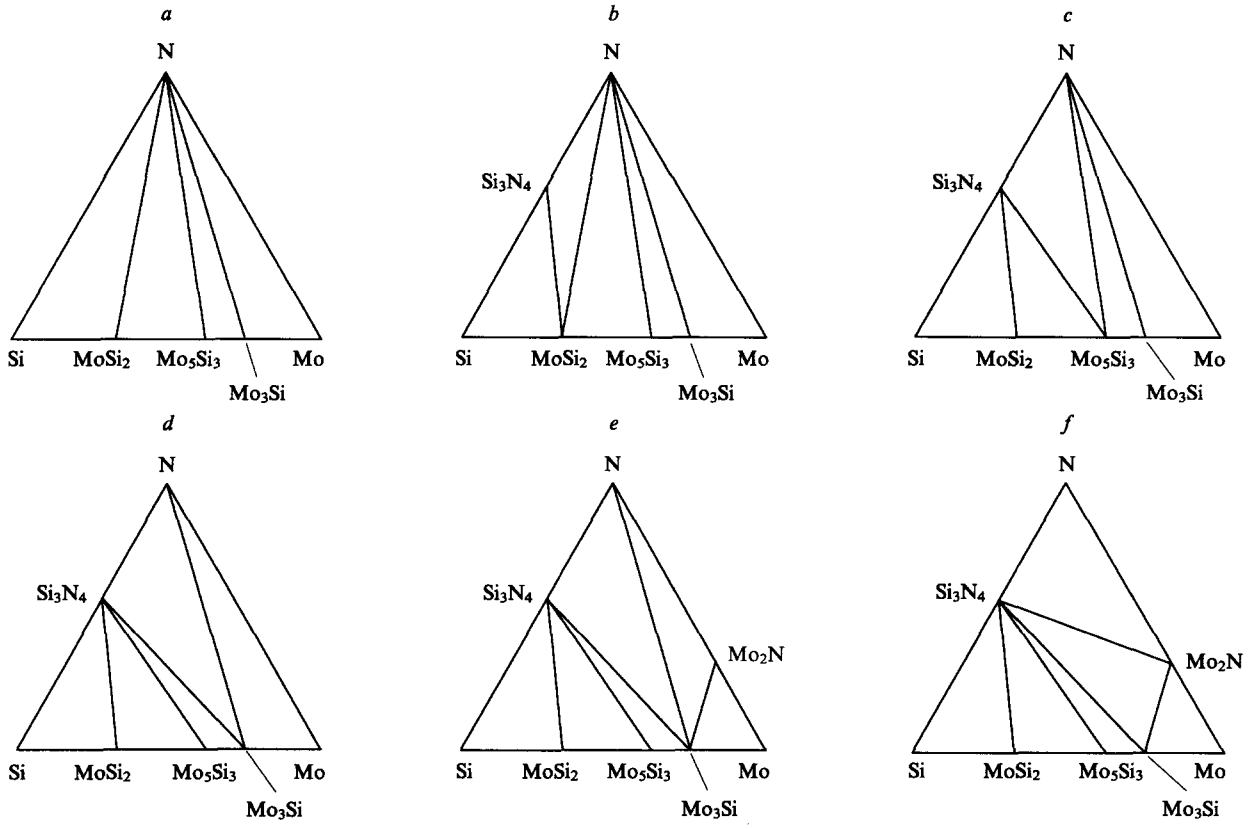


Figure 21. The influence of nitrogen pressure p_{N_2} on phase equilibria in the Mo–Si–N system at 1573 K.[155]
(*a*) < 18 Pa, (*b*) 18 ⩽ p_{N_2} < 3×10^3 Pa, (*c*) 3×10^3 ⩽ p_{N_2} < 7×10^5 Pa, (*d*) 7×10^5 ⩽ p_{N_2} < 88×10^5 Pa, (*e*) 88×10^5 ⩽ p_{N_2} < 98×10^5 Pa, (*f*) p_{N_2} ⩾ 98×10^5 Pa.

solution of silicon in iron). In the presence of pure iron at 1390 ± 10 K Si_3N_4 starts to decompose yielding the solid solution of α-Fe containing 6–8 at.% of silicon.

At 1423 K the nitride Si_3N_4 coexists with silicides Fe_2Si_5, FeSi, Fe_2Si, and Fe_3Si, and also with α-Fe (the solid solution of silicon in iron). No ternary phases have been detected in the Fe–Si–N system.

The Co–Si–N system. When Si_3N_4 reacts with liquid cobalt, it decomposes to give cobalt silicides and gaseous nitrogen. In the absence of an external nitrogen pressure at 1273 K, the silicon nitride is in an equilibrium with $CoSi_2$, CoSi, the low-temperature silicide Co_2Si, α-Co and ε-Co (the solid solutions of silicon in cobalt), and cobalt.[145] The reaction between Co and Si_3N_4 with the decomposition of the latter starts at 1440 K. Nitrogen is insoluble in cobalt silicides. No ternary compounds have been found in the Co–Si–N system.

The Ni–Si–N system. The interaction of molten nickel with the silicon nitride Si_3N_4 is accompanied by the decomposition of the latter. At temperatures above 1440 K, the decomposition occurs very rapidly. Without an external nitrogen pressure at 1173 K, the silicon nitride Si_3N_4 coexists with nickel and with all the nickel silicides stable at this temperature. Nickel silicides do not dissolve nitrogen. No ternary compounds have been detected in this system.

The phase equilibria in the Ni–Si–N system have been studied at 1373 K and at a nitrogen pressure of 1×10^5 Pa.[155] Under these conditions, the silicides Ni_2Si, Ni_5Si_2 ($Ni_{31}Si_{12}$), and Ni_3Si and the solid solution of silicon in nickel exist in equilibrium with the silicon nitride Si_3N_4. Nickel dissolves up to 15 at.% of silicon.

The Ru–Si–N system. There are no ternary phases in the Ru–Si–N system at temperatures from 1270 K to 1520 K and at an argon pressure of 1×10^5 Pa.[157] At 1273 K the nitride Si_3N_4 coexists with ruthenium and with its silicides Ru_2Si_3, RuSi, and Ru_4Si_3 (Fig. 22*a*). At 1480 K, decomposition of Si_3N_4 begins

$$Si_3N_4 + Ru \longrightarrow Ru_4Si_3 + N_2,$$

and the appearance of the phase diagram changes. At 1520 K, the nitride Si_3N_4 exists in equilibrium with Ru_2Si_3 and RuSi, and the silicides RuSi, Ru_4Si_3, and Ru_2Si are in equilibrium with nitrogen (Fig. 22*b*).

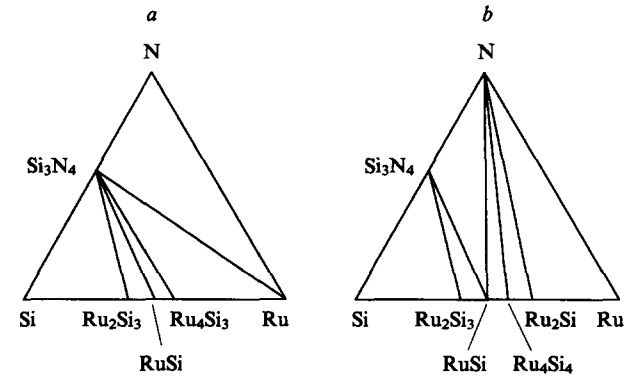


Figure 22. Isothermal cross-sections through the Ru–Si–N system at 1273 K (*a*) and 1520 K (*b*) under an argon atmosphere.[157]

V. Phase equilibria in M – Al – X ternary systems (X = C, N, Si)

1. The common types of the crystal structures of ternary compounds in the M – Al – X systems

Aluminidocarbides and aluminidonitrides of transition metals have, as a rule, one of several specific crystal structures peculiar to these compounds.

The cubic structure [space group $Pm3m(O_h^1)$] of the perovskite $CaTiO_3$ ($E2_1$) type, which is usually found in double oxides, for example, in barium titanate $BaTiO_3$, is the most common among these structures. The M and Al atoms in the aluminidocarbides and aluminidonitrides M_3AlX with the perovskite type of structure form an ordered metallic Fcc-sublattice: the aluminium atoms occupy the vertices of a cube, whilst the transition metal atoms M are located at the centres of the faces of the cube; the M atoms constitute octahedra in the centres of which the interstitial atoms X are located (Fig. 23). The interstitial atoms X (C, N) occupy all or some of the octahedral interstices formed by the transition metal atoms M; this accounts for the fact that most of aluminidocarbides and aluminidonitrides with the perovskite type of structure have fairly extensive homogeneity regions. The presence of the metallic Fcc-lattice, with interstitial atoms located in its octahedral interstices, and the existence of the homogeneity regions make these compounds very similar to the classical nonstoichiometric interstitial compounds, namely, carbides and nitrides MX_y with the structure of the $B1$ (NaCl) type. In addition, in some cases the X atoms in the aluminidocarbides and aluminidonitrides M_3AlX with the perovskite type of structure can not only fill the octahedral interstices, but can also substitute aluminium.

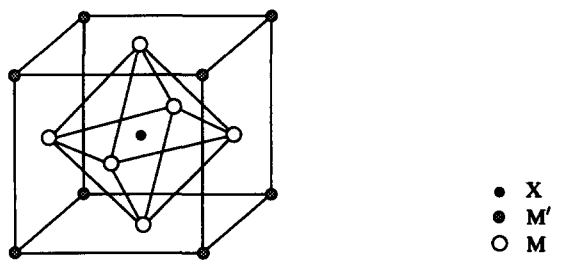


Figure 23. Unit cell of the ternary compounds $M_3M'X$ with the ideal cubic structure (space group $Pm3m$) of the perovskite $CaTiO_3$ type.

Another group of transition metal aluminidocarbides and aluminidonitrides $M_2M'X$ (H-phases) have the hexagonal structure (space group $P6_3/mmc$) of the Cr_2AlC type (Fig. 24). A significant element of this structure, as well as of the previous one, is the octahedron XM_6 formed by six transition metal atoms M with the nonmetal atom X located at the centre of it. In the $M_2M'X$ H-phases, each XM_6 octahedron is joined with the adjacent octahedra via its six edges; thus layers with tetrahedral vacancies between the octahedra are formed (Fig. 24*b*). The nontransition metal atoms M′ are located over these tetrahedral vacancies in the trigonal prisms formed by six M atoms. The octahedral layers separated by the layer of the M′ atoms are packed in such a way that the tetrahedral interstices are located above one another. The unit cell of the H-phases incorporates two $M_2M'X$ formula units.

The frequently occurring aluminidocarbides and aluminidonitrides of the composition $M_3M'_2X$ have a cubic structure [space group $P4_132$ (O^7)] of the β-Mn type ($A13$) in which twenty atoms of the transition and nontransition metals occupy the 12(d) and 8(c) sites, respectively. The transition metal atoms M constitute slightly distorted octahedra that are connected to one another via their vertices; the octahedral interstices correspond to the 4(a) sites in the structures of the β-Mn type, and in the compounds $M_3M'_2X$

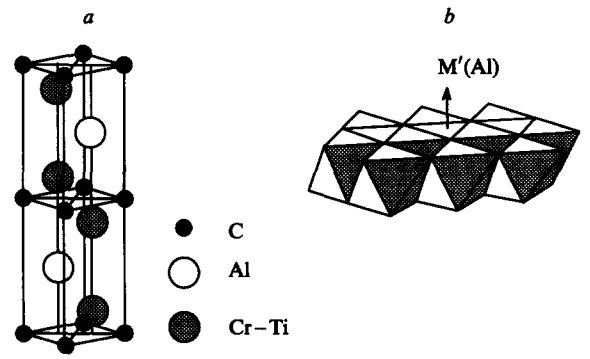


Figure 24. Crystal structure of the Nowotny phase (H-phase) of the Cr_2AlC type ($M_2M'X$).
(a) unit cell (space group $P6_3/mmc$); (b) the layer of the XM_6 octahedra joined via six edges; nontransition metal atoms in compounds with the Cr_2AlC type of structure are arranged over tetrahedral vacancies.

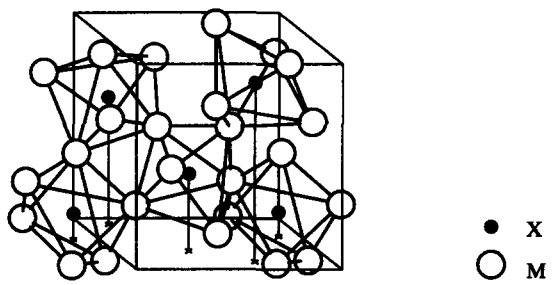


Figure 25. Filled crystal structure of the β-Mn(A13) type of the ternary cubic (space group $P4_132$) compounds $M_3M'_3X$.
Only the transition metal atoms M at the 12(d) sites and interstitial nonmetal atoms X (C,N) at the 4(a) sites are shown; these atoms form distorted XM_6 octahedra joined via all the vertices.

of the stoichiometric composition they are occupied by the nonmetallic interstitial atoms X, that is, carbon or nitrogen atoms (Fig. 25). In the case where the composition of a ternary carbide or nitride with the structure of the β-Mn type deviates from the stoichiometry, some of the octahedral interstices remain vacant.

A filled structure of the Mn_5Si_3 type ($D8_8$) (see Fig. 10), which is common for the transition metal silicoborides, carbosilicides, and siliconitrides $M_5Si_3B_x$, $M_5Si_3C_x$, and $M_5Si_3N_x$ considered above, is also a frequently encountered type of the structure of the ternary compounds in the M – Al – C and M – Al – N systems. It is of interest that this structure is hardly found among the transition metal aluminosilicides.

2. The M – Al – C ternary aluminidocarbide systems

The structural characteristics of the ternary phases formed in the M – Al – C aluminidocarbide systems are presented in Table 9.

Some lanthanides form aluminium and carbon cubic ternary compounds Ln_3AlC (Ln = Tb, Er, Tm) with the perovskite type of structure.[158]

The Ti – Al – C system. In a study of the phase equilibria in the Ti – Al – C system,[179] the existence of the ternary cubic compound Ti_3AlC with the perovskite structure [159] and of the ternary hexagonal compound Ti_2AlC (the H-phase) with the Cr_2AlC type of structure [169–172] has been confirmed (Table 9). The following pseudobinary equilibria occur in the Ti – Al – C system under equilibrium conditions at 1273 K (Fig. 26): $Al_4C_3 - TiC_y$, $TiAl_3 - TiC_y$, $Ti_2AlC - TiAl_3$, $Ti_2AlC - TiAl$, $Ti_2AlC - Ti_3Al$, $Ti_2AlC - Ti_3AlC$, $Ti_2AlC - TiC_y$, $Ti_3AlC - TiC_y$, $Ti_3AlC - Ti_3Al$, Al(liq) – TiC_y, Ti_3AlC – α-Ti(sol) and Ti_3AlC – β-Ti(sol) [Al(liq) is molten aluminium, and α-Ti(sol) and β-Ti(sol) are solid solutions of aluminium in α-Ti and β-Ti, respectively]. Titanium is

Table 9. Some ternary phases in the M–Al–C systems.

Compound	Symmetry and type of structure	Space group	Z	Unit cell parameters / nm		Ref.
				a	c	
Tb_3AlC	Cubic, the perovskite $CaTiO_3$ ($E2_1$) type	$Pm3m$	1	0.4876	–	158
Er_3AlC	"	$Pm3m$	1	0.4792	–	158
Tm_3AlC	"	$Pm3m$	1	0.4776	–	158
Ti_3AlC_x ($x = 1.0$)	"	$Pm3m$	1	0.4156	–	159
Cr_3AlC_x	–	–	–	–	–	160
Mn_3AlC_x ($x = 1.0-1.2$)	Cubic, the perovskite $CaTiO_3$ ($E2_1$) type	$Pm3m$	1	0.3869	–	161–165
Fe_3AlC_x ($x \approx 0.66$)	"	$Pm3m$	1	0.3728–0.3788	–	163, 164
Co_3AlC_x ($x \approx 0.59$)	"	$Pm3m$	1	0.3697	–	163, 164, 166
Ni_3AlC_x ($x \approx 0.3$)	Cubic (a solid solution of carbon in Ni_3Al)	$Pm3m$	1	0.3617	–	163, 164, 167, 168
Ni_3AlC_x ($x \approx 0.3$)	"	$Pm3m$	1	0.3583	–	168
Ti_2AlC	Hexagonal (H-phase of the Cr_2AlC type)	$P6_3/mmc$	2	0.304	1.360	169–172
V_2AlC	"	$P6_3/mmc$	2	0.2913	1.314	169–172
Nb_2AlC	"	$P6_3/mmc$	2	0.3103	1.383	169–172
Ta_2AlC	"	$P6_3/mmc$	2	0.3075	1.383	169–172
Cr_2AlC	"	$P6_3/mmc$	2	0.286	1.282	169–172
Nb_3Al_2C	Cubic, the β-Mn ($A13$) type	$P4_132$	4	0.7065–0.7079	–	172–174
Ta_3Al_2C	"	$P4_132$	4	0.7038	–	172–174
Mo_3Al_2C	"	$P4_132$	4	0.6860–0.6866	–	172, 174–176
$Zr_2Al_3C_5$	Hexagonal	$P31c$	2	0.3345	2.2231	177
$Hf_2Al_3C_5$	"	$P31c$	2	0.3319	2.209	177
$ZrAlC_2$	"	$P6_3/mcm$	6	0.3345	2.761	177
$HfAlC_2$	"	$P6_3/mcm$	6	0.3319	2.742	177
Zr_5Al_3C	Hexagonal, filled structure of the Mn_5Si_3 type ($D8_8$)	$P6_3/mcm$	2	0.822	0.568	177
Hf_5Al_3C	"	$P6_3/mmc$	2	0.812	0.5679	172, 177
Ta_5Al_3C	"	$P6_3/mmc$	2	0.7734	0.5245	177
$Th_4Al_2C_5$	–	–	–	–	–	178
$ThAlC_2$	–	–	–	–	–	178
$ThAl_4C_4$	Hexagonal	–	–	0.823	0.334	178

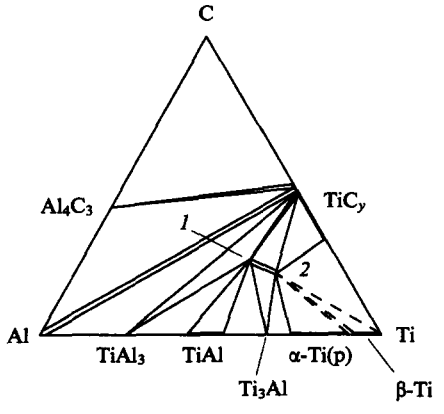


Figure 26. Isothermal cross-section through the Ti–Al–C system at 1273 K (the dark areas denote one-phase regions).[179]
(*1*) Ti_2AlC; (*2*) Ti_3AlC.

insoluble in Al_4C_3, carbon is insoluble in titanium aluminides, and aluminium is insoluble in TiC_y. α-Ti dissolves up to 10 at.% of aluminium. The Ti_2AlC H-phase annealed at 973 K has no homogeneity region. The variation of the unit cell parameters on the substitution of titanium by aluminium in the ternary phases is relatively greater than the variation caused by a similar change in the carbon content.[179] Thus, the lattice period of the Ti_3AlC annealed at 1273 K decreases on the substitution of titanium by aluminium and increases with an increase in the concentration of carbon. The unit cell parameters of the Ti_2AlC H-phase annealed at 1273 K vary in the ranges $a = 0.3045$ to 0.3065 nm and $c = 1.3636$ to 1.3671 nm. The variation of the unit cell parameters points to the existence of small homogeneity regions of the ternary phases annealed at 1273 K.

While considering the phase equilibria in the Ti–Al–C system, one should mention a study[180] published in 1988, when the ternary compounds Ti_2AlC and Ti_3AlC were already known, in which a wrong variant of the phase diagram with no allowance for the existence of the ternary phases was suggested for the Ti–Al–C system.

The Zr–Al–C system. All the known zirconium aluminides except for Zr_2Al, Zr_5Al_4, and Zr_5Al_3, have been found in the Zr–Al–C system.[177] The Zr_2Al phase may be stabilised only in the presence of silicon.[181] The aluminide Zr_5Al_4 decomposes at a

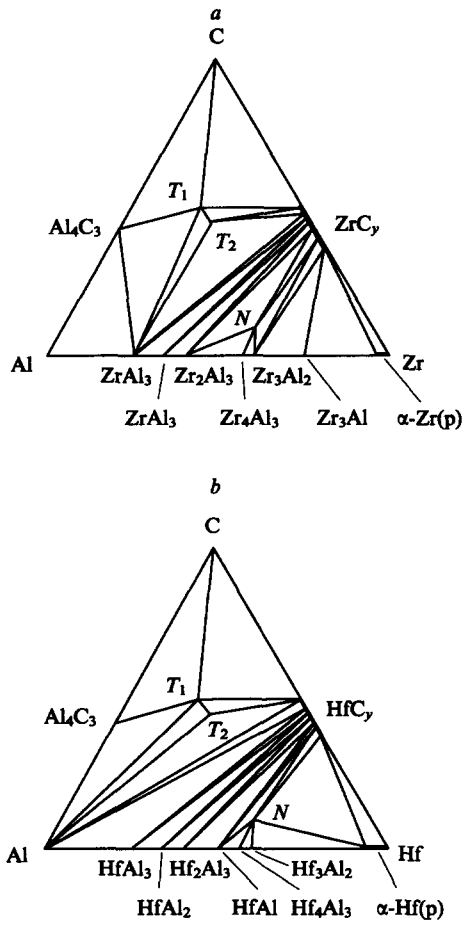


Figure 27. Isothermal cross-sections through the Zr–Al–C (*a*) and Hf–Al–C (*b*) systems at 973 K (dark sections denote single-phase homogeneity regions of carbides and of solid solutions of aluminium in transition metals).[177]
$T_1 = M_2Al_3C_{5-x}$, $T_2 = MAlC_{2-x}$, $N = M_5Al_3C$ (M = Zr, Hf).

temperature of ~1250 K, and Zr_5Al_3 almost coincides in its composition with Zr_3Al_2.

Three ternary phases have been found in the Zr–Al–C system: $Zr_2Al_3C_{5-x}$, $ZrAlC_{2-x}$, and Zr_5Al_3C (see Table 9). The new ternary compound with the ideal formula $Zr_2Al_3C_5$ has a hexagonal structure [space group $P31c$ (C_{3v}^4)] with the unit cell parameters $a = 0.3345$ nm and $c = 2.2230$ nm; carbon atoms are located in the octahedral interstices. The $ZrAlC_2$ phase also crystallises with a hexagonal structure [space group $P6_3/mmc$ (D_{6h}^4)], carbon being located in the octahedral interstices. The Zr_5Al_3C phase has a structure of the Mn_5Si_3 type the octahedral interstices of which are filled with carbon.

The greatest number of pseudobinary equilibria in the Zr–Al–C system are formed by the very stable zirconium carbide ZrC_y (Fig. 27*a*). However, in contrast to the Ti–Al–C system, ZrC_y does not form pseudobinary equilibria with aluminium at temperatures below ~1300 K. Carbon is soluble only in the aluminide Zr_3Al_2 (Zr_5Al_3), thus stabilising its structure (Mn_5Si_3 type); aluminium is insoluble in ZrC_y. The distribution of the phase fields near the ternary compound Zr_5AlC_3 at 1273 K differs from that at 973 K, namely, the ZrC_y–Zr_3Al_2 and ZrC_y–Zr_3Al equilibria disappear, the Zr_5Al_3C–Zr_3Al and Zr_5Al_3C–β-Zr(sol) appearing instead [β-Zr(sol) is the solid solution of aluminium in β-Zr].

The Hf–Al–C system. Three ternary compounds exist in the Hf–Al–C system, their structures and compositions (see Table 9) being similar to those of the corresponding ternary compounds formed in the Zr–Al–C system.[177] However, in contrast to the zirconium-containing system, there is no Al_4C_3–$HfAl_3$ equilibrium in the system under consideration, and aluminium coexists with $Hf_2Al_3C_5$, $HfAlC_2$, and HfC_y (Fig. 27*b*). Carbon is insoluble in the hafnium aluminides and aluminium is insoluble in hafnium carbide. The phase equilibria in the Hf–Al–C system at 973 K and 1273 K are virtually identical, differing only in that the solubility of aluminium in α-Hf increases (up to 12 at.% of Al at 1273 K) and some solubility of carbon in α-Hf appears.

The V–Al–C system. One ternary compound, namely V_2AlC with a hexagonal structure of the Cr_2AlC type, is formed in the V–Al–C system (see Table 9).[169–172] At 1273 K this compound coexists with molten aluminium, the carbides Al_4C_3, VC_y, ζ-V_4C_3, and V_2C, and with V(sol) [V(sol) is the solid solution of aluminium in vanadium]; Al_4C_3 exists in an equilibrium with VC_y (V_8C_7), and V_2C is in an equilibrium with V(sol).[179] The solid solution V(sol) coexisting with V_2AlC and V_2C contains up to 23 at.% of Al. Note that both the disordered carbide VC_y and the ordered phase V_8C_7 have been observed in this system at 1273 K.[179] The V_2AlC ternary phase has no homogeneity region, binary phases do not dissolve the third component.[179]

The Nb–Al–C system. The data[169–172] concerning the existence of the Nb_2AlC ternary *H*-phase in this system (see Table 9) have been confirmed by Schuster et al.[177] At 973 K this phase exists in equilibrium with $NbAl_3$, Nb_2Al, Nb_3Al, NbC_y, and Nb_2C; NbC_y coexists with Al_4C_3 and $NbAl_3$, and Al_4C_3 coexists with $NbAl_3$ (Fig. 28*a*). The carbide Nb_3Al_2C with the β-Mn type of structure (see Table 9) is unstable at 973 K and is not shown in Fig. 28*a*.

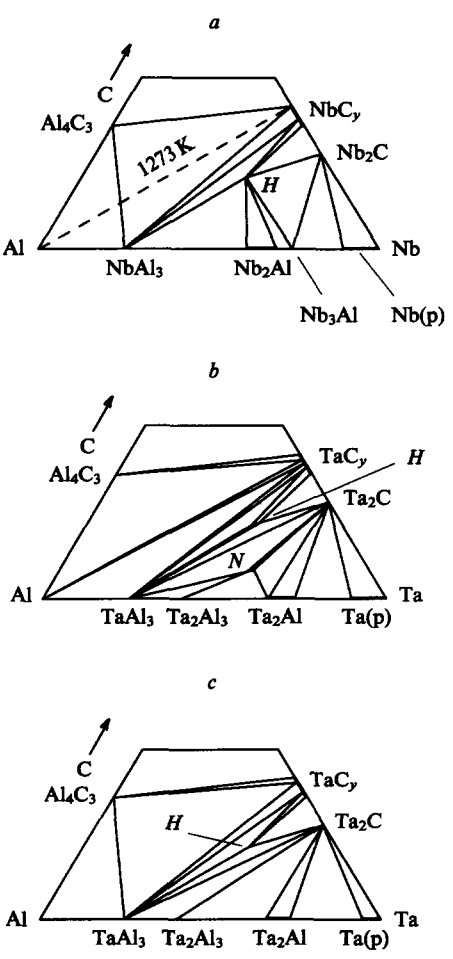


Figure 28. Isothermal cross-sections through the Nb–Al–C system at 973–1273 K (*a*) and through the Ta–Al–C system at 1273 K (*b*) and 973 K (*c*).[177]
$H = Nb_2AlC$ (*a*), Ta_2AlC (*b*, *c*), $N = Ta_5Al_3C$.

At a higher temperature of 1273 K the $Al_4C_3-NbAl_3$ equilibrium disappears, and the carbide NbC_y coexists directly with liquid aluminium (similarly to the Ti–Al–C system in which the carbide TiC_y is in an equilibrium with liquid aluminium). In all other aspects, the isothermal cross-sections through the Nb–Al–C system at 973 K and 1273 K are similar.

The variation of the parameters of the *H*-phase (*a* varies from 0.3105 nm to 0.3115 nm and *c* varies from 1.3860 nm to 1.3921 nm) indicates the existence of a small homogeneity region corresponding to the formula $Nb_{2-x}Al_{1+x}C_{1-x/2}$, which was suggested in a previous study.[169] Carbon is insoluble in the niobium aluminides, and aluminium is insoluble in the niobium carbides.

The Ta–Al–C system. The isothermal cross-sections through the Ta–Al–C system at 973 K and 1273 K are shown in Fig. 28*b,c*. At 973 K one ternary compound with the formula Ta_2AlC exists in this system, and at 1273 K the second ternary compound appears, namely, $Ta_5Al_3C_x$ with a filled structure of the Mn_5Si_3 type (see Table 9). The ternary compound Ta_3Al_2C is unstable at these temperatures and is not shown in Fig. 28*b,c*. At 1273 K carbon populates only some of the octahedral interstices of the tantalum sublattice in $Ta_5Al_3C_x$ ($x < 1.0$), and the occupation of all the interstices can be achieved at a higher temperature.

As the temperature increases, carbon stabilises the Ta_5Al_3C phase with the $D8_8$ type of structure; as this takes place an equilibrium arises between the carbide TaC_y and liquid aluminium, and the $Al_4C_3-TaAl_3$ equilibrium disappears (see Fig. 28*b,c*).

The Cr–Al–C system. There is one ternary compound in this system: Cr_2AlC (see Table 9), which is more stable at 1073 K than the carbides Al_4C_3 and Cr_3C_2 and exists in an equilibrium directly with carbon (graphite); with an increase in the temperature, the *H*-phase becomes less stable than Al_4C_3 and Cr_3C_2, and the Cr_2AlC-C equilibrium disappears (Fig. 29). According to the data obtained by Schuster et al.,[179] the compound Cr_2AlC has no homogeneity region. There is no solubility of the third component in the binary phases of the Cr–Al–C system. The existence of the Cr_3AlC carbide phase with an unknown structure has been reported;[160] however, these data have not been confirmed subsequently.

The Mo–Al–C system. One ternary compound has been detected in this system, namely, the compound Mo_3Al_2C with a cubic structure of the β-Mn type, similar to the analogous compounds formed in the Nb–Al–C and Ta–Al–C systems. The aluminidocarbide Mo_3Al_2C exists in equilibrium with the carbides Al_4C_3 and Mo_2C and with the aluminides Mo_3Al_8 and Mo_3Al; Al_4C_3 coexists with Mo_2C, $MoAl_3$, and Mo_3Al_8; the carbide Mo_2C is in equilibrium with Mo_3Al and with the solid solution of aluminium and carbon in molybdenum Mo(Al,C).[176] The ternary compound Mo_3Al_2C has a small homogeneity region and is formed via a peritectic reaction between the carbide Mo_2C and the aluminium melt. A ternary eutectic ($Mo_3Al_2C + Mo_3Al + Mo_3Al_8$) with a melting point of ~1823 K exists in the system. The compound Mo_3Al_2C has a small homogeneity region: as the content of molybdenum increases from 47 to 51 at.%, the content of carbon being constant and equal to 16.7 at.%, the cubic lattice period increases from 0.6860 nm to 0.6866 nm.[171,172] A small amount of carbon can be dissolved in all the molybdenum aluminides, whereas molybdenum (up to 3 at.%) is soluble in Al_4C_3. In all probability, the $Al_4C_3-MoC_y$ (Mo_3C_2) pseudobinary equilibrium should exist in the Mo–Al–C system at $T > 1750$ K.

The W–Al–C system. There are no ternary compounds in the W–Al–C system at 1173 K.[176] The intermetallide WAl_2 exists in equilibrium with the carbides Al_4C_3, WC, and W_2C, whereas Al_4C_3 is in equilibrium with the hexagonal carbide WC (the WC_y high-temperature cubic phase was not taken into account). It should be kept in mind that the designation of the intermetallide WAl_2, which is formed from tungsten and aluminium melt via the peritectic reaction and is stable in the narrow temperature range from 1600 K to 1830 K, is somewhat arbitrary.[182]

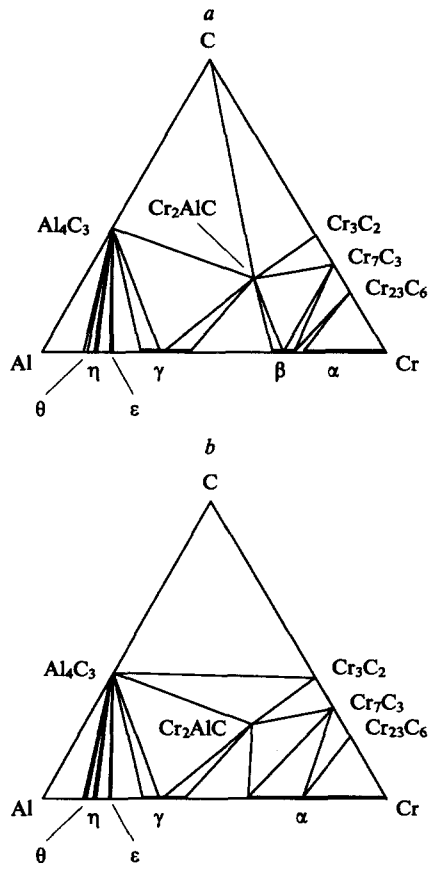


Figure 29. Isothermal cross-sections through the Cr–Al–C system at 1073 K (*a*) and 1273 K (*b*) (dark sections denote single-phase regions).[179]

The Mn–Al–C system. A study of the phase equilibria in the Mn–Al–C system has provided evidence for the existence of the ternary compound Mn_3AlC with the perovskite type of structure[183] (see Table 9). At 973 K this compound is in equilibrium with Al_4C_3 and with solid solutions of aluminium in α-Mn(sol) and β-Mn(sol) as well as with the carbides Mn_7C_3, Mn_5C_2, and $Mn_{23}C_6$ and with carbon, whereas Al_4C_3 is in equilibrium with all the manganese aluminides (Fig. 30*a*). The period of the lattice of Mn_3AlC annealed at 973 K varies from 0.3856 nm to 0.3873 nm. This apparently reflects the variation of the carbon content in the compound rather than the alteration of the ratio between the manganese and aluminium. A similar conclusion can be drawn from the results of another study.[163]

At 1273 K γ-Mn dissolves ~5 at.% of carbon and 25 at.% of aluminium thus forming a broad one-phase region; the high-temperature ε-MnAl phase dissolves up to 5 at.% of carbon (Fig. 30*b*). The parameters of the cubic lattice in the compounds Mn_3AlC thus formed differ from each other and are equal to 0.3840 nm and 0.3874 nm. It should be noted that two phases (apart from the γ-Mn Fcc structure) with the perovskite structure and different parameters, $a = 0.384$ nm and $a = 0.387$ nm, have been also observed in the Mn_7Al_2C alloy.

The temperature of the congruent melting of Mn_3AlC is 2000 K.

The Fe–Al–C system. Figure 31 presents a fragment of the Fe–Al–C ternary system at 1273 K.[184] The carbide Fe_3AlC_x with the perovskite type of structure is formed in this system (see Table 9); the metal atoms in this compound form an ordered Fcc-lattice. The corresponding aluminide Fe_3Al has a cubic structure (space group $Fm3m$) of the $BiLi_3$ or BiF_3 ($D0_3$) type. This structure consists of four interpenetrating Fcc sublattices.

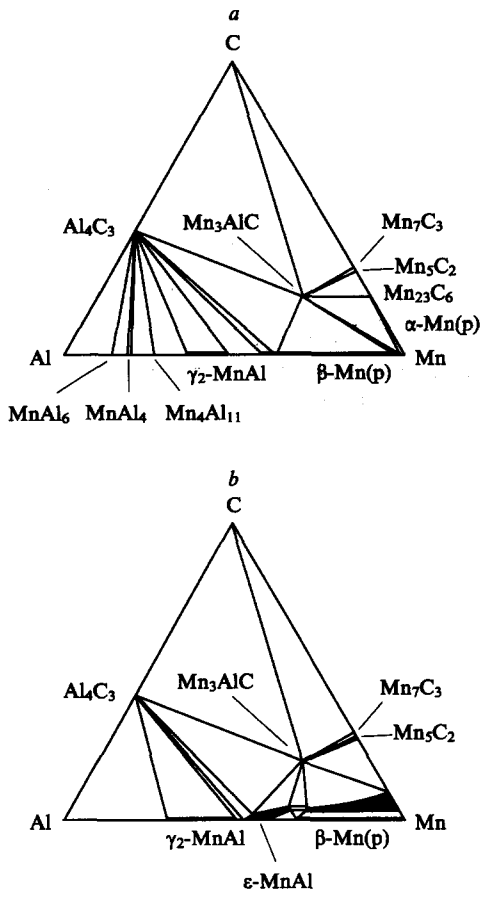


Figure 30. Isothermal cross-sections through the Mn–Al–C system at 973 K (*a*) and 1273 K (*b*) (dark sections denote single-phase regions).[183]

The aluminium atoms are located at the unit cell vertices and at the centres of faces, whereas iron atoms occupy the centres of octahedral and tetrahedral interstices of the aluminium Fcc-sublattice. As a whole, the atoms in Fe_3Al populate the same positions as do the atoms in the eight cells of a body-centred cubic (Bcc) lattice of the CsCl(*B*2) type. This permits Fe_3Al to be regarded as a superstructure based on a Bcc lattice. The introduction of carbon into Fe_3Al leads to the formation of the ternary carbide Fe_3AlC with the perovskite type of structure. The carbide Fe_3AlC has an extended homogeneity region that is connected to the homogeneity region of austenite γ-Fe(C) via a two-phase region. The ternary compound Fe_3AlC_x exists in equilibrium with Fe_3Al, FeAl, the solid solution of aluminium in α-Fe, γ-Fe(C), carbon, and possibly with the cementite Fe_3C.

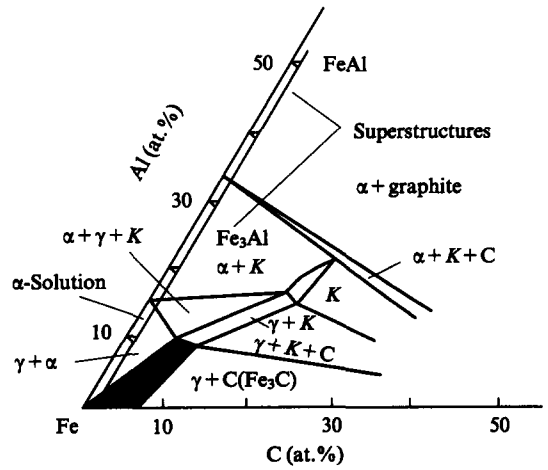


Figure 31. Fragment of the isothermal cross-section through the Fe–Al–C system at 1273 K.[184]
K is the ternary compound Fe_3AlC_x with the perovskite type of structure; dark area indicates the region of austenite γ-Fe(C).

The Co–Al–C system. One ternary compound Co_3AlC_x with the perovskite type of structure is formed in the Co–Al–C system.[163,164,166] The proportions of carbon in Co_3AlC_x and Fe_3AlC_x are approximately equal ($x \approx 0.6$).[163,164] The carbide Co_3AlC_x is formed via a peritectic reaction of CoAl with carbon and aluminium melt. The ternary compound Co_3AlC_x forms pseudobinary equilibria with α-Co (more precisely, with the limited solid solution of aluminium and carbon in cobalt), CoAl, C, and probably with Al_4C_3.

The Ni–Al–C system. In the Ni–Al–C system, the nickel aluminide Ni_3Al [Cu_3Au ($L1_2$) structural type, space group $Pm3m(O_h^1)$] has an ordered cubic lattice and dissolves up to 7 at.% of carbon, the symmetry of the metallic lattice being retained and the period of the lattice increasing from 0.3587 nm to 0.3617 nm.[163,164] Thus, the Ni_3AlC_x phase is an interstitial solid solution of carbon in Ni_3Al. The structure of this solid solution is characterised by the same distribution of atoms as in the carbides M_3AlC_x with the perovskite structure, which has been confirmed in a special study.[168] The method of forming the Ni_3AlC_x solid solution and its crystal structure (the $L1_2$ type with some of the octahedral interstices being filled with carbon atoms) indicate that the compounds M_3AlC_x with the perovskite structure are interstitial compounds, like the cubic [with the structure of the NaCl(*B*1) type] carbides and nitrides MX_y ($y \leqslant 1.00$).

It has been found[168] that carbon is markedly soluble not only in Ni_3Al, but also in NiAl. According to this study, on passing from Ni_3Al to $Ni_3Al(C_{1.0})$, the period of the metallic lattice increases from 0.3557 nm to 0.3583 nm.

3. The ternary M–Al–N aluminidonitride systems

The interest in the use of the compounds and heterophase compositions formed in the M–Al–N systems as abrasives is due to their high chemical stability and hardness. In addition, the ability of the aluminium nitride AlN to retain its high mechanical properties at elevated temperatures $T > 1000$ K makes the development of construction materials based on it particularly attractive, since these materials can be used under drastic conditions, for example, in aggressive media, at high temperatures, and under great loads.

The structural characteristics of the ternary phases formed in the M–Al–N systems are listed in Table 10.

The Sc–Al–N system. All the alloys formed in the Sc–Al–N systems in which the concentration of scandium is more than 50 at.% contain the Sc_3AlN_x ternary cubic phase with the perovskite structure.[185] The ternary compound Sc_3AlN_x is in equilibrium with ScAl, Sc_2Al, ScN, and Sc(sol) (the solid solution of Al and N in scandium). In addition, the following pseudobinary equilibria exist in the Sc–Al–N system: AlN–$ScAl_3$, AlN–$ScAl_2$, AlN–ScN, ScN–$ScAl_2$, ScN–ScAl, ScN–Sc(sol), and Sc_2Al–Sc(sol) (Fig. 32*a*). The lattice period of Sc_3AlN_x is 0.4396 nm (in equilibrium with ScAl and Sc_2Al), 0.4405 nm [in equilibrium with Sc(sol) and ScN], and 0.4435 nm (in equilibrium with ScN and ScAl). Scandium dissolves up to 15 at.% of nitrogen and more than 5 at.% of aluminium.

The Yl–Al–N system. According to Schuster and Bauer,[185] there are no ternary phases in this system at temperatures from 1073 K to 1573 K. At 1273 K the yttrium nitride YN coexists with AlN, YAl_2, YAl, and Y_3Al_2, whereas the aluminium nitride AlN coexists with YAl_2 (Fig. 32*b*). At 1573 K the aluminides YAl and Y_3Al_2 disappear from the Y–Al–N system, the AlN + YN + YAl_2 region being retained as the only solid three-phase region.

Table 10. Some ternary phases in M–Al–N systems.

Compound	Symmetry and type of structure	Space group	Z	Unit cell parameters / nm			Ref.
				a	b	c	
Sc_3AlN_x	Cubic, the perovskite $CaTiO_3$ ($E2_1$) type	$Pm3m$	1	0.4396–0.4435	–	–	185
La_3AlN_x	"	$Pm3m$	1	0.507	–	–	186
Nd_3AlN_x	"	$Pm3m$	1	0.4910	–	–	187
Nd_3AlN_x	"	$Pm3m$	1	0.4939	–	–	186
Sm_3AlN_x	"	$Pm3m$	1	0.4862	–	–	186
$Ce_3Al(N)$	Cubic, a solid solution of nitrogen in Ce_3Al [the Cu_3Au ($L1_2$) type]	$Pm3m$	1	0.5008	–	–	186
$Pr_3Al(N)$	Cubic, a solid solution of nitrogen in Pr_3Al [the Cu_3Au ($L1_2$) type]	$Pm3m$	1	0.4977	–	–	186
Ti_3AlN	Cubic, the perovskite $CaTiO_3$ ($E2_1$) type	$Pm3m$	1	0.4120	–	–	188
$Fe_4N(Al)$ (Fe_3AlN)	Cubic, a solid solution of aluminium in γ-Fe_4N ($L'1$)	–	1	0.380	–	–	189
$Ni_3Al(N)$	Cubic (a solid solution of nitrogen in Ni_3Al (the Cu_3Au ($L1_2$) type)	$Pm3m$	1	0.380	–	–	189
Ti_2AlN_x	Hexagonal (H-phase the Cr_2AlC type)	$P6_3/mmc$	2	0.2991–0.304	–	1.361–1.369	188, 190–192
$Ti_3Al_2N_2$	Trigonal	$P31c$	2	0.2988	–	2.335	188
Zr_3AlN	Monoclinic	–	–	0.5988	0.8966	0.3367[a]	193
Hf_3AlN	"	–	–	0.5901	0.8865	0.3319[b]	194
Zr_3AlN	Orthorhombic, the type of filled Re_3B	$Cmcm$	4	0.3369	1.1498	0.8983	195
Hf_3AlN	"	$Cmcm$	4	0.3319	1.1326	0.8865	195
$Zr_5Al_3N_x$ ($0.1 \leqslant x \leqslant 0.9$)	Hexagonal, the type of filled Mn_5Si_3 ($D8_8$)	$P6_3/mcm$	2	0.8170–0.8240	–	0.5655–0.5694	193, 194
$Hf_5Al_3N_x$	"	$P6_3/mcm$	2	0.8062	–	0.5603	194
$Ta_5Al_3N_x$	Tetragonal, the Cr_5B_3 ($D8_l$) type	$I4/mcm$	4	–	–	–	196
Nb_3Al_2N	Cubic, the β-Mn type	$P4_132$	4	0.7031–0.7039	–	–	174, 196, 197

[a] In the unit cell $\beta = 106.39°$. [b] In the unit cell $\beta = 106.33°$.

The Ln–Al–N systems. A study has shown [186] that there are no ternary phases in the Ln–Al–N systems with Ln = Gd, Tb, Dy, Ho, Er, Tm, Yb, and Lu. In the La–Al–N, Nd–Al–N, and Sm–Al–N systems, the Ln_3AlN_x ternary phases with the perovskite type of structure are formed, whereas in the Ce–Al–N and Pr–Al–N systems, the Ce_3AlN_x and Pr_3AlN_x ternary phases based on the aluminides Ce_3Al and Pr_3Al with structures of the Cu_3Al ($L1_2$) type are formed. The latter result from filling of the octahedral interstices of the lanthanide sublattice with nitrogen atoms.

Figure 33 presents the isothermal cross-section through the Pr–Al–N system at 873 K.[186] The ternary compound Pr_3AlN coexists with $PrAl_2$, $PrAl_3$, PrN, and Pr, the aluminium nitride

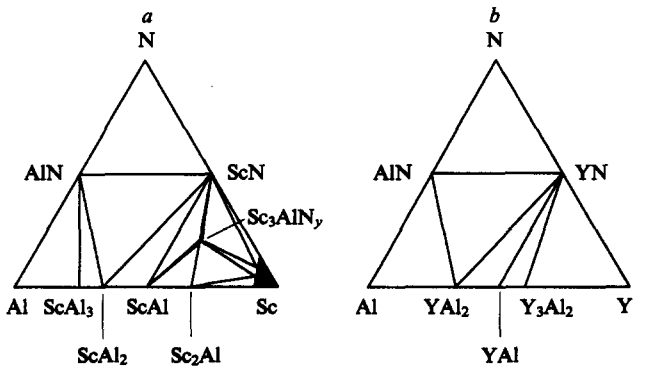


Figure 32. Isothermal cross-sections through the Sc–Al–N (*a*) and Y–Al–N (*b*) systems at 1273 K (dark areas indicate single-phase regions).[185]

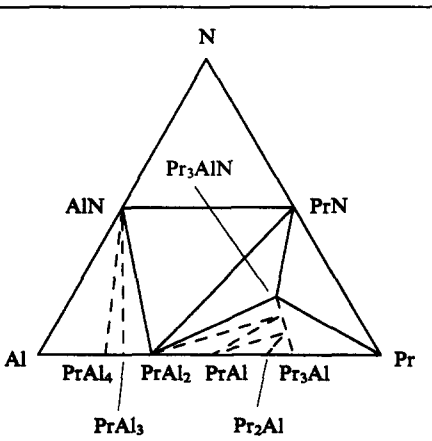


Figure 33. Isothermal cross-section through the Pr–Al–N system at 873 K (pseudobinary equilibria marked by dashed lines are shown conventionally).[186]

AlN coexists with $PrAl_4$, $PrAl_3$, $PrAl_2$, and PrN, and $PrAl_2$ is in an equilibrium with PrN. The $Pr_3Al-Pr_3AlN_x$ pseudobinary equilibrium is shown with a dashed line, because the ternary phase is actually a solid solution of nitrogen in the aluminide Pr_3Al. The equilibria in the $PrAl_4-AlN-PrAl_3$ and $PrAl_2-Pr_3AlN_x-Pr_3Al$ regions are shown arbitrarily and require additional investigation.

The Ti–Al–N system. Numerous studies of the phase relationships in the Ti–Al–N ternary system have shown that depending on the temperature, two or three ternary compounds can exist in it under equilibrium conditions. At 1273 K there are two ternary phases Ti_3AlN and Ti_2AlN.[188] The cubic phase Ti_3AlN with the perovskite structure (see Table 10) is iso-structural to the carbide Ti_3AlC[159] and has a negligibly small homogeneity region. The hexagonal Ti_2AlN *H*-phase has been detected for the first time by Jeitschklo et al.[190] Its existence has been confirmed in other studies.[188,191,192] This phase is isostructural to the analogous Ti_2AlC phase[169–172] crystallising with the Cr_2AlC type of structure and, judging from the difference in the lattice parameters determined in a number of studies,[188,190,191] it possesses a certain homogeneity region, which is defective with respect to nitrogen. At 1273 K, the ternary cubic Ti_3AlN phase coexists with Ti_3Al, TiN_y, and Ti_2AlN, whereas the Ti_2AlN *H*-phase is in an equilibrium with TiAl, Ti_3Al, Ti_3AlN, TiN_y, and AlN. In addition, the AlN–TiAl, AlN–TiN_y, and TiN_y–Ti_3Al pseudobinary equilibria exist in the Ti–Al–N system. The solubility of aluminium in TiN_y is less than 2 at.%. The lower hexagonal titanium nitride ε-Ti_2N does not form any equilibria with ternary compounds or titanium aluminides; it coexists only with TiN_y and with the solid solution of aluminium and nitrogen in α-Ti.

Apart from Ti_2AlN and Ti_3AlN, the $Ti_3Al_2N_2$ ternary phase with a layered trigonal structure (see Table 10) arises in the Ti–Al–N system at 1573 K. It coexists with AlN, TiN_y, TiAl, $TiAl_3$, and Ti_2AlN (Fig. 34) and exists in the narrow temperature range 1473–1573 K.

The Zr–Al–N system. The phase equilibria in this system have been studied.[193,195] The ternary compound Zr_3AlN exists in the Zr–Al–N system at 1273 K (see Table 10). Initially this compound was believed to crystallise with a monoclinic symmetry;[193] however, an X-ray diffraction structural study of its single crystal[195] has shown that Zr_3AlN has an orthorhombic structure of the Re_3B type. The aluminium atoms in the compound Zr_3AlN are located at the centres of trigonal prisms formed by six zirconium atoms, whereas the nitrogen atoms are arranged in the weakly distorted octahedral interstices of the zirconium sublattice. The formation of the second ternary phase $Zr_5Al_3N_x$ is associated with the stabilisation of the hexagonal structure of the Mn_5Si_3 type with nitrogen; at 1273 K the nitrogen content in $Zr_5Al_3N_x$ is low ($x < 0.2$).

At a temperature of 1273 K the compound Zr_3AlN exists in equilibrium with AlN, Zr_2Al_3, ZrAl, $Zr_5Al_3N_x$ ($x < 0.2$), ZrN_y, and α-Zr(sol) (the solid solution of aluminium and nitrogen in α-Zr); the aluminium nitride coexists with $ZrAl_3$, $ZrAl_2$, Zr_2Al_3, and ZrN_y; the $Zr_5Al_3N_x$ phase exists in equilibrium with ZrAl, Zr_5Al_4, Zr_3Al_2, Zr_5Al_3, Zr_2Al, and α-Zr(sol); and ZrN_y is in equilibrium with α-Zr(sol) (Fig. 35*a*). Note that in a study of the Zr–Al–C system, Schuster and Nowotny[177] did not find such zirconium aluminides as Zr_2Al, Zr_5Al_4, and Zr_5Al_3, which have been observed in the related Zr–Al–N ternary system.[193]

An increase in the temperature to 1573 K leads to a substantial extension of the homogeneity region of the Zr_5Al_3N ternary phase, which contains up to 10 at.% of nitrogen under these conditions. At 1573 K the appearance of the phase diagram of the Zr–Al–N system (Fig. 35*b*) changes somewhat, since the ZrN_y-ZrAl_2, $ZrN_y-Zr_2Al_3$, $ZrN_y-Zr_5Al_3N$, $Zr_2Al_3-Zr_5Al_3N$, $ZrAl-Zr_5Al_3N$, and Zr_5Al_3N–β-Zr(sol) pseudobinary equilibria arise [β-Zr(sol) is the solid solution of aluminium in β-Zr].

The Hf–Al–N system. Only one stable ternary phase exists in this system at 1273 K, namely, the Hf_3AlN phase with a monoclinic structure determined using a powder.[194] A single-crystal X-ray diffraction study[195] has shown that Hf_3AlN has an orthorhombic structure of the Re_3B type. The Hf_3AlN phase coexists with HfN_y, AlN, Hf_2Al_3, HfAl, Hf_4Al_3, Hf_3Al_2, and α-Hf(sol) (the solid solution of aluminium and nitrogen in hafnium, Fig. 35*c*). The line connecting HfN_y and α-Hf(sol) confines the possible area of the existence of the nitrides Hf_4N_{3-x} and Hf_3N_{2-x}, which are unstable at 1273 K.

The X-ray diffraction patterns of the samples, the compositions of which corresponded to the $Hf_2Al_3-Hf_3AlN-HfAl$ region, exhibited an additional set of reflections due to a fourth phase.[194] In all probability, this phase exists in the equilibrium state only at lower temperatures or is stabilised by admixtures.

Two ternary phases Hf_3AlN and Hf_5Al_3N exist in the Hf–Al–N system at 1673 K (Fig. 35*d*). The Hf_5Al_3N phase has a structure of the Mn_5Si_3 type; its unit cell parameters ($a = 0.8062$ nm, $c = 0.5603$ nm) are smaller than those of the analogous carbide phase Hf_5Al_3C ($a = 0.8120$ nm, $c = 0.5679$ nm). It follows from the comparison of the unit cell dimensions of Zr_5Al_3C and Zr_5Al_3N, Hf_5Al_3C and Hf_5Al_3N that nitrogen occupies only some of the octahedral interstices of the transition metal sublattice. It should be noted that the Hf_5Al_3N and Hf_3AlN ternary phases have no homogeneity regions.

The V–Al–N system. In the temperature range from 1273 to 1773 K no ternary compounds exist in this system, although the attempts to synthesise the nitride V_2AlN with a structure of the *H*-phase have resulted in some cases in multiphase samples, the X-ray diffraction patterns of which contained lines due to the *H*-phase.[198] However, the observed lattice parameters were close to those of the carbide V_2AlC *H*-phase. In addition, the sample containing the *H*-phase was nonequilibrium and incorporated more than three phases. The $V_{0.50}Al_{0.25}N_{0.25}$ alloy corresponding to the ideal stoichiometric composition of the *H*-phase contained only the nitrides VN_y and AlN even at a nitrogen pressure of 3×10^6 Pa. Thus, no ternary phases were detected in the V–Al–N system in the experiment described above.[198]

At $T = 1273$ K the aluminium nitride AlN is in equilibrium with VAl_3, V_5Al_8, VN_y, and V(sol) [V(sol) is the solid solution of aluminium and nitrogen in vanadium]; VN_y and V_9N_4 exist in equilibrium with V(sol). At 1573 K the cubic nitride VN_y does not exist, therefore the AlN–V_9N_4 equilibrium arises. The V(sol) solid solution existing in equilibrium with AlN and V_9N_4 has the

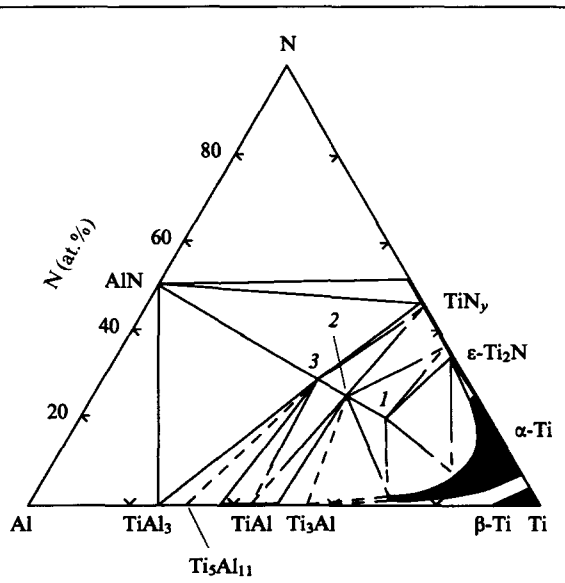


Figure 34. Isothermal cross-section through the Ti–Al–N system at 1573 K (dark areas denote single-phase regions).[188]
(*1*) Ti_3AlN, (*2*) Ti_2AlN, (*3*) $Ti_3Al_2N_2$.

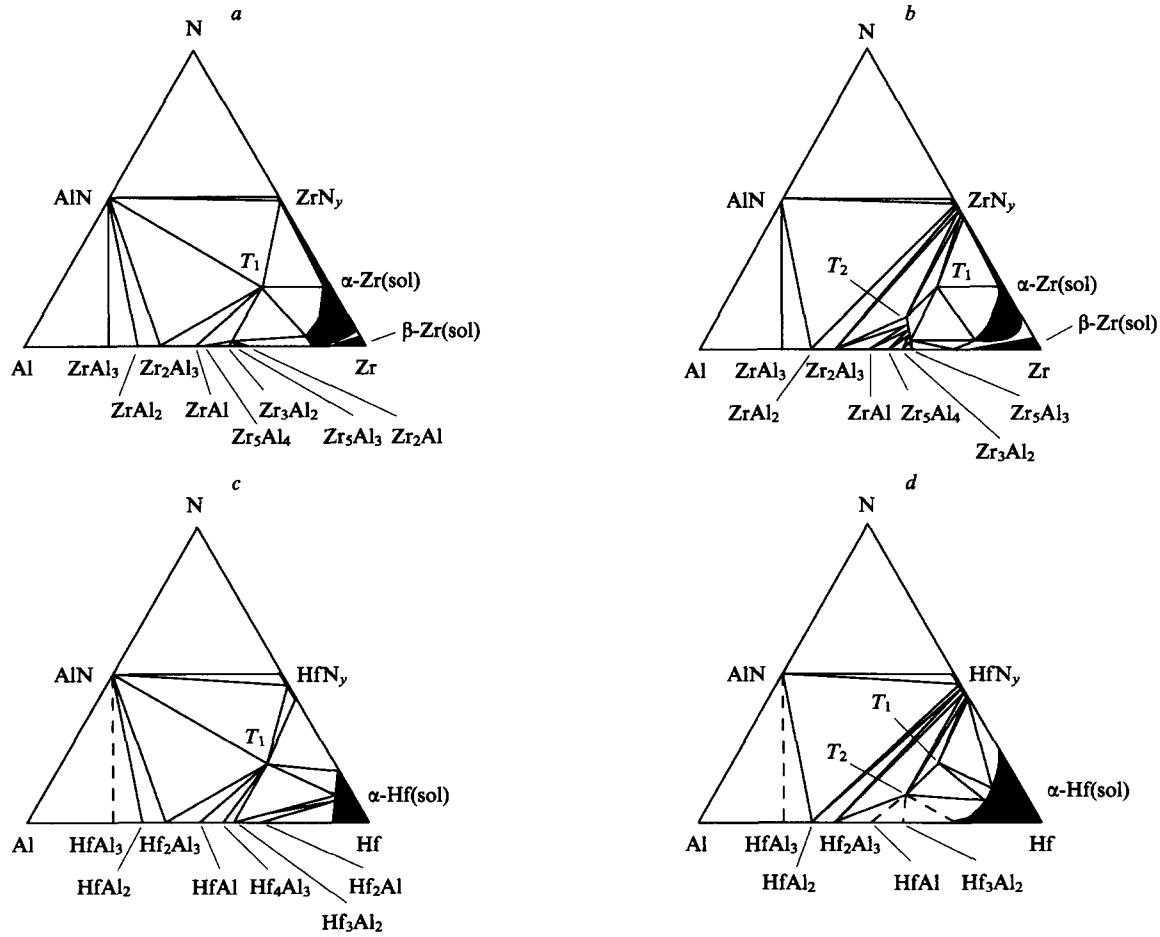


Figure 35. Isothermal cross-sections of the Zr – Al – N system at 1273 K (*a*) and 1573 K (*b*) and of the Hf – Al – N system at 1273 K (*c*) and 1673 K (*d*).[193,194] Dark areas denote single-phase regions; pseudobinary equilibria marked by dashed lines are shown conventionally; T_1 = M_3AlN, T_2 = M_5Al_3N (M = Zr, Hf).

composition $V_{0.67}Al_{0.33}$. At 1773 K the AlN + V_9N_4 + V(sol) field is the main region where ternary phase equilibria exist. The solubility of nitrogen in the V(sol) solid solution with high aluminium proportions is low, but it increases markedly with the decrease in the amount of aluminium. The homogeneity region of the V(sol) solid solution expands with an increase in the temperature.

The Nb – Al – N system. The phase equilibria in the Nb – Al – N system have been studied by Schuster and Nowotny.[197] The samples for the investigation were prepared by sintering Nb – Al alloys with the nitrides AlN and NbN under an argon atmosphere. Previously the ternary compound Nb_3Al_2N with a structure of the β-Mn type has been found in this system.[174,196] According to Schuster and Nowotny,[197] this compound is stable in the temperature range from 1273 to 1773 K studied and melts congruently. The compound Nb_3Al_2N exists in equilibrium with AlN, Nb_2N, $NbAl_3$, and Nb_2Al; the nitride AlN is in equilibrium with $NbAl_3$ and with the niobium nitrides Nb_4N_3 and Nb_2N; and Nb_2N also coexists with Nb_2Al, Nb_3Al, and the solid solution of aluminium and nitrogen in niobium (Fig. 36*a*). The solubility of Nb or Nb-containing compounds in AlN is negligibly small. The compound Nb_3Al_2N has apparently a narrow homogeneity region, since the period of its lattice varies from 0.70314 nm (in equilibrium with Nb_2Al and Nb_2N) to 0.70387 nm (in equilibrium with $NbAl_3$ and Nb_2Al).

The nitride NbN_y becomes stable at 1273 K, and the AlN – NbN_y equilibrium arises instead of AlN – Nb_4N_3. In all other aspects, the phase diagram for the Nb – Al – N system at 1273 K is identical to that at 1773 K.

The Ta – Al – N system. The ternary compound $Ta_5Al_3N_x$ with a structure of the Cr_5B_3 type having vacancies in the nitrogen sublattice has been found in the Ta – Al – N system.[196] However, in another study [197] no ternary compounds have been observed in this system at temperatures from 1273 to 1773 K. The following pseudobinary phase equilibria occur in this system at 1273 K and 1523 K: AlN – $TaAl_3$, AlN – Ta_2Al_3 (as the low-temperature modification at 1273 K and as the high-temperature modification at 1573 K), AlN – Ta_2Al, AlN – Ta_2N, and AlN – ε-TaN (Fig. 36*b*).

At low temperatures AlN coexists with tantalum, but the reaction between AlN and Ta slowly yields Ta_2N and Ta_2Al. At 1773 K the major part of the ternary system is liquid, and the melt is in an equilibrium with all the binary solid phases.

The Cr – Al – N system. This system contains no ternary phases under the equilibrium conditions in the temperature range 1273 – 1773 K.[198] The X-ray diffraction patterns of the samples, the composition of which was close to Cr_2AlN, exhibited reflections corresponding to a ternary compound of this composition with a structure of the *H*-phase. Nevertheless, an equilibrium *H*-phase could not be detected in the Cr – Al – N system even at a nitrogen pressure of 3×10^6 Pa. Four solid-phase equilibria exist in this system at 1273 K, namely, AlN – $CrAl_4$, AlN – Cr_4Al_9, AlN – Cr_5Al_8, and AlN – α-Cr (α-Cr is the solid solution of aluminium in chromium having the composition $Cr_{0.58}Al_{0.42}$ – $Cr_{0.98}Al_{0.02}$). Chromium is insoluble in AlN.

The Mo – Al – N system. Two solid three-phase fields (Mo_3Al_8 + AlN + Mo_3Al) and (Mo_3Al + AlN + Mo) exist in the Mo – Al – N system in the temperature range 1273 – 1773 K.[198] Molybdenum is insoluble in AlN, and nitrogen

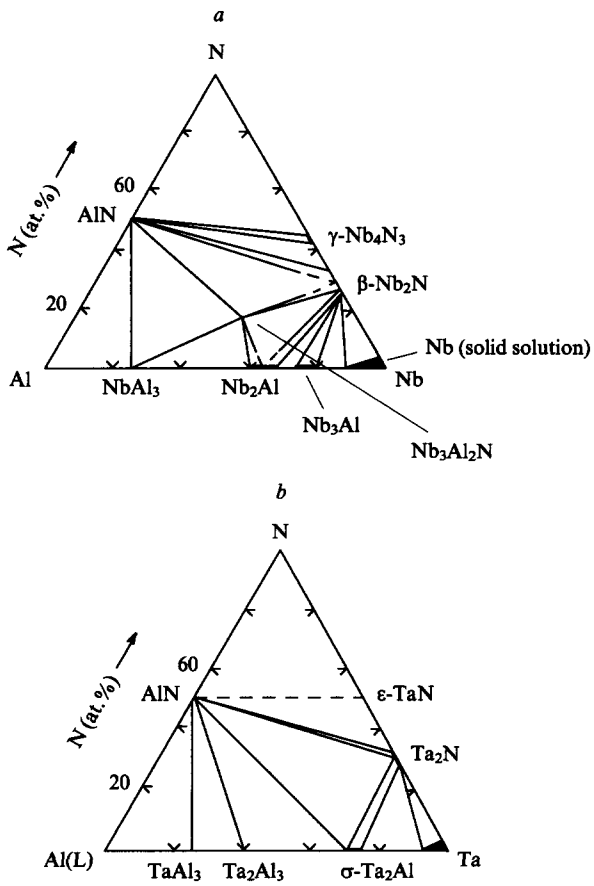


Figure 36. Isothermal cross-sections of the Nb–Al–N system (*a*) at 1773 K and the Ta–Al–N system (*b*) at 1523 K (dark areas denote homogeneity regions of binary phases and of solid solutions).[197]

is insoluble in the molybdenum aluminides. The molybdenum nitride Mo_2N becomes stable at low temperatures or at high partial pressures of nitrogen (for example, at 1273 K and 1×10^6 Pa). The molybdenum nitride Mo_2N apparently exists in equilibrium with AlN. No ternary phases have been found in the Mo–Al–N system.

The W–Al–N system. There are two pseudobinary solid-phase equilibria, namely, AlN–WAl_4 and AlN–W(sol) [W(sol) is the solid solution of aluminium in tungsten], and no ternary compounds in the W–Al–N system at temperatures from 1273 K to 1773 K. The solubility of tungsten in AlN and the solubility of nitrogen in WAl_4 and W(sol) are negligibly small.

The Mn–Al–N system. No ternary phases exist in the Mn–Al–N system at 873 K; the $Mn_{88.4}Al_{9.8}N_{1.8}$ and $Mn_{68.1}Al_{29.2}N_{2.7}$ alloys studied have a cubic structure of the β-Mn type with the periods *a* equal to 0.637 nm and 0.643 nm, respectively, and the $Mn_{75.9}Al_{8.3}N_{15.8}$ alloy incorporates two cubic phases, one of which has $a = 0.900$ nm and a structure of the β-Mn type, and the other is characterised by $a = 0.637$ nm and the α-Mn type of structure (the *A*12 structural type, space group $I\bar{4}3m$).[189]

Schuster and Nowotny[198] also have not found any ternary phases in the Mn–Al–N system at temperatures of up to 1273 K. At 1073 K the nitride AlN coexists with $MnAl_4$, Mn_4Al_{11}, MnAl, β-Mn (the solid solution of aluminium in manganese), γ-Mn (the solid solution of aluminium and nitrogen in manganese), and with the hexagonal nitride ζ-Mn_2N. Neither solubility of manganese in AlN or solubility of nitrogen in manganese aluminides was observed, while γ-Mn dissolves up to 10 at.% of aluminium and 8 at.% of nitrogen. The only solid-phase equilibrium existing at 1273 K is the equilibrium between AlN and β-Mn.

The Re–Al–N system. There are no ternary phases in the Re–Al–N system in the temperature range from 1273 to 1773 K at a nitrogen pressure of 2×10^7 Pa.[198] At 1273 K aluminium nitride exists in an equilibrium with $ReAl_4$, $ReAl_3$, ReAl, Re_2Al, and Re. Only two aluminides $ReAl_3$ and Re_2Al coexisting with AlN are stable at 1773 K.

The Fe–Al–N system. No ternary compounds were found in this system after nitriding the metal alloys at 873 K.[189] The $Fe_{57}Al_{19}N_{24}$ (Fe_3AlN_{1+x}) alloy contains only the hexagonal iron nitride ε-Fe_3N with the parameters $a = 0.276$ nm and $c = 0.442$ nm and contains no aluminium nitride AlN. The alloy of the composition $Fe_{63.9}Al_{21.3}N_{14.8}$ (Fe_3AlN_{1-x}), apart from ε-Fe_3N ($a = 0.273$ nm, $c = 0.438$ nm), incorporates also the cubic austenite γ-Fe (the A1 structural type, space group $Fm3m$) with $a = 0.356$ nm. The main phases in the $Fe_{35.8}Al_{35.8}N_{28.4}$ ($FeAlN_{1-x}$) alloy are the hexagonal nitrides ε-Fe_3N ($a = 0.273$ nm, $c = 0.439$ nm) and AlN. Finally, the cubic iron nitride γ′-Fe_4N (the L′1 structural type) with the unit cell period $a = 0.380$ nm and the hexagonal aluminium nitride AlN [the wurtzite ZnS (*B*4) structural type, space group $P6_3mc$] are present in the alloy of composition $Fe_{43.1}Al_{43.1}N_{13.8}$ ($FeAlN_{0.32}$). The results obtained by Stadelmaier and Yun[189] indicate that γ′-Fe_4N dissolves substantial amounts of aluminium, and the homogeneity region is extended forming a ternary system.

The Co–Al–N system. There are no ternary compounds in this system.[189] The aluminium nitride is in an equilibrium with α-Co and with the only stable cobalt aluminide β-CoAl.

The Ni–Al–N system. In this system, the dissolution of up to 8 at.% of nitrogen in the cubic nickel aluminide Ni_3Al (the $L1_2$ structural type, $a = 0.358$ nm) leads to the formation of the ternary cubic phase Ni_3AlN_x (the $L'1_2$ structural type) with the lattice period $a = 0.380$ nm.[189]

4. The ternary M–Al–Si aluminidosilicide systems

The ternary systems of transition metals with silicon and aluminium have been studied with regard to their resistance to oxidation at high temperatures and the possibility of using them for protective coatings. A characteristic feature of M–Al–Si systems is the ability of aluminium and silicon atoms to substitute each other, which leads to continued solid solutions (or limited solid solutions with high mutual solubilities) of silicides and aluminides. In particular, continued or limited solid solutions arise in those systems where the silicides MSi_2 and M_5Si_3 are formed. Virtually no ternary phases with filled structures of the Mn_5Si_3 type, which are highly typical of the M–B–Si, M–Si–C, M–Si–N, M–Al–C, and M–Al–N systems, are produced in the M–Al–Si systems. Nevertheless, ternary phases with the Mn_5Si_3 type of structure and with vacant octahedral interstices appear in the Zr–Si and Hf–Si systems in the presence of aluminium.

The structural characteristics of the ternary phases formed in the M–Al–Si systems are listed in Table 11.

The Ti–Al–Si system. The phase equilibria and the crystal structures of the compounds formed in this system have been studied in a number of works.[199–201] The alloys were prepared by sintering the powders and were annealed at 1473 K. The $(Ti,Si)_{2-3}Al$ ternary phase with a structure of the Mg_3Gd (BiF_3) type was found in the Ti–Al–Si system. The homogeneity region of this phase is located from Ti_2Al to Ti_3Al, and it dissolves up to 5 at.% of silicon. A slight amount of silicon (no more than 2 at.%) is also dissolved in the γ-TiAl solid solution [the CuAu($L1_0$) structural type, space group $P4/mmm$]. A limited substitution solid solution containing up to 12 at.% of silicon is also formed based on the tetragonal aluminide $TiAl_3$ (the $D0_{22}$ structural type, space group $I4/mmm$). The orthorhombic disilicide $TiSi_2$ (the *C*54 structural type, space group *Fddd*) dissolves up to 5 at.% of aluminium. The hexagonal disilicide Ti_5Si_3 with the Mn_5Si_3 type of structure also dissolves up to 5 at.% of aluminium, some of the aluminium atoms substituting the silicon atoms and the rest filling the octahedral interstices. The ternary

Table 11. Some ternary phases in M–Al–Si systems.

Compound	Symmetry and type of structure	Space group	Z	Unit cell parameters / nm			Ref.
				a	b	c	
$TiAl_xSi_{2-x}$ ($x = 0.3-0.6$) [Ti(Si, Al)$_2$]	Orthorhombic (pseudo-tetragonal), the $ZrSi_2$ ($C49$) type	$Cmcm$	4	0.3590–0.3618	0.3590–0.3618	1.3517	199, 200
Ti_2AlSi_3	Orthorhombic, the $ZrSi_2$ ($C49$) type	$Cmcm$	4	0.3635	1.419	0.3613	201
Ti_2AlSi_3	Tetragonal, the $ZrSi_2$ ($C49$) type	–	4	0.360	0.360	1.353	201
$Ti_7Al_5Si_{12}$	–	–	–	0.3570–0.3645	–	2.715–2.865	201
$Ti_{2-3}Al(Si)$	Cubic, the $BiLi_3$ [BiF_3 ($D0_3$)] type	$Fm3m$	4	–	–	–	199, 200
Zr(Si,Al) ($ZrAl_{0.3}Si_{0.7}$)	Orthorhombic, the CrB [B_f($B33$)] type, high-temperature	$Cmcm$	4	0.3762–0.3788	0.9912–1.007	0.3754–0.3788	200, 202
	Orthorhombic, the FeB ($B27$) type, low-temperature	$Pnma$	4	–	–	–	200, 202
$Zr(Al,Si)_3$	Tetragonal, the $TiAl_3$ ($D0_{22}$) type	$I4/mmm$	2	0.5520	–	0.9008	200, 202
Zr_2Al_5Si	"	$I4/mmm$	2	0.392–0.400	–	0.8938–0.8960	201
$Zr_3Al_4Si_5$	Tetragonal	$I4_1/amd$	2	0.371	–	2.935	201
Zr_2Al–Zr_2Si	Tetragonal, the $CuAl_2$ ($C16$) type, CSSS [a]	$I4/mcm$	4	–	–	–	201
Zr_5Al_3–Zr_5Si_3	Hexagonal, the Mn_5Si_3 ($D8_8$) type	$P6_3/mcm$	2	–	–	–	200, 201
$Zr(Al)Si_2$	Orthorhombic, the $ZrSi_2$ ($C49$) type, LSS [a] of Al in $ZrSi_2$	$Cmcm$	4	0.372	1.473	0.3663	201
$HfAl_{0.35}Si_{0.65}$	Orthorhombic, the CrB [B_f($B33$)] type	$Cmcm$	4	0.3714	0.9890	0.3754	200, 202
$Hf_5(Si,Al)_3$	Hexagonal, the Mn_5Si_3 ($D8_8$) type	$P6_3/mcm$	2	–	–	–	200
Hf_2Al–Hf_2Si	Tetragonal, the $CuAl_2$ ($C16$) type, CSSS [a]	$I4/mcm$	4	–	–	–	200, 202
VAl_xSi_{2-x} ($x = 0-0.7$)	Hexagonal, the $CrSi_2$ ($C40$) type, LSS [a] of Al in VSi_2	$P6_222$	3	0.4566–0.4608	–	0.6372–0.6439	203, 204
$NbAl_{0.6}Si_{1.4}$ [Nb(Si,Al)$_2$]	Orthorhombic, the $TiSi_2$ ($C54$) type	$Fddd$	8	0.8402	0.4901	0.8794	204, 205
$Nb_5Al_xSi_{3-x}$ ($x = 1.8-1.4$) [Nb_5(Si,Al)$_3$]	Tetragonal, the W_5Si_3 ($D8_m$) type	$I4/mcm$	4	1.016–1.021	–	0.508	204, 205
$TaAl_xSi_{2-x}$ ($x = 0-0.9$) [Ta(Si,Al)$_2$]	Hexagonal, the $CrSi_2$ ($C40$) type	$P6_222$	3	0.4773–0.4800	–	0.6558–0.6635	206
$Cr_4Al_{13}Si_4$	Hexagonal, the Mn_3Al_9Si type	–	–	–	–	–	207
$MoAl_{1.3}Si_{0.7}$	Orthorhombic, the $TiSi_2$ ($C54$) type	$Fddd$	8	0.8239	0.4783	0.8758	199
$MoAl_xSi_{2-x}$ ($x = 0.3-1.0$) [Mo(Si,Al)$_2$]	Hexagonal, the $CrSi_2$ ($C40$) type	$P6_222$	3	0.4618–0.4722	–	0.6563	208, 209
MoAlSi	–	–	–	0.4709	–	0.6556	210
$Mo(Si,Al)_2$	Tetragonal, the α-$MoSi_2$ ($C11_b$) type, LSS [a] of Al in $MoSi_2$	$I4/mmm$	2	0.3199	–	0.7847	209, 210
Mo_3Al–Mo_3Si	Cubic, the W_3O ($A15$) type, CSSS	$Pm3n$	2	–	–	–	210
$Mo_3Al_{0.77}Si_{0.23}$ [Mo_3(Al,Si)]	Cubic, the W_3O ($A15$) type	$Pm3n$	2	0.4923	–	–	210
WAl_xSi_{2-x} ($x = 0.6-1.4$) [W(Al,Si)$_2$]	Hexagonal, the $CrSi_2$ ($C40$) type	$P6_222$	3	0.4696–0.4741	–	0.6556–0.6615	206

Table 11 (continued).

Compound	Symmetry and type of structure	Space group	Z	Unit cell parameters / nm			Ref.
				a	b	c	
$Mn_3Al_2Si_4$ ($MnAl_{0.75}Si_{0.25}$)	Hexagonal, the $CrSi_2$ ($C40$) type	$P6_222$	3	0.4475	–	0.6427	201, 211
$Mn_3Al_4Si_2$ ($MnAl_{1.3}Si_{0.7}$)	Orthorhombic, the $TiSi_2$ ($C54$) type	$Fddd$	8	0.7889	0.4570	0.8506	201, 211
β-Mn_3Al_9Si	Hexagonal	–	2	0.7513	–	0.7745	201, 211
Mn_3Al_9Si	"	$C6/mmc$	2	0.7519	0.7500	0.7768 – 0.7722	212
Mn_3AlSi_5	–	–	–	–	–	–	201
α-$Mn_3Al_{21}Si_5$	–	–	–	–	–	–	211
γ-Mn_2Al_2Si	–	–	–	–	–	–	211
δ – $Mn(Si,Al)_4$	–	–	–	–	–	–	211
$Fe_2Al_9Si_2$ ($FeAl_5Si$, m-AlFeSi)	Monoclinic	–	–	0.6122	0.6122	4.1484 [b]	213
$Fe_5Al_{20}Si_2$ ($Fe_3Al_{12}Si$, c-AlFeSi)	Cubic [c]	–	–	1.2548	–	–	213
$Fe_5Al_{20}Si_2$ (α-AlFeSi)	"	$Im3$	–	1.256	–	–	214
α-AlFeSi ($Fe_5Al_{19}Si_2$)	Hexagonal	–	–	1.23	–	2.62	215
γ-AlFeSi ($Fe_{18}Al_{60}Si_{22}$)	Monoclinic	–	–	1.78	1.0.25	0.89 [d]	215
$Fe_3(Al,Si)$	Cubic, the Fe_3Al type with ordering of aluminium and silicon	–	–	0.5685	–	–	216
$FeAl_4Si_2$ (t-AlFeSi)	Tetragonal	–	–	0.6122	0.6122	0.9479	213
$FeAl_3Si_2$ ($FeAl_{2.7}Si_{2.3}$)	Orthorhombic, isostructural to $PdGa_5$, but is a superstructure	$Pbcn$	4	0.6011	–	0.9525	217
$Co_3Al_3Si_4$	Cubic, the Ir_3Ge_7 ($D8_f$) type	$Im3m$	4	0.8091	–	–	218
Co_2AlSi_2	Hexagonal, the Ni_2Al_3 ($D5_{13}$) type	$P\bar{3}m1$	1	0.387 – 0.391	–	0.4750 – 0.4791	218
$NiAl_{0.5}Si_{0.5}$	Cubic, the FeSi ($B20$) type	$P2_13$	4	0.4537	–	–	219
$Ni_3(Al,Si)_7$	Cubic, the Ir_3Ge_7 ($D8_f$) type	$Im3m$	4	0.8291	–	–	219

[a] The following designations are used: CSSS is a continuous series of solid solutions; LSS is a limited solid solution. [b] In the unit cell α = 91°. [c] The unit cell of the aluminosilicide $Fe_5Al_{20}Si_2$ incorporates 138 atoms (100 aluminium atoms, 24 iron atoms and 14 silicon atoms). [d] In the unit cell α = 132°.

pseudotetragonal (orthorhombic) $TiAl_{0.3-0.6}Si_{1.7-1.4}$ phase [$Ti(Si,Al)_2$] has a structure of the $ZrSi_2$ type and possesses a significant homogeneity region.

A titanium silicide containing ~45 at.% of silicon and dissolving considerable amounts of aluminium has also been found. This compound has been reported to be a solution of aluminium in Ti_5Si_4.[201] The same authors[201] also showed that the orthorhombic silicide TiSi [the FeB ($B27$) structural type, space group $Pnma$] dissolves up to 8 at.% of aluminium. One more unknown ternary compound has been detected near the $Ti(Si,Al)_2$ ternary phase;[200] its composition has been determined as $Ti_7Al_5Si_{12}$.[201] This compound is stable at least up to 1173 K; with allowance for the data of Schob et al.,[200] it is stable up to 1473 K.

The Zr – Al – Si system. The phase equilibria in the Zr – Al – Si system have been studied at 973 K[201] and at 1273 – 1473 K.[200,202] Two ternary phases exist in this system at 1473 K, namely, the orthorhombic Zr(Si,Al) phase and the tetragonal $Zr(Al,Si)_3$ phase. The ideal composition of the ternary tetragonal phase was determined[201] to be Zr_2Al_5Si. One more ternary compound $Zr_3Al_4Si_5$ with a narrow homogeneity region was found in this system at 973 K.

Continued solid solutions are formed in this system over the $Zr_2Al – Zr_2Si$ pseudobinary cross-section. It has been reported[200] that the mutual solubility of the components over the $Zr_5Al_3 – Zr_5Si_3$ cross-section is absent only in a narrow region near Zr_5Si_3; according to another study,[201] the mutual solubility is infinite. Limited solid solutions of silicon in $ZrAl_3$ (up to 5 at.%) and of aluminium in $ZrSi_2$ (up to 8 at.%[200] or up to 24 at.%[201]) are also formed in the Zr – Al – Si system.

At 973 K aluminium is highly soluble in the silicide ZrSi substituting both zirconium and silicon up to the composition $Zr_{0.33}Al_{0.33}Si_{0.34}$. The high-temperature modification of this solution has the CrB type of structure, whereas the low-temperature modification crystallises with the FeB type of structure.

The Hf – Al – Si system. The isothermal cross-section through the Hf – Al – Si system at 1473 K has been constructed.[200] The ternary compound Hf(Si,Al) ($HfAl_{0.35}Si_{0.65}$) with the orthorhombic structure of the CrB type was found in this system. A continuous series of solid solutions is formed over the $Hf_2Al – Hf_2Si$ pseudobinary cross-section. The $Hf_5(Al,Si)_3$

ternary phase with a structure of the Mn_5Si_3 ($D8_8$) type possesses an extended homogeneity region, although there are no compounds M_5X_3 with the Mn_5Si_3 type of structure in the Hf–Al and Hf–Si binary systems. Thus, in the presence of aluminium, there is no need for boron, carbon, or nitrogen admixtures to stabilise the $D8_8$ structural type. The silicide Hf_3Si_2 dissolves aluminium yielding a solid solution of the composition $Hf_3Al_{0.5}Si_{1.5}$. Limited solid solutions of silicon (up to 10 at.%) in $HfAl_3$ and of aluminium (up to 10 at.%) in $HfSi_2$ are also formed. The Hf(Si,Al) ternary phase with a structure of the CrB type is in an equilibrium with $HfAl_3$ (the $ZrAl_3$ type) and with the silicides Hf_3Si_2 and HfSi.

The V–Al–Si system. No ternary compounds have been found in the V–Al–Si system.[203,204] Vanadium disilicide VSi_2 dissolves substantial amounts of aluminium, which substitutes silicon thus yielding a limited solid solution with the $CrSi_2$ ($C40$) type of structure. The composition of the solid solution with the highest aluminium content can be written as $V(Si_{0.67}Al_{0.33})_2$. The unit cell parameters of the solid solution increase with an increase in the content of aluminium.

The Nb–Al–Si system. There are two ternary phases in the Nb–Al–Si system at 1673 K, namely, $Nb_5(Al,Si)_3$ with a tetragonal structure of the W_5Si_3 ($D8_m$) type and $Nb(Si,Al)_2$ with an orthorhombic structure of the $TiSi_2$ ($C54$) type.[204,205] These phases are in equilibrium with each other and have homogeneity regions in which silicon is substituted by aluminium. The tetragonal silicide Nb_5Si_3 with the Cr_5B_3 ($D8_l$) type of structure dissolves up to 18 at.% of aluminium; further increase in the aluminium content leads to the transition from the $Nb_5(Si,Al)_3$ substitution solid solution with the Cr_5B_3 type of structure to the $Nb_5(Al,Si)_3$ ternary phase with the W_5Si_3 structure. A substitution solid solution containing up to 10 at.% of aluminium is also formed based on the silicide $NbSi_2$ with the $CrSi_2$ ($C40$) structure. The aluminide Nb_3Al [the W_3O ($A15$) structural type, space group $Pm3n$] dissolves up to 7 at.% of silicon thus yielding a substitution solid solution. The ternary σ-phase containing up to 2 at.% of silicon may be regarded as a solid solution of silicon in niobium aluminide in the region between Nb_2Al and Nb_3Al.

The Ta–Al–Si system. The isothermal cross-section through the Ta–Al–Si system at 1673 K has been constructed.[206] No ternary compounds were found in this system. On the basis of tantalum silicides, limited solid solutions are formed in which silicon is substituted by aluminium: Ta_2Si dissolves 9 at.% of Al; Ta_5Si_3 with the W_5Si_3 structure dissolves up to 20 at.% of Al (as a consequence, the unit cell parameters of Ta_5Si_3 increase somewhat); and $TaSi_2$ with a structure of the $CrSi_2$ ($C40$) type dissolves more than 20 at.% of aluminium. A solid solution with a low silicon content (up to 2 at.%) is formed on the basis of the σ-phase having the homogeneity region from Ta_2Al to Ta_3Al.

The Cr–Al–Si system. The phase equilibria in the Cr–Al–Si system have been studied at 1573 K.[204] There are no ternary compounds in this system, but the silicides Cr_3Si [the W_3O ($A15$) structural type], Cr_5Si_3 [the W_5Si_3 ($D8_m$) structural type], and $CrSi_2$ dissolve 12, 7, and 22 at.% of aluminium, respectively. The solid solutions resulting from the substitution of silicon by aluminium retain the crystal structures of the chromium silicides. The extended solid solution of aluminium in chromium also dissolves up to 4 at.% of Si. It has been reported[207] that the ternary cubic compound $Cr_4Al_{13}Si_4$ having a homogeneity region is formed from the Cr–Al–Si melt (see Table 11). This compound is stable at temperatures below 870 K, and at 870 K it melts incongruently.

The Mo–Al–Si system. The phase equilibria and the ternary phases existing in the Mo–Al–Si system have been studied by a number of authors.[199,204,208–210] Two ternary compounds were found: $Mo(Si,Al)_2$ with the hexagonal structure of the $CrSi_2$ ($C40$) type, having a broad homogeneity region from $MoAl_{0.3}Si_{1.7}$ to MoAlSi, and $Mo(Si,Al)_2$ with a rhombic structure of the $TiSi_2$ ($C54$) type and a narrow homogeneity region (see Table 11). A continuous series of cubic solid solutions with the $A15$ type of structure are formed over the Mo_3Al–Mo_3Si pseudobinary cross-section. The silicide Mo_5Si_3 dissolves up to 12 at.% of aluminium, which substitutes silicon. The limited solid solution of aluminium in Mo_5Si_3 with the highest content of aluminium (Mo_5Si_2Al) exists in equilibrium with a solid solution of the composition $Mo_3Al_{0.77}Si_{0.23}$ from the Mo_3Al–Mo_3Si continuous series of solid solutions.

The W–Al–Si system. The isothermal cross-section through the W–Al–Si system at 1773 K has been reported.[206] The tetragonal silicides W_5Si_3 and WSi_2 dissolve 4 at.% and 15 at.% of aluminium, respectively, thus forming the $W_5(Si,Al)_3$ and $W(Si,Al)_2$ limited solid solutions; a limited solid solution of aluminium and silicon in tungsten also exists in the W–Al–Si system. In addition, there exists the $W(Al,Si)_2$ hexagonal ternary phase with the $CrSi_2$($C40$) structure. It possesses a broad homogeneity region from $WAl_{0.6}Si_{1.4}$ to $WAl_{1.4}Si_{0.6}$, the unit cell parameters increasing as the content of silicon decreases (see Table 11). The $W(Al,Si)_2$ hexagonal ternary phase is in equilibrium with aluminium and silicon, with the $W_5(Si,Al)_3$ and $W(Si,Al)_2$ limited tetragonal solid solutions [the α-$MoSi_2$ ($C11_b$) structural type], and also with WAl_2 and with tungsten [more precisely, with the limited solid solution of aluminium (~2 at.%) and silicon (~8 at.%) in tungsten].

The Mn–Al–Si system. Six ternary phases exist in this system at 1073 K,[211] namely, γ-Mn_2Al_2Si, $MnAl_{1.3}Si_{0.7}$ (near γ-Mn_2Al_2Si), $MnAl_{0.75}Si_{1.25}$ ($Mn_3Al_2Si_4$) with the $CrSi_2$($C40$) type of structure, α-$Mn_3Al_{21}Si_5$, δ-$Mn(Si,Al)_4$, and Mn_3Al_9Si with a hexagonal structure (see Table 11). The Mn_3Al_9Si ternary phase results from the dissolution of silicon in Mn_3Al_{10} and is apparently an ordered solid solution of silicon in this compound [silicon atoms replace only those aluminium atoms, which occupy the 2(a) sites]. It has been shown[211] that MnSi dissolves up to 3 at.% of aluminium; however, in another study,[201] the solubility of aluminium in MnSi has been found to reach 20 at.%. The silicide Mn_3Al_9Si exists in an equilibrium with γ-Mn_2Al_2Si, $Mn_3Al_2Si_4$, and δ-$Mn(Si,Al)_4$. The $Mn_3Al_2Si_4$ ternary phase forms pseudobinary equilibria with γ-Mn_2Al_2Si and δ-$Mn(Si,Al)_4$, whereas δ-$Mn(Si,Al)_4$ is in an equilibrium with α-$Mn_3Al_{21}Si_5$.

The Fe–Al–Si system. The Fe–Al–Si system has been studied repeatedly. The superstructure $Fe_3(Al,Si)$ has been discovered in the homogeneity region of the solid solution of aluminium and silicon in iron.[216] The solid solution of iron and silicon in aluminium is in equilibrium with two ternary phases: $Fe_5Al_{20}Si_2$ (which has also been written as $Fe_5Al_{19}Si_2$, $Fe_3Al_{12}Si$, and α-AlFeSi) with a cubic[213,214] or hexagonal[215] structure and the monoclinic[213] $Fe_2Al_9Si_2$. Other ternary phases are also known (see Table 11).

The compounds $FeAl_4Si_2$ and $FeAl_3Si_2$ ought to be identical, in view of the similarity of their unit cell dimensions. However, it has been found[217] that the lattice of $FeAl_3Si_2$ is a superstructure with respect to the tetragonal disordered phase of the same composition isostructural to $PdGa_5$.

The great number of ternary compounds with similar compositions and close unit cell dimensions indicates that the majority of the ternary phases in the Fe–Al–Si system possess homogeneity regions. It is of interest that most of the ternary phases contain from 14 at.% to 25 at.% of iron.

The Co–Al–Si system. Two ternary phases have been found in this system:[218] $Co_3Al_3Si_4$ with a cubic structure of the Ir_3Ge_7($D8_f$) type and Co_2AlSi_2 with a hexagonal structure (see Table 11). In all probability, the Co_2AlSi_2 ternary phase exists in equilibrium with CoSi and $Co_3Al_3Si_4$. Judging by the substantial alteration of unit cell parameters, Co_2AlSi_2 possesses a noticeable homogeneity region. The cobalt atoms in the $Co_3Al_3Si_4$ cubic ternary phase occupy the 12(e) sites, while the aluminium and silicon atoms are likely to be statistically distributed among the 12(d) and 16(f) sites; the predominant location of the aluminium atoms at the 12(d) sites, with the silicon atoms filling predominantly the 16(f) sites, should lead to a superstructure based on the Ir_3Ge_7 structural type.

The Ni–Al–Si system. Three ternary phases exist in this system at 1000 K:[219,220] Ni_4AlSi (there is no information concerning its structure), $NiAl_{0.5}Si_{0.5}$, and $Ni_3(Al,Si)_7$ with a high content of aluminium (see Table 11). The $NiAl_{0.5}Si_{0.5}$ ternary phase is in equilibrium with all the nickel silicides, with the aluminide NiAl, and with the $Ni_3(Al,Si)_7$ and Ni_4AlSi ternary phases; Ni_4AlSi is in equilibrium with the aluminides NiAl and Ni_3Al and with the silicide Ni_3Si, and $Ni_3(Al,Si)_7$ coexists with silicon, aluminium, $NiAl_3$, Ni_2Al_3, and $NiSi_2$. At temperatures above 1370 K all the alloys in the Ni–Al–Si system containing less than 50 at.% of Ni are in the molten state.

VI. Phase equilibria in X–X′–X″ ternary systems (X, X′, X″ = B, C, N, Si, Al)

The overwhelming majority of the currently existing oxygen-free ceramic materials are multicomponent systems and, apart from metals, they contain such elements as B, C, N, Si, or Al. Therefore, for understanding the equilibria in complex multicomponent systems, it is important to know what compounds and phase equilibria exist in simpler ternary systems formed by boron, carbon, nitrogen, silicon, and aluminium. The X–X′–X″ ternary systems (X, X′, X″ = B, C, N, Si, Al) are constituents of M–X–X′–X″ four-component systems containing transition metals M. The X–X′–X″ ternary systems have not been adequately studied so far, and phase diagrams have not been constructed for all of them. The crystal-chemical characteristics of the ternary compounds found in these systems are listed in Table 12.

The Si–B–C system. The phase equilibria in the Si–B–C system have been studied at temperatures of 1973 K and 2173 K.[229] At these temperatures, the silicon carbide SiC exists in an equilibrium with the silicon melt, with the boride SiB_6, and with the carbides B_4C and $B_{13}C_2$; and the boron carbides coexist with SiB_6 and SiB_{12+x} (Fig. 37*a*). The SiC–B_4C pseudobinary cross-section is an eutectic system. The composition of the eutectics is close to SiB_5C_2 and its melting point is ~2530 K. These data are in good agreement with the results obtained by Dokukina et al.[230] As the temperature increases to 2273 K, the SiC–SiB_6 equilibrium disappears, and the carbide $B_{13}C_2$ coexists with the silicon and boron melt (Fig. 37*b*).

The authors of a number of studies[51,229,230] of the Si–B–C system have not found the ternary compounds SiB_5C_2 and $Si_2B_3C_2$, which have been reported by Portnoi et al.[231]

The Si–C–N system. The phase equilibria in the Si–C–N system have been studied at 1900 K and 2000 K at a nitrogen pressure of 1×10^5 Pa.[232,233] At 1900 K the silicon nitride Si_3N_4 exists in equilibrium with the silicon carbide SiC, cyanogen C_2N_2, and carbon (Fig. 37*c*). As the temperature increases, the nitride Si_3N_4 reacts with carbon yielding the carbide SiC; therefore, the SiC–C_2N_2 equilibrium arises instead of Si_3N_4–C (Fig. 37*d*). The carbide β-SiC forms the nitride Si_3N_4 on heating in nitrogen [$T = 2273$ K, $p_{N_2} = (1-30) \times 10^5$ Pa].[232]

The possible phase equilibria involving the carbon nitride β-C_3N_4 are shown by the dashed lines in the isothermal cross-sections through the Si–C–N system (Fig. 37*c*,*d*). This compound, the existence of which had been predicted,[26-28,234] has been recently discovered experimentally.[20]

Data concerning the existence of the ternary compounds Si_2C_2N and Si_3C_3N have found no support. A number of researchers, who have studied this system, have not found any silicon carbonitrides.[232,233,235]

The Al–Si–C system. Several ternary compounds have been found in this system (see Table 12). However, these data are very contradictory. For example, the existence of two modifications α- and β-Al_4SiC_4 has been reported.[236] Later the existence of α-Al_4SiC_4 has been confirmed;[225,228,237] however, the β-modification was not found. The ternary compound $Al_4Si_2C_5$ has been reported by Inoue et al.;[225,226] however, it was not detected in another study.[228] The hexagonal carbosilicide Al_8SiC_7 has been observed.[227,228] The aluminium carbosilicides Al_4SiC_4 and Al_8SiC_7 were found to decompose incongruently at 2353 and at 2358 K, respectively.[228] Both ternary compounds are formed with great difficulty at relatively low temperatures (below 1800 K).

The isothermal cross-sections through the Al–Si–C system at 900 and 2273 K are presented in Fig. 37*e*,*f*. At 900 K (below the melting point of aluminium), silicon carbide exists in equilibrium with Al_4SiC_4 and Al, Al_4C_3 coexists with Al_8SiC_7, and the ternary compounds are in equilibrium with each other, and also with carbon and aluminium (see Fig. 37*e*). When the liquid phase appears, silicon carbide and aluminium carbosilicides coexist with the aluminium melt (Fig. 37*f*).

Table 12. Some ternary compounds in the Al–B–C, Al–C–N, and Al–Si–C systems.

Compound	Symmetry and type of structure	Space group	Z	Unit cell parameters / nm			Ref.
				a	b	c	
$Al_3B_{48}C_2$	Orthorhombic	*Cmma*	2	1.234	1.263	0.508	28
$Al_3B_{48}C_2$	"	*Ammm*	2	0.617	1.263	1.016	28
$Al_3B_{48}C_2$	Tetragonal, high-temperature	*P4/mmm*	1	0.882	–	0.509	28
$AlB_{24}C_4$	Orthorhombic	*Bbmm*	2	0.888	0.910	0.569	221
$Al_{2.1}B_{51}C_8$	"	*Cmcm*	2	0.5690	0.8881	0.9100	222
$AlB_{40}C_4$	Hexagonal	$R\bar{3}m$	1	0.5642	–	1.2367	223
$Al_8B_4C_7$	"	$P6_3cm$	3	0.5906	–	1.5901	224
Al_5C_3N	Hexagonal	$P6_3mc$	2	0.3281	–	2.167	25
$Al_6C_3N_2$	Trigonal	$R\bar{3}m$	3	0.3248	–	4.003	25
$Al_7C_3N_3$	Hexagonal	$P6_3mc$	2	0.3226	–	3.170	25
$Al_8C_3N_4$	Trigonal	$R\bar{3}m$	3	0.3211	–	5.508	25
$Al_9C_3N_5$[a]	Hexagonal	$P6_3mc$	2	0.3197	–	4.169	25
$Al_{10}C_3N_6$[a]	Trigonal	$R\bar{3}m$	3	0.3186	–	7.000	25
α-Al_4SiC_4	Hexagonal	$P6_3mc$	2	0.3277	–	2.1676	225
$Al_4Si_2C_5$	"	$R\bar{3}m$	3	0.3251	–	4.0108	225, 226
Al_8SiC_7	"	–	1	0.3313	–	1.9242	227, 228

[a] The carbonitrides $Al_9C_3N_5$ and $Al_{10}C_3N_6$ have not been observed experimentally, their hypothetical structural characteristics have been reported.[25]

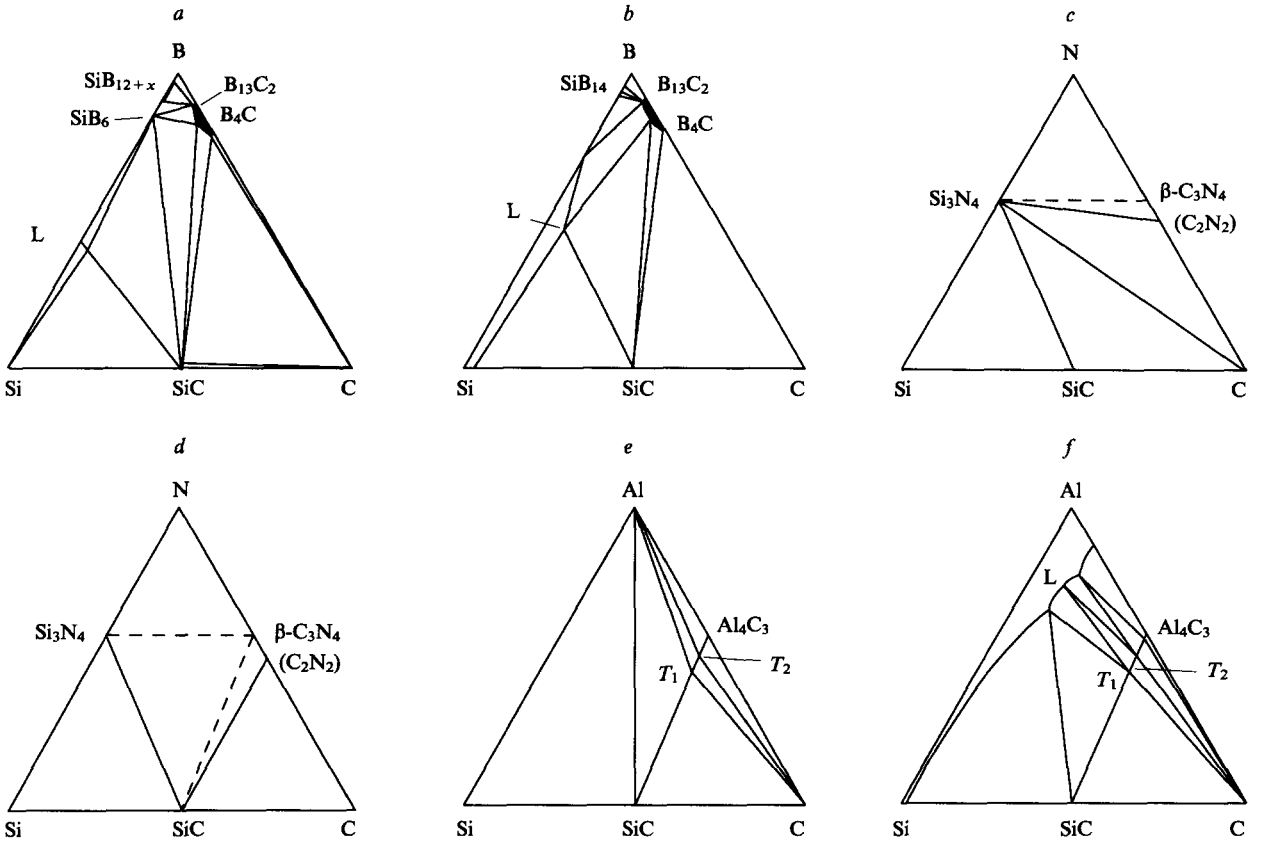


Figure 37. Isothermal cross-sections of ternary systems of silicon with boron, carbon, nitrogen, and aluminium (dark areas denote single-phase homogeneity regions). (*a*) the Si–B–C system at 1973 K; (*b*) the Si–B–C system at 2273 K; (*c*) the Si–C–N system at 1900 K, $p_{N_2} = 1 \times 10^5$ Pa; (*d*) the Si–C–N system at 2000 K, $p_{N_2} = 1 \times 10^5$ Pa; (*e*) the Al–Si–C system at 900 K; (*f*) the Al–Si–C system at 2273 K; $T_1 = Al_4SiC_4$, $T_2 = Al_8SiC_7$.

The Si–B–N system. The silicon nitride Si_3N_4 in the Si–B–N system at temperatures below 1700 K coexists with the boron nitride BN and the boride SiB_6; the $BN-SiB_{12+x}(SiB_{14})$ pseudobinary equilibrium also exists (Fig. 38*a*).

The Al–Si–N system. The isothermal cross-section through the Al–Si–N system at 873 K is presented in Fig. 38*b*.[238] The aluminium nitride AlN exists in equilibrium with Si and Si_3N_4; however, the Si_3N_4–Al metastable equilibrium should also be taken into account. Its existence is caused by the following: the interaction of Si_3N_4 with aluminium leads to the appearance on the surface of aluminium grains of an AlN film, which acts as a diffusion barrier and prevents further occurrence of the reaction even during prolonged annealing. No ternary compounds have been found in the Al–Si–N system.

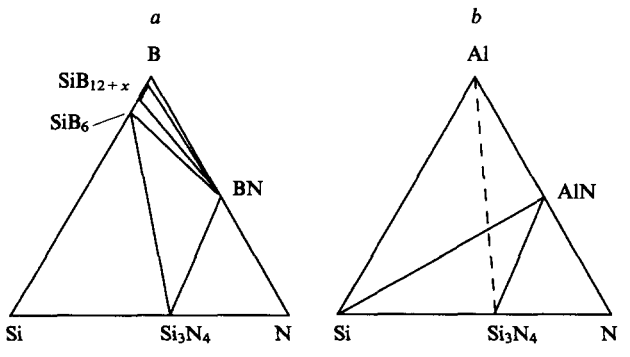


Figure 38. Isothermal cross-sections through the Si–B–N system (*a*) at 1700 K (the dark area denotes the single-phase homogeneity region of SiB_{12+x}) and through the Al–Si–N system at 873 K (*b*) (the dashed line marks a metastable equilibrium).

The Al–B–C system. Several aluminium borocarbides have been found in this system (see Table 12). In all probability, the ternary compound $Al_8B_4C_7$ exists in equilibrium with the carbide Al_4C_3 and also with aluminium and carbon. The $AlB_{24}C_4$ phase observed by Will,[221] has the composition $Al_{2.1}B_{51}C_8$, according to Perotta et al.[222] The $Al_3B_{48}C_2$ phase exists at high temperatures as a tetragonal modification, which decomposes to two related orthorhombic phases of the same composition at $T < 800$ K (see Table 12).

The Al–C–N system. The carbide Al_4C_3 and the aluminium nitride AlN in the Al–C–N system form several ternary compounds, namely, aluminium carbonitrides $(Al_4C_3)(AlN)_n$, where $n = 1-4$ (see Table 12). The structures of aluminium carbonitrides have been studied.[25] The aluminium atoms in these ternary compounds form close-packed planes, the carbon and nitrogen atoms being arranged between these planes (the carbon atoms occupy the tetrahedral or octahedral interstices, while the nitrogen atoms populate only tetrahedral interstices). Thus, the Al_2C_2, Al_2C, and AlN layers can be distinguished in the structure of aluminium carbonitrides. It has been suggested[25] that two other ternary compounds $Al_9C_3N_5$ and $Al_{10}C_3N_6$ also exist (see Table 12).

Aluminium carbonitrides are in equilibrium with aluminium and carbon as well as with the carbonitrides closest to them; Al_5C_3N is also in equilibrium with Al_4C_3, and $Al_8C_3N_4$ coexists with AlN.

VII. Conclusion

The thermodynamic state of a multicomponent system containing several phases is described by a set of equations of state $\varphi(c,p,T)$ characterising each of the phases. The numerical values of the c, p, and T parameters unambiguously determine the state of the system, which is represented graphically as a point in the three-dimensional c, p, T system of coordinates. If two of these parameters are known, the third one can be found from the equation of state. This means that to determine the state of the system, it is sufficient to find the position of the figurative point in a two-dimensional system of coordinates, usually in the c,T-coordinates. This graphical representation of the equation of state of a system is its state diagram.

The real equations of state of multicomponent systems are unknown; therefore, the state diagrams are of great importance. By virtue of these diagrams, the actual relationship between the physical and chemical parameters determining the state of the system can be clearly represented on the basis of experimental data. Each characteristic of the system varies continuously as a function of one or several parameters within the limits of a particular phase region. The boundaries of phase regions are represented by singular points (inflection, break, or discontinuity points, cusps, etc.). Hence it is obvious, how important it is to know the positions of phase boundaries, which are the main information provided by state diagrams.

The problem of constructing state diagrams has been solved at present to a very small extent. In particular, no more than 5% of the state diagrams of ternary systems are known. In the present review, the author has attempted to generalise and to make available the results of experimental studies of the phase equilibria in the M–X–X′ and M–Al–X ternary oxygen-free systems (M is a transition metal, X, X′ are B, C, N, Si), which provide a basis for the development of new ceramic materials.

The greatest contribution to the systematic studies of phase diagrams of the ternary systems considered was made by scientists of the Austrian school: H Nowotny, W Jeitschko, F Benesovsky, E Rudy, P Rogl, J Schuster, and their colleagues.

It follows from the analysis performed that the interaction of a transition metal with the two other components of a M–X–X′ or M–Al–X ternary system is often accompanied by the formation of one or several ternary phases. This leads to a substantial complication of the phase equilibria, to the appearance of a large number of phase boundaries, and to the splitting of the state diagram into many phase fields. The allowance for these data will permit researchers to carry out the target-directed synthesis of compounds and heterogeneous compositions with specified properties.

The analysis of the crystal structures of the ternary compounds formed in the M–X–X′ or M–Al–X systems considered has shown that an ideal or a distorted octahedron built of six transition metal atoms M is the main structural unit of the majority of these compounds. The octahedral interstice can be either occupied by an interstitial nonmetal atom X (B, C, N) or vacant. The possibility of the complete or partial population of the octahedral interstices causes the existence of the homogeneity regions (fairly broad or narrow) for many ternary compounds. Those of the considered ternary compounds, which incorporate the XM_6 octahedral units and possess homogeneity regions, constitute an extensive group of ternary nonstoichiometric interstitial compounds, which are related to the binary nonstoichiometric interstitial compounds MX_y and M_2X_y (X = C, N) with structures of the NaCl ($B1$) and W_2C ($L'3$) types. The ternary nonstoichiometric interstitial compounds have looser structures than the binary compounds, due to the presence of the third element, i.e. the V/n volume, which corresponds to one atom in the ternary compounds, is greater than in the binary compounds (V is the unit cell volume and n is the number of atoms in the unit cell).

In this connection, it is of interest to compare various carbide and nitride phases of the same transition metal differing in the X/M ratio of the atomic concentrations of the interstitial element and the metal. The titanium compounds, namely, the cubic Ti_3AlC and Ti_3AlN with the perovskite type of structure; the hexagonal Ti_2AlC and Ti_2AlN with a structure of the Cr_2AlC type; the hexagonal carbosilicide Ti_3SiC_2 and the trigonal aluminidonitride $Ti_3Al_2N_2$; the cubic carbide $TiC_{1.0}$ and the cubic nitride $TiN_{1.0}$ with the NaCl ($B1$) type of structure (Table 13) can be considered as typical examples. Each pair of these compounds (except for Ti_3SiC_2 and $Ti_3Al_2N_2$) have the same structure. The structure of $Ti_3Al_2N_2$ differs from that of Ti_3SiC_2 in that in the former case, the double-stranded layers of the XTi_6 octahedra are separated by two layers of nontransition metal

Table 13. Interatomic distances in carbide and nitride phases of titanium with different degrees of filling of the titanium sublattice with interstitial atoms.

Stoichiometric composition	Symmetry and type of structure, space group	Unit cell parameters / nm		Interatomic distances/ nm			V/ nm^3	$V n^{-1}$/ nm^3 (see[a])
		a	c	Ti–C	Ti–Ti	Ti–N		
Ti_3AlC	Cubic, perovskite $CaTiO_3$ type, space group $Pm3m$	0.4156	–	0.208	0.294	–	0.0718	0.0144
Ti_2AlC	Hexagonal H-phase, the Cr_2AlC type, space group $P6_3/mmc$	0.304	1.360	0.212	0.292	–	0.1088	0.0136
Ti_3SiC_2	Hexagonal, space group $P6_3/mmc$	0.3068	1.7669	0.215	0.297	–	0.1440	0.0120
$TiC_{1.0}$	Cubic, the NaCl ($B1$), type, space group $Fm3m$	0.4328	–	0.216	0.306	–	0.0811	0.0101
Ti_3AlN	Cubic, the perovskite $CaTiO_3$ type ($E2_1$), space group $Pm3m$	0.4120	–	–	0.291	0.206	0.0699	0.0140
Ti_2AlN	Hexagonal H-phase, the Cr_2AlC type, space group $P6_3/mmc$	0.2991	1.3621	–	0.290	0.208	0.1055	0.0132
$Ti_3Al_2N_2$	Trigonal, space group $P31c$	0.2988	2.3350	–	0.297	0.209	0.1805	0.0129
$TiN_{1.0}$	Cubic, the NaCl ($B1$), type, space group $Fm3m$	0.4244	–	–	0.300	0.213	0.0764	0.0096

[a] V is the unit cell volume, n is the number of atoms in the unit cell.

atoms, whereas in Ti_3SiC_2, they are separated by one layer of nontransition element atoms.

A general feature of the structures of all these compounds is that the interstitial atoms (carbon or nitrogen) are located at the octahedral interstices formed by six transition metal atoms. In the compounds with an ideal stoichiometric composition, all the octahedral vacancies are filled with the interstitial atoms. The structures of the compounds under consideration differ in the manner in which the XM_6 octahedra are linked to one another. In the compounds $M_3M'X$ the octahedra are joined via all their six vertices (see Fig. 23); in the $M_2M'X$ *H*-phases, each octahedron is linked to the adjacent octahedra via six edges thus forming an octahedral layer of the composition M_2X (see Fig. 24); in the next pair of compounds, namely, Ti_3SiC_2 and $Ti_3Al_2N_2$, the XM_6 octahedra are joined with one another via nine edges thus forming a double octahedral layer of the composition M_3X_2 (see Fig. 14); finally, the XM_6 octahedra in the cubic carbides and nitrides $MX_{1.0}$ are joined via all their twelve edges and form the closest packing (see Fig. 1).

In the sequence $M_3M'X \rightarrow M_2M'X \rightarrow M_3M'X_2$ $(M_3M_2'X_2)$ $\rightarrow MX$ the X/M ratio increases in the following way: $\frac{1}{3} \rightarrow \frac{1}{2} \rightarrow \frac{2}{3} \rightarrow 1$, which indicates an increase of the degree of filling of the transition metal sublattice with the interstitial atoms. For the cubic carbides and nitrides MX_y, the increase in the degree of filling of the octahedral vacancies of the metallic sublattice (i.e. the increase in the content of interstitial atoms) is accompanied by an increase in the period of the crystal lattice and by an increase in the interatomic distances. By analogy with the cubic carbides and nitrides MX_y, one may expect a similar variation of the interatomic distances and a similar decrease in the V/n volume corresponding to one atom in the sequence $M_3M'X \rightarrow M_2M'X \rightarrow M_3M'X_2$ $(M_3M_2'X_2) \rightarrow MX$.

Table 13 presents the Ti–X and Ti–Ti interatomic distances and the V/n volume for the binary and ternary titanium compounds considered as examples. With an increase in the X/M ratio the Ti–C interatomic distances in the series of carbide phases and the Ti–N distances in the series of nitride phases increase monotonically, whereas the V/n volume decreases. A similar increase is observed for the Ti–Ti interatomic distances, except for those in the *H*-phases.

Thus, the majority of the compounds of transition metals with B, C, N, Si, and Al retain the octahedral fragment consisting of six transition metal atoms M as the main structural unit; this fragment is either vacant or filled with interstitial nonmetal atoms. The atoms of the third element make the structure of the ternary compound more complex and more loose than the structure of the corresponding binary compound of the transition metal.

The ternary compounds with the homogeneity regions discussed in this review can exist in two structural states, namely, the disordered and the ordered state. In the former case, the interstitial atoms are randomly distributed among the octahedral interstices, and in the latter case, they are regularly distributed. The ordering phenomenon in the binary nonstoichiometric interstitial compounds has been studied fairly extensive-ly;[1, 2, 6, 239, 240] however, ordering in the ternary nonstoichiometric compounds and its influence on the properties of these compounds are scarcely known. It may be expected that the investigation of the ordering effects will become one of the major directions in the research on ternary nonstoichiometric compounds of transition metals with boron, carbon, nitrogen, silicon, and aluminium.

The work was supported by the Russian Foundation for Basic Research (project 95-02-03549a) and the State scientific and technical programme 'New materials' (project 07.02.0103m).

References

1. A I Gusev, A A Rempel' *Strukturnye Fazovye Perekhody v Nestekhiometricheskikh Soedineniyakh* (Structural Phase Transitions in Nonstoichiometric Compounds) (Moscow: Nauka, 1988)
2. A I Gusev *Fizicheskaya Khimiya Nestekhiometricheskikh Tugoplavkikh Soedinenii* (Physical Chemistry of Nonstoichiometric High-Melting Compounds) (Moscow: Nauka, 1991)
3. A I Gusev, S I Alyamovskii, Yu G Zainulin, G P Shveikin *Usp. Khim.* **55** 2067 (1986) [*Russ. Chem. Rev.* **55** 1175 (1986)]
4. A I Gusev *Usp. Khim.* **57** 1595 (1988) [*Russ. Chem. Rev.* **57** 913 (1988)]
5. A I Gusev *Phys. Status Solidi, B* **156** 11 (1989)
6. A I Gusev *Phys. Status Solidi, B* **163** 17 (1991)
7. V I Matkovich (Ed.) *Boron and Refractory Borides* (Berlin: Springer, 1977)
8. H J Goldschmidt *Interstitial Alloys* (London: Butterworth, 1967) (Translated into Russian; Moscow: Mir, 1971)
9. W B Pearson *The Crystal Chemistry and Physics of Metals and Alloys* (New York: Wiley, 1972)
10. A Kirfel, A Gupta, G Will *Acta Crystallogr., Sect. B, Struct. Crystallogr.* **35** 1052 (1979)
11. R S Pease *Acta Crystallogr.* **5** 356 (1952)
12. R H Wentorf *J. Chem. Phys.* **26** 956 (1957)
13. V A Kurdyumov, A N Pilyankevich *Fazovye Prevrashcheniya v Uglerode i Nitride Bora* (Phase Transformations in Carbon and in Boron Nitride) (Kiev: Naukova Dumka, 1979)
14. R F Adamsky *Acta Crystallogr.* **11** 744 (1958)
15. R F Giese, J J Economy, V I Matkovich *Z. Kristallogr.* **122** 144 (1965)
16. E J Felten *J. Am. Ceram. Soc.* **78** 5977 (1956)
17. V I Matkovich, R F Giese, J J Economy *Z. Kristallogr.* **122** 116 (1965)
18. I Higashi, T Sakurai, T Atoda *J. Solid State Chem.* **20** 67 (1977)
19. I Higashi *J. Solid State Chem.* **47** 333 (1983)
20. K M Yu, M L Cohen, E E Haller, W L Hansen, A Y Liu, I C Wu *Phys. Rev. B* **49** 5034 (1994)
21. P T B Schaffer *Acta Crystallogr., Sect. B, Struct. Crystallogr.* **25** 477 (1969)
22. G A Jeffrey, V Y Wu *Acta Crystallogr.* **16** 559 (1963)
23. A J Moulson *J. Mater. Sci.* **14** 1017 (1979)
24. G A Slack *J. Phys. Chem. Solids* **34** 321 (1973)
25. V I Matkovich, R F Giese, J J Economy *Z. Kristallogr.* **122** 108 (1965)
26. A Y Liu, M L Cohen *Science* **245** 841 (1989)
27. A Y Liu, M L Cohen *Phys. Rev. B* **41** 10727 (1990)
28. M L Cohen *Phys. Rev. B* **32** 7988 (1985)
29. H Holleck *Binäre und Ternäre Carbid- und Nitridsysteme der Übergangsmetalle* (Berlin: Gebrüder Borntraeger, 1984) (Translated into Russian; Chelyabinsk: Metallurgiya, 1988)
30. R A Andrievskii, I I Spivak *Prochnost' Tugoplavkikh Soedinenii i Materialov na Ikh Osnove* (The Strength of High-Melting Compounds and of Materials Based on Them) (Chelyabinsk: Metallurgiya, 1989)
31. Yu B Kuz'ma, N F Chaban *Dvoinye i Troinye Sistemy, Soderzhashchie Bor* (Binary and Ternary Boron-containing Systems) (Moscow: Metallurgiya, 1990)
32. J Bauer *J. Less-Common Met.* **87** 45 (1982)
33. G S Smith, Q Johnson, P C Nordine *Acta Crystallogr.* **19** 668 (1965)
34. J Bauer, H Nowotny *Monatsh. Chem.* **102** 1129 (1971)
35. J Bauer, J Debuigne *J. Inorg. Nucl. Chem.* **37** 2473 (1975)
36. N A Fishel, H A Eick *J. Inorg. Nucl. Chem.* **31** 891 (1969)
37. J Bauer, O Bars *Acta Crystallogr., Sect. B, Struct. Crystallogr.* **36** 1540 (1980)
38. L Ya Markovskii, N V Vekshina, G F Pron' *Zh. Prikl. Khim.* **35** 2090 (1962)
39. J Bauer, O Bars *J. Less-Common Met.* **83** 17 (1982)
40. R W Johnson, A H Daane *J. Phys. Chem.* **65** 909 (1961)
41. P K Smith, P W Gilles *J. Inorg. Nucl. Chem.* **29** 375 (1967)
42. J Bauer, C Politis *J. Less-Common Met.* **88** L1 (1982)
43. J Bauer, J Debuigne *C. R. Hebd. Seances. Acad. Sci., Ser. C, Sci. Chim.* **274** 1271 (1972)
44. J Bauer, P Vennegues, J L Vergneau *J. Less-Common Met.* **110** 295 (1985)
45. E T Bezruk, L Ya Markovskii *Zh. Prikl. Khim.* **45** 3 (1972)
46. L Ya Markovskii, N V Vekshina, Yu D Kondrashev *Zh. Prikl. Khim.* **45** 1183 (1972)
47. L Brewer, H Haraldsen *J. Electrochem. Soc.* **102** 399 (1955)
48. H Nowotny, F Benesovsky, C Brukl, O Schob *Monatsh. Chem.* **92** 403 (1961)

49. E Rudy *Compendium of Phase Diagram Data. Final Report AFML TR-65-2* Part V (Ohio, USA: Metals and Ceramics Division, Air Force Materials Laboratory, Wright-Patterson Air Force Base, 1969)
50. M Schouler, M Dicarroir, C Bernard *Rev. Int. Hautes, Temp. Refract.* **20** 261 (1983)
51. R Telle, R J Brook, G Petzow *J. Hard Mater.* **2** 79 (1991)
52. A I Gusev, G P Shveikin *Izv. Akad. Nauk SSSR, Neorg. Mater.* **10** 2144 (1974)
53. H Nowotny, E Rudy, F Benesovsky *Monatsh. Chem.* **92** 394 (1961)
54. H Nowotny, E Rudy, F Benesovsky *Monatsh. Chem.* **91** 963 (1960)
55. F W Glaser *J. Met.* **4** 391 (1952)
56. L E Toth, F Benesovsky, H Nowotny, E Rudy *Monatsh. Chem.* **92** 956 (1961)
57. P Rogl *J. Nucl. Mater.* **80** 187 (1979)
58. P Rogl *J. Nucl. Mater.* **79** 154 (1979)
59. P Rogl, P Fischer *J. Solid State Chem.* **78** 294 (1989)
60. Yu D Kondrashev *Kristallografiya* **11** 559 (1966)
61. H Nowotny, P Rogl, J C Schuster *J. Solid State Chem.* **44** 126 (1982)
62. W Jeitschko, H Nowotny, F Benesovsky *Monatsh. Chem.* **94** 565 (1963)
63. L E Toth, H Nowotny, F Benesovsky, E Rudy *Monatsh. Chem.* **92** 794 (1961)
64. P Rogl, J Bauer, J Debuigne *J. Nucl. Mater.* **165** 74 (1989)
65. H H Stadelmaier, J B Ballance *Z. Metallkd.* **58** 449 (1967)
66. L Ya Markovskii, E T Bezruk *Zh. Prikl. Khim.* **39** 258 (1966)
67. H H Stadelmaier *Metall* **17** 412 (1963)
68. M E Nicholson *J. Met.* **9** 1 (1957)
69. L Ya Markovskii, E T Bezruk, G E Berlova *Izv. Akad. Nauk SSSR, Neorg. Mater.* **7** 56 (1971)
70. E Rudy, F Benesovsky, L E Toth *Z. Metallkd.* **54** 345 (1963)
71. G Papesch, H Nowotny, F Benesovsky *Monatsh. Chem.* **104** 933 (1973)
72. M Lucco Borlera, G Pradelli *Met. Ital.* **59** 907 (1967)
73. M Lucco Borlera, G Pradelli *Met. Ital.* **60** 140 (1968)
74. P Rogl, H Klesnar, P Fischer *J. Am. Ceram. Soc.* **73** 2634 (1990)
75. J Gaude, P L'Haridon, J Guyader, J Lang. *J. Solid State Chem.* **59** 143 (1985)
76. P Rogl, H Klesnar *J. Solid State Chem.* **98** 99 (1992)
77. J Gaude *C. R. Hebd. Seances Acad. Sci., Ser. 2* **297** 717 (1983)
78. P Rogl, H Klesnar, P Fischer *J. Am. Ceram. Soc.* **71** C450 (1988)
79. P Rogl, H Klesnar, P Fischer, B Chevalier, B Buffat, G Demazeau, J Etourneau *J. Mater. Sci. Lett.* **7** 1229 (1988)
80. P Rogl, J C Schuster *Phase Diagrams of Ternary Boron Nitride and Silicon Nitride Systems* (Materials Park, OH: American Society of Material Science, 1992)
81. H P Klesnar, P Rogl *High Temp.-High Press.* **22** 453 (1990)
82. I Šmid, P Rogl, F Weitzer, in *Proceedings of the 12th International Plansee Seminar* Vol. 2 (Eds H Bildstein, H M Ortner) (Reutte, Austria: Metallwerk Plansee, 1989) p. 577
83. H Klesnar, P Rog, in *Proceedings of the 12th International Plansee Seminar* Vol. 2 (Eds H Bildstein, H M Ortner) (Reutte, Austria: Metallwerk Plansee, 1989) p. 599
84. E Rudy, F Benesovsky *Monatsh. Chem.* **92** 415 (1961)
85. K E Spear, H Schäfer, P W Gilles *J. Less-Common Met.* **14** 449 (1968)
86. M P Asanova, A F Gerasimov, V N Konev *Fiz. Met. Metalloved.* **9** 689 (1960)
87. R Kiessling, Y H Liu *J. Met.* **3** 639 (1951)
88. R W Fountain, J Chipman *Trans. Metall Soc. AIME* **224** 599 (1962)
89. H Nowotny, B Lux, H Kudielka *Monatsh. Chem.* **87** 447 (1956)
90. H Kudielka, H Nowotny, G Findeisen *Monatsh. Chem.* **88** 1048 (1957)
91. H Nowotny, R Kieffer, F Benesovsky *Planseeber. Pulvermetall.* **5** 86 (1957)
92. H Nowotny, F Benesovsky, E Rudy, A Wittman *Monatsh. Chem.* **91** 975 (1960)
93. E Parthe, J T Norton *Monatsh. Chem.* **91** 1127 (1960)
94. R Kieffer, F Benesovsky *Hartstoffe* (Wien: Springer, 1963)
95. H Nowotny, E Piegger, R Kieffer, F Benesovsky *Monatsh. Chem.* **89** 611 (1958)
96. B Aronsson *Acta Chem. Scand.* **12** 31 (1958)
97. V N Konev, A F Nesterov, I P Glazkova *Fiz. Met. Metalloved.* **16** 86 (1963)
98. B Aronsson, G Lundgren *Acta Chem. Scand.* **13** 433 (1959)
99. B Aronsson, I Engström *Acta Chem. Scand.* **14** 1403 (1960)
100. S Rundqvist, F Jellinek *Acta Chem. Scand.* **13** 425 (1959)
101. J C Schuster, in *Proceedings of the 13th International Plansee Seminar* Vol. 2 (Eds H Bildstein, R Eck) (Reutte, Austria: Metallwerk Plansee, 1993) p. 571
102. J C Schuster *Int. J. Refract. Hard Met.* **12** 173 (1993–1994)
103. J C Schuster *Ceram. Trans.* **35** 43 (1993)
104. W Jeitschko, H Nowotny *Monatsh. Chem.* **98** 329 (1967)
105. J J Nickl, K K Schweitzer, P Luxenberg *J. Less-Common Met.* **26** 335 (1972)
106. T Goto, T Hirai *Mater. Res. Bull.* **22** 1195 (1987)
107. E Parthe, H Nowotny, H Schmid *Monatsh. Chem.* **86** 385 (1955)
108. L Brewer, O Krikorian *J. Electrochem. Soc.* **103** 38 (1956); **103** 701 (1956)
109. E Parthe, H Schachner, H Nowotny *Monatsh. Chem.* **86** 182 (1955)
110. P W Pellegrini, B C Giessen, J M Feldman *J. Electrochem. Soc.* **119** 535 (1972)
111. E Parthe, W Jeitschko, V Sadagopan *Acta Crystallogr.* **19** 1031 (1965)
112. F J J Van Loo, F M Smet, G D Rieck, G Verspui *High Temp.-High Press.* **14** 25 (1982)
113. P Guinet, H Vaugoyeau *C. R. Hebd. Seances Acad. Sci., Ser. C, Sci. Chim.* **262** 1856 (1966)
114. P L Blum, P Guinet, G Silvestre *C. R. Hebd. Seances Acad. Sci.* **260** 1911 (1965)
115. P L Blum, G Silvestre *C. R. Hebd. Seances Acad. Sci., Ser. B, Sci. Phys.* **263** 709 (1966)
116. P Guinet, H Vaugoyeau, J Laugier, P L Blum *J. Nucl. Mater.* **21** 21 (1967)
117. W Jeitschko, H Nowotny, F Benesovsky *Monatsh. Chem.* **94** 844 (1963)
118. W J J Wakelkamp, F J J Van Loo, R Metselaar *J. Eur. Ceram. Soc.* **8** 135 (1991)
119. W Wakelkamp *Tijdschr. Klei. Glas Keram.* **13** 18 (1992)
120. M Maline, M Ducarroir, F Teyssandier, R Hillel, R Berjoan, F J J Van Loo, W Wakelkamp *Surf. Sci.* **286** 82 (1993)
121. C E Brukl, in *Ternary Phase Equilbria in Transition Metal–Boron–Carbon–Silicon Systems. Technical Report AFML TR-65-2* Part II, Vol. VII (Ohio, USA: Metals and Ceramics Division, Air Force Materials Laboratory, Wright-Patterson Air Force Base, 1966) p. 35
122. N P Lyakishev, M I Gasik, O I Polyakov *Izv. Akad. Nauk SSSR, Metally* 5 (1991)
123. S Sambasivan, W T Petuskey *J. Mater. Res.* **7** 1473 (1992)
124. C E Brukl, in *Technical Report AD 489752* (US Clearinghouse Federal Scientific Technical Information, 1966) p. 37
125. K Yvon, E Parthe *Acta Crystallogr., Sect. B. Struct. Crystallogr.* **26** 149 (1970)
126. B V Khaenko, V G Fak *Izv. Akad. Nauk SSSR, Neorg. Mater.* **14** 1294 (1978)
127. J C Schuster *J. Chim. Phys. Phys.-Chim. Biol.* **90** 373 (1993)
128. H Nowotny, E Parthe, R Kieffer, F Benesovsky *Monatsh. Chem.* **85** 255 (1954)
129. Z M Alekseeva *Izv. Akad. Nauk SSSR, Metally* 212 (1990)
130. P Guinet, H Vaugoyeau, J Jolivet *J. Nucl. Mater.* **36** 94 (1970)
131. A W Searcy, L N Finnie *J. Am. Ceram. Soc.* **45** 268 (1962)
132. R C J Schiepers, F J J Van Loo, G de With *J. Am. Ceram. Soc.* **71** C284 (1988)
133. Y C Chen, C M Chen, K C Su, K Yang *Mater. Sci. Eng. A, Struct. Mater.* **133** 596 (1991)
134. M R Jackson, R L Mehan, A M Davies, E L Hall *Metall. Trans. A, Phys. Metall. Mater. Sci.* **14** 355 (1983)
135. A Inoue, S Furukawa, T Masumoto *J. Mater. Sci.* **22** 1670 (1987)
136. T C Chou *J. Mater. Sci.* **26** 1412 (1991)
137. Z Inoue, M Mitomo, N Il *J. Mater. Sci.* **15** 2915 (1980)
138. C E Holcombe, L Kovach *Am. Ceram. Soc. Bull.* **60** 546 (1981)
139. J Gaude, J Lang, D Louër *Rev. Chim. Miner.* **20** 523 (1983)
140. F Weitzer, J C Schuster, J Bauer, B Jounel *J. Mater. Sci.* **26** 2076 (1991)
141. J C Schuster, H Nowotny, in *Proceedings of the 11th International Plansee Seminar* Vol. 1 (Eds H Bildstein, H M Orlrer) (Reutte, Austria: Metallwerk Plansee, 1985) p. 899
142. J C Schuster, F Weitzer, J Bauer, H Nowotny *Mater. Sci. Eng. A, Struct. Mater.* **105/106** 201 (1988)

143. R Marchand, M Maunaye, J Lang *C. R. Hebd. Seances Acad. Sci., Ser. C* **272** 1654 (1991)
144. M Maunaye, R Marchand, J Guyader, Y Laurent, J Lang *Bull. Soc. Fr. Mineral. Cristallogr.* **94** 561 (1972)
145. F Weitzer, J C Schuster *J. Solid State Chem.* **70** 178 (1987)
146. Yu I Krylov,V A Bronnikov *Poroshk. Metall.* (1) 52 (1976)
147. Yu S Borisov, A L Borisova, Yu A Kocherzhinskii, E A Shishkin *Poroshk. Metall.* (3) 63 (1978)
148. T Hirai, S Hayashi *J. Mater. Sci.* **17** 1320 (1982)
149. S Hayashi, T Hirai, K Hiraga, M Hirabayashi *J. Mater. Sci.* **17** 3336 (1982)
150. R Beyers, R Sinclair, M E Thomas *J. Vac. Sci. Technol. B* **2** 781 (1984)
151. W Wakelkamp, PhD, Teshnische Universiteit Eindhoven, Eindhoven, Nederlands, 1991
152. T Onozuka *Trans. Jpn. Inst. Met.* **23** 315 (1982)
153. J C Schuster *J. Mater. Sci.* **23** 2792 (1988)
154. T Kato, M Yoshimura, S Somiya *Yogyo-Kyokai-Shi* **89** 221 (1981)
155. E Heikinheimo, A Kodentsov, J A Van Beek, J T Klomp, F J J Van Loo *Acta Metall. Mater.* **40** S111 (1992)
156. R Pompe *Thermochim. Acta* **34** 245 (1979)
157. F Weitzer, P Rogl, J C Schuster *Z. Metallkd.* **79** 154 (1988)
158. H Haschke, H Nowotny, F Benesovsky *Monatsch. Chem.* **98** 273 (1967)
159. W Jeitschko, H Nowotny, F Benesovsky *Monatsch. Chem.* **95** 319 (1964)
160. D S Bloom, N J Grant *J. Met.* **2** 41 (1950)
161. E R Morgan *J. Met.* **6** 983 (1954)
162. R G Butters, H P Myers *Philos. Mag.* **46** 895 (1955)
163. L J Hütter, H H Stadelmaier *Acta Metall.* **6** 367 (1958)
164. L J Hütter, H H Stadelmaier *Z. Metallkd.* **50** 199 (1959)
165. M L Swanson *Can. J. Phys.* **40** 719 (1962)
166. L J Hütter, H H Stadelmaier, A C Fraker *Metall* **14** 113 (1960)
167. H H Stadelmaier *Z. Metallkd.* **52** 758 (1961)
168. J C Schuster, H Nowotny *Monatsch. Chem.* **113** 163 (1982)
169. W Jeitschko, H Nowotny, F Benesovsky *Monatsh. Chem.* **94** 672 (1963)
170. W Jeitschko, H Nowotny, F Benesovsky *J. Less-Common Met.* **7** 133 (1964)
171. H Nowotny, W Jeitschko, F Benesovsky *Planseeber. Pulvermetall.* **12** 31 (1964)
172. H Nowotny *Angew. Chem.* **84** 973 (1972)
173. W Jeitschko, H Nowotny, F Benesovsky *Monatsh. Chem.* **94** 332 (1963)
174. W Jeitschko, H Nowotny, F Benesovsky *Monatsh. Chem.* **95** 1212 (1964)
175. W Jeitschko, H Nowotny, F Benesovsky *Monatsh. Chem.* **94** 245 (1963)
176. W Jeitschko, H Nowotny, F Benesovsky *Monatsh. Chem.* **95** 30 (1964)
177. J C Schuster, H Nowotny *Z. Metallkd.* **71** 341 (1980)
178. C Brisi, F Abbatista *Ann. Chim. (Roma)* **51** 452 (1961)
179. J C Schuster, H Nowotny, C Vaccaro *J. Solid State Chem.* **32** 213 (1980)
180. T Lundström, M M Korsukova, V N Gurin *Prog. Cryst. Growth Charact.* **16** 143 (1988)
181. H Nowotny, O Schob, F Benesovsky *Monatsch. Chem.* **92** 1300 (1961)
182. A E Vol *Stroenie i Svoistva Dvoinykh Metallicheskikh Sistem* T. 1 (The Structure and Properties of Binary Metal Systems, Vol. 1) (Moscow: Fizmatgiz, 1959)
183. J C Schuster, H Nowotny *Z. Metallkd.* **72** 63 (1981)
184. F R Morral *J. Iron Steel Inst.* **130** 419 (1934)
185. J C Schuster, J Bauer *J. Less-Common Met.* **109** 345 (1985)
186. J C Schuster *J. Less-Common Met.* **105** 327 (1985)
187. H Haschke, H Nowotny, F Benesovsky *Monatsch. Chem.* **98** 2157 (1967)
188. J C Schuster, J Bauer *J. Solid State Chem.* **53** 260 (1984)
189. H H Stadelmaier, T S Yun *Z. Metallkd.* **52** 477 (1961)
190. W Jeitschko, H Nowotny, F Benesovsky *Monatsh. Chem.* **94** 1198 (1963)
191. M J Kaufman, D G Konitzer, R D Shull, H L Fraser *Scr. Metall.* **20** 103 (1986)
192. F Ueda, M Yageta, I Tajima *J. Hard Mater.* **2** 233 (1991)
193. J C Schuster, J Bauer, J Debuigne *J. Nucl. Mater.* **116** 131 (1983)
194. J C Schuster *J. Nucl. Mater.* **120** 133 (1984)
195. J C Schuster *Z. Kristallogr.* **175** 211 (1986)
196. W Jeitschko, H Nowotny, F Benesovsky *Monatsh. Chem.* **95** 156 (1964)
197. J C Schuster, H Nowotny *Z. Metallkd.* **76** 728 (1985)
198. J C Schuster, H Nowotny *J. Mater. Sci.* **20** 2787 (1985)
199. C Brukl, H Nowotny, O Schob, F Benesovsky *Monatsch. Chem.* **92** 781 (1961)
200. O Schob, H Nowotny, F Benesovsky *Planseeber. Pulvermetall.* **10** 65 (1962)
201. A Raman, K Schubert *Z. Metallkd.* **56** 40 (1965)
202. O Schob, H Nowotny, F Benesovsky *Monatsch. Chem.* **92** 1218 (1961)
203. E Gerhardt, G Joseph *Z. Metallkd.* **52** 310 (1961)
204. C Brukl, H Nowotny, F Benesovsky *Monatsch. Chem.* **92** 967 (1961)
205. H Nowotny, F Benesovsky, C Brukl *Monatsch. Chem.* **92** 193 (1961)
206. H Nowotny, C Brukl, F Benesovsky *Monatsch. Chem.* **92** 116 (1961)
207. K Robinson *Acta Crystallogr.* **6** 854 (1953)
208. H Nowotny, C Brukl *Monatsch. Chem.* **91** 313 (1960)
209. C Brukl, F Benesovsky, H Nowotny *Planseeber. Pulvermetall.* **11** 20 (1963)
210. H Holleck, F Benesovsky, E Laube, H Nowotny *Monatsch. Chem.* **93** 1075 (1962)
211. J B Kusma, H Nowotny *Monatsch. Chem.* **95** 1266 (1964)
212. K Robinson *Acta Crystallogr.* **5** 397 (1952)
213. G L Phragmen *J. Inst. Met.* **77** 489 (1950)
214. M Cooper *Acta Crystallogr.* **23** 1106 (1967)
215. D Munson *J. Inst. Met.* **95** 217 (1967)
216. R I Garrod, L M Hogen *Acta Metall.* **2** 887 (1954)
217. C Gueneau, C Servant, F d'Yvoire, N Rodier *Acta Crystallogr. Sect. C, Cryst. Struct. Commun.* **51** 177 (1995)
218. K O Burger, A Wittmann, H Nowotny *Monatsch. Chem.* **93** 9 (1962)
219. A Wittmann, K O Burger, H Nowotny *Monatsch. Chem.* **93** 674 (1962)
220. R W Guard, E A Smith *J. Inst. Met.* **88** 369 (1960)
221. G Will *Acta Crystallogr., Sect. B, Struct. Crystallogr.* **25** 1219 (1969)
222. A J Perrotta, W D Townes, J A Potenza *Acta Crystallogr., Sect. B, Struct. Crystallogr.* **25** 1223 (1969)
223. H Neidhard, R Mattes, H J Becher *Acta Crystallogr., Sect. B, Struct. Crystallogr.* **26** 315 (1970)
224. Z Inoue, H Tanaka, Y Inomata *J. Mater. Sci.* **15** 3036 (1980)
225. Z Inoue, Y Inomata, H Tanaka, H Kawabata *J. Mater. Sci.* **15** 575 (1980)
226. Z Inoue, Y Inomata, H Tanaka, H Kawabata *J. Mater. Sci.* **15** 255 (1980)
227. B L Kidwell, L L Oden, R A McCune *J. Appl. Crystallogr.* **17** 481 (1984)
228. L L Oden, R A McCune *Metall. Trans. A, Phys. Metall. Mater. Sci.* **18** 2005 (1987)
229. R Kieffer, E Gugel, G Leimer, P Ettmayer *Ber. Deutsch. Keram. Ges.* **49** 41 (1972)
230. N V Dokukina, A A Kalinina, M I Sokhor, F I Shamrai *Izv. Akad. Nauk SSSR, Neorg. Mater.* **3** 630 (1967)
231. K I Portnoi, G V Samsonov, L A Solonnikova *Zh. Neorg. Khim.* **5** 2032 (1960)
232. R Kieffer, E Gugel, P Ettmayer, A Schmidt *Ber. Deutsch. Keram. Ges.* **43** 621 (1966)
233. E Gugel, P Ettmayer, A Schmidt *Ber. Deutsch. Keram. Ges.* **45** 395 (1968)
234. M L Cohen *J. Hard. Mater.* **2** 13 (1991)
235. M Billy, F Colombeau *C. R. Hebd. Seances Acad. Sci., Ser. C, Sci. Chim.* **264** 392 (1967)
236. V J Barczak *J. Am. Ceram. Soc.* **44** 299 (1961)
237. G Schneider, L J Gauckler, G Petzow, A Zangvil *J. Am. Ceram. Soc.* **62** 574 (1979)
238. F Weitzer, K Remsching, J C Schuster, P Rogl *J. Mater. Res.* **5** 2152 (1990)
239. A A Rempel' *Effekty Uporyadocheniya v Nestekhiometricheskikh Soedineniyakh Vnedreniya* (Ordering Effects in Nonstoichiometric Interstitial Compounds) (Ekaterinburg: Nauka, 1992)
240. A I Gusev, A A Rempel *Phys. Status Solidi A* **135** 15 (1993)